University of Alberta

Detection of Clandestine Tunnels using Seismic Refraction and Electrical Resistivity Tomography

By

Grey Riddle

A thesis submitted to the Faculty of Graduate Studies and Research
in partial fulfillment of the requirements for the degree of

Master of Science
in
Geophysics

Department of Physics

Fall 2011
Edmonton, Alberta

ABSTRACT

The detection of clandestine tunnels is a major issue along the US-Mexico border, the use of these tunnels leads to illegal transportation of drugs, immigration, and weapons. The study that was performed here was to see if using high resolution seismic refraction techniques and electrical resistivity tomography can be used to detect tunnels. The study has two main target sites, the first in Oxford, MS; looking at surrogate tunnel sites along an abandoned railway track. The second site looking at a plugged found clandestine tunnel that runs from Agua Prieta, MX to a warehouse in Douglas, AZ. The results show that the use of seismic and electrical techniques can detect the presence of a tunnel anomaly. The use of using multiple geophysical techniques can be advantageous for joint interpretation to increase reliability and confidence in the location of the tunnel.

TABLE OF CONTENTS

LIST OF FIGURES

LIST OF TABLES

LIST OF SYMBOLS AND ABBREVIATIONS

NCPA	National center of Physical Acoustics
UofA	University of Alberta
MS	Mississippi
AZ	Arizona
US	United States
DHS	Department of Homeland Security
CBP	Customs and Border Patrol
MX	Mexico
ERT	Electrical resistivity tomography
SRI	Stanford research institute
GPR	Ground penetrating radar
EM	Electromagnetic
FDEM	Frequency domain electromagnetic method
TDEM	Time domain electromagnetic method
MASW	Multichannel analysis of surface waves
KGS	Kansas geological survey
RMS	Root mean square
GPS	Global positioning system
VSP	Vertical seismic processing
CA	California
SEG	Society of exploration geophysicist
SARIS	Scintrex automated resistivity imaging system
DC	Direct Current
FDVEP	Finite difference viscoelastic program
FD	Finite difference
GSLS	Generalized standard linear solid
SRT	Seismic refraction tomography
P-wave	Compressional wave
S-wave	Shear wave
SV wave	Vertical surface wave
QC	Quality control

CSG	Common shot gather
GLI	Generalized linear inversion
NMO	Normal moveout correction
LMO	Linear moveout correction
WET	Wavepath eikonal traveltime
AGC	Automated gain control
FWI	Full waveform inversion
S/N	Signal to noise
V_s	Shear wave
V	Compressional wave
fc	central frequency
DH	grid spacing
DT	time sampling
Q	Quality factor
T	stress relation time/tortuosity
J	Electric current density
ρ	Density
E	Electric field
L	Length
A	Cross sectional area
C	Curvature
I	Current
ΔV	Potential difference
k	geometric factor
Δq	Resistivity model parameter change vector
F	Resistivity smoothness constrain matrix
f	Resistivity model response vector
g	Resistivity discrepancy vector
J	Jacobian matrix
y	Resistivity data vector
2D	Two dimensional
3D	Three dimensional
k	Bulk modulus

μ	Shear modulus
v	Velocity
λ	Wavelength
E	Least squares error
P	Probability
T	Temperature of annealing

CHAPTER 1
1.0 OUTLINE

The work that will be presented below is the work of a joint cooperation between the University of Alberta and the National Center for Physical acoustics (NCPA) in Olemiss, MS. The collaboration was with a Department of Homeland Security (DHS) contract to look at the feasibility of using high resolution seismic methods to detect clandestine tunnels. Along with this it was deemed that electrical methods could be used to help delineate some features and was also collected at two test sites. The first site was in Oxford, MS along an abandoned railway track that had numerous different cavities cutting underneath it. The second site was in Douglas, AZ where a real clandestine tunnel crosses the US Mexico border. The work presented is split up into eight sub chapters; a brief description is given below for each chapter.

The first Chapter is an outline chapter that goes over basic project premise and the description of each chapter thereafter.

The second Chapter is an overview of multiple different geophysical methods that have been used in the past to detect tunnels with a brief overview on how they detect a void in the subsurface. The chapter starts off with a brief motivation on how this project came about, and the prevailing issues associated with tunnels across the US-Mexico border. This is followed up with a description of how various geophysical techniques have detected subsurface voids. The literature review of various authors experience using different methods on detecting tunnels gives good insight on how tunnels have been detected in the past. The end of the chapter involves a brief description of how tunnels are constructed and some limitations and advantages of each method are summarized.

The information that is gathered from the second chapter is used for the third chapter which gives an overview of the data acquisition and equipment that was used for the tunnel sites. This chapter is used to explore in general; the target

sites, the general layout of the terrain; and the equipment used. A description of the equipment and how it is implemented in the field is also discussed.

The fourth chapter is the beginning of the work that was done for detecting subsurface tunnels; this was done by synthetic modeling for both seismic and electrical methods. The chapter shows how using synthetic modeling can optimize some of the acquisition parameters and gives a basic premise of the signature of what should be seen in the real data. The geological models that were used for modeling are simple and are there just to guide the acquisition of both the seismic and electrical methods. The electrical modeling used was to figure out which electrical array is needed to image the subsurface model and also to see the effects of an air filled void on both Wenner and dipole-dipole arrays. Using a finite difference forward modeling program the synthetic seismograms are used to display what the effect of a tunnel has on a seismic wave. A description of the program and the parameterization of the modeling program is discussed.

The electrical method theory, application, and examples are described in the fifth chapter. The chapter starts by going over some basic resistivity theory followed by a description of the electrical resistivity tomography (ERT) method. How electrical data is displayed is then described and how the subsurface is imaged for both dipole-dipole and Wenner arrays. The data collected at Oxford, MS is then analyzed with the results feeding into the interpretation of the real clandestine site in Douglas, AZ. The main objective of this chapter is to show how electrical methods can detect tunnels.

The sixth chapter discusses the seismic method and how it can be used for tunnel detection. It starts with a description of elastic wave theory and the different types of seismic waves. A brief description of seismic resolution, and how refraction tomography and seismic ray tracing can image the subsurface. The inversion algorithm is discussed and the seismic refraction data is discussed in detail. The refraction profiles from both Oxford, MS and Douglas, AZ are analyzed with both surface and borehole models interpreted.

The seventh chapter describes how using both the seismic and electrical methods can help delineate any false anomalies. The data is discussed ~~described~~ by

analyzing what could be done better and hence points towards some of future work. The joint interpretation shows why some of the surveys fail and why others are interpreted in certain ways. The interpretation also shows what could be done to with other parts of the seismic wave to detect tunnels using diffractions off the tunnel itself. The final part of the chapter discusses some of the feasibility, repeatability and criteria needed for the next level in tunnel detection

~~The study is finally wrapped up with conclusions of the study and~~ what was done during the duration of the project is concluded in chapter eight. This chapter describes what was learned and summarizes how using refraction and electrical methods can be used for tunnel detection.

At the end of the dissertation there is an appendix that has the notes and a brief description of some of the key acquisition parameters of each tunnel site. This is used as a guide if some of the information of each tunnel site is vague. The information about each site gives ~~detailed information about~~ the field record notes and a basic description of the tunnel sites and pictures associated with each test site.

CHAPTER 2
2.0 BACKGROUND INFORMATION

The following chapter discusses how geophysical techniques can be used to detect subsurface voids such as tunnels, cavities and karst features. This is done by analyzing how different geophysical methods measure basic physical properties and some of the basic limitations and advantages of each method. Previous case studies on tunnel detection will be analyzed and how various studies have helped develop new advances in processing and acquisition for detection of near surface voids. Later in the chapter how tunnels are constructed, ~~and~~ some technical limitations of the equipment and software held by the University of Alberta and University of Mississippi ~~will be analyzed.~~

2.1 INTRODUCTION

Tunnel detection has been a difficult field of research in the near surface for a long time. The reason for this is that most tunnels and subsurface cavities are in densely populated regions with large amount of surface and subsurface heterogeneity. Due to this, the best way to find a tunnel using geophysics depends on ~~a site to site basis.~~ The research is the same geophysical methodology as for finding any subsurface void such as bunkers, caves, karst features, tombs, culverts, and any subsurface void. The reason for this, geophysically speaking, is a subsurface void is just a zone of high contrast in physical properties with a solid and fluid wall. In the near surface the void is completely fluid filled and in most cases air and water. The way the subsurface void is created also affects the ~~surrounding~~ rocks which cause a change in the stresses to the surrounding material. The type of casing also greatly affects what type of geophysical technique can be used, with this in mind great caution has to be taken into account when dealing with interpretation of tunnel data. To get around this, multiple methods should be used to limit false artifacts and increase reliability in detecting tunnels.

Clandestine tunnels crossing the USA and Mexico border have been transporting large amounts of drugs and illegal immigrants for years. The government started to take notice and held its first symposium on tunnel detection in 1977 at Colorado school of mines and to date more and more attention has been given to near surface clandestine tunnels. The reason is that using conventional intelligence methods are not ~~plausible~~ to detect all tunnels, so more attention ~~has been~~ given to other more direct methods ~~to locate tunnels.~~ Locating clandestine tunnels gives more border security and greater control of illegal transportation of drugs and immigrants. ~~Later in the chapter details on how tunnel detection has progressed and how the University of Alberta and University of Mississippi have been involved.~~

To date the best way to find a clandestine tunnel is ~~mostly~~ indirectly through intelligence (i.e., rumours, tips) and not from a scientific perspective. This is mainly due to the cost and the lack of reliability of most geophysical methods, but as data acquisition technology progresses cheaper and more effective ways are being found to detect tunnels. From geophysics perspective multiple methods have been used in the past to detect tunnels, but all have some limitations from both a scientific and acquisition perspective. New advances in acquisition have been ~~able to make it possible for~~ cheap and reliable data, but ~~due to~~ the small sizes of the underground void ~~they are~~ nearly impossible to detect. The goal of the research is to see how practical using seismic and electrical resistivity tomography can be in detection of clandestine tunnels. To do this other geophysical methods have been used both currently and in the past and how these methods detect subsurface voids. Will finally conclude with an assessment of the capabilities of the University of Alberta`s equipment by listing some of the technical limitations of the equipment and software available.

Later in this chapter information about how tunnels are constructed and how the construction changes the physical properties of the surrounding rock. The construction technique used depends on the lithology in the region and the accessibility to heavy machinery. The main type of tunnel construction in urban environments is known as the cut and cover method. The other type of contrustion which is popular is clandestine tunnels is known as boring, which tunnels through

the subsurface without removing the material above it. The tunnel construction will just be gone over to help with the interpretation later in the dissertation but will not be discussed in detail.

2.2 MOTIVATION

In general, tunnel detection is a difficult area of research since most clandestine tunnels constructed are made not to be detected. On the USA and Mexico border clandestine tunnels are constructed to transport drugs, weapons, and illegal aliens to the USA undetected by the government. Tunnels have also been detected at the Canada-USA border. Quite a series of tunnels have been constructed for military or terrorist access in places such as the borders between North and South Korea and between Israel and the Palestinian territories. To date most tunnels are detected using human intelligence, and the application of geophysical techniques is not completely reliable due to the large amount of near surface heterogeneity. One of the goals of this research is to evaluate reliability of near surface geophysical methods.

To do this, multiple types of geophysical methods were considered but only a few were field tested as appropriate methods for the actual test sites. This material is based upon work supported by the U.S. Department of homeland Security under Grant Award Number 2007-ST-108-000003.

From a research prospective multiple workshops and conferences have been convened on the subject of tunnel detection due to the complexities and hazards associated with near surface voids. The very first few conferences held for tunnel detection were to see how plausible the use of geophysical techniques could be to detect a subsurface tunnel. The first technical symposium on tunnel detection tunnels (Anon 1981) found that methods could be used to detect tunnels , and the second technical symposium on tunnel detection (Anon 1988) was held to reconvene to see if new research made detection more accurate.. A major report was also done by SRI international to see the technology used in tunnel detection (Vesecky, Nierenberg and Despain 1980). The main issue found in this report was

that there was a resolution issue in nearly all geophysical techniques. Multiple other conferences were held to try and remedy this issue but in general detecting tunnels has always had this problem.

Recently there have been conferences to try and remedy this issue by looking to see if newer acquisition technology has increased the resolution for detecting subsurface voids. The conference held in Oxford, MS was first used to see how tunnels could be detected during construction (Sabatier and Muir 2006). In particular, it discussed the use of passive techniques that record the unavoidable noise created from constructing the tunnel in the subsurface. Other active techniques were also discussed but what was decided is that more information and data was needed to be collected to see if tunnels could be found. Other assemblies around the same time were done to see if tunnels or voids can be detected (Halihan and Nyquist 2006, Mckenna and Ketchum 2006). To date the resolution of the tunnel is still the main source of unpredictability in detecting tunnels, to get around this the goal of this report was to see how combining multiple methods could be used to detect tunnels. The other way to do this is to use multiple methods for joint inversion to decrease false anomalies such as (Cardarelli et al. 2010). This method uses electrical resistivity to make an estimated subsurface model of the subsurface and uses that as the initial model for refraction tomography. The goal taken in this research is to use multiple methods and process them individual to limit false artifacts in interpretation of data (Riddle, Hickey and Schmitt 2010)

The University of Mississippi became involved with the USA Department of Homeland Security during the 2006 convention (Sabatier and Muir 2006). The goal of the grant was to look at using refraction tomography and if it has advanced far enough and to see if they can detect tunnels using high resolution seismic technology. The idea first came from looking at infiltration of water through a test earthern damsite, trying to test if the movement of water can be detected in a time lapse sense (Hickey and Howard 2006). What was seen was that as the water went through a buried pipe a void of air was created and it possible to detect the void by looking at the seismic ray coverage. Using the same methodology as the earthen dam the goal of this study was todetect tunnels using high resolution seismic tomography

by using a 2-D ray coverage plot and velocity tomography. Electrical methods were also considered to be used to look at basic geological structure and its previous experience in finding high contrast voids. The University of Alberta got involved due to Dr. Doug Schmitt's field experience and the equipment available to the university. Dr. Craig Hickey was a previous grad of the University of Alberta and a mutual collaboration was developed. The goal of the University of Alberta was to test using electrical resistivity tomography and to see if other seismic methods such as reflection or other high resolution seismic methods are able to detect tunnels.

2.3 Tunnel Detection Review

There are multiple methods for finding geological information in the vadose zone, the partially saturated zone from earth's surface to the ground water table; but in general all methods have draw backs. The vadose zone is generally the region where a clandestine tunnel will be dug; as below the water table opening and maintaining a dry tunnel becomes problematic. One of the key features in the vadose zone is that you have unsaturated to partially saturated rocks in this region. For detection of any subsurface void you look for the large changes in the physical properties of the void and the surrounding rock. The main issue is that the resolution of the tunnel site is on par or smaller than that of the geophysical technique`s resolution. To look at this the following paragraphs will describe case studies used to detect subsurface voids focusing on the limitations, advantages and disadvantages of most major geophysical technique.

In general the most common type of way to find a tunnel is during the construction or when the tunnel itself is being used. For this reason along the US Mexico border a large amount of permanent seismometers and sensors are in place to find tunnels that are being constructed. The noise from the construction in the seismic data can be correlated to find general locations of tunnels (Sabatier, Matalkah and Ieee 2008). Large amount of seismometers are needed to get an accurate location of a tunnel, but information on the general location can be easily confirmed. The installed sensors can detect tunnel location by comparing similar signal from different sensors and by back propagating the location of the noise. The

way the waves propagate through a tunnel can be described by (Ketcham et al. 2006) and can be used to help find a tunnel signature. The study describes that the activity in a tunnel pulsates in a harmonic motion seen in seismic data, and could be cross correlated to create maps of possible tunnel locations. Other types of permanent geophysical sensors can be implemented and used to gather data to help limit false artifacts in clandestine tunnel detection by using statistical measures and comparing to synthetic measurements (Senglaub et al. 2010). The advantage of passive methods is that once the sensors are in place they can look over a large area for possible tunnel sites. The main problem associated with this method is that in urban environments the energy caused by the construction for tunnels may be too weak relative to the urban noise at the seismometer locations. In these locations active source geophysics need to be applied to detect clandestine tunnels. In urban environments many geophysical techniques have troubles operating due to large amount of situational noise and large man made obstacles in the way of optimal acquisition conditions.

Once in an urban environment the type of technique used depends on the situation, and the type of terrain. In situations of very resistive soil with very little surface metal in the region ground penetrating radar (GPR) is usually the best imaging technique. The technique uses high frequency electromagnetic waves (EM) and pulsates a signal into the ground using an antenna. Two antennas are used, one to transmit signal into the ground acting as the source while the other one is a receiver. The transmitted sends a polarized short pulse of a given frequency, the wave propagates through the ground and when it hits a buried object of different dielectric constant it reflects back. The depth of penetration all depends on the electrical conductivity of the subsurface and the transmitted frequency. In situations where the conductivity is high this method can only go into the very near surface and wont detect any anomaly. In these regions using GPR is a very poor choice and other techniques need to be used. More information about the technique itself can be seen (Telford, Geldart and Sheriff 1990). GPR was one of the first techniques to readily be able to detect tunnels due to the high accuracy of the technique. The technique has been used quite extensively in situations of mapping karst features (Benson 1995, Chamberlain et al. 2000). The reason the method is so popular is the

onsite data analysis, fast acquisition, and ability to distinguish very small subsurface features. This can be seen in (Kruse et al. 2006) where GPR was used to map subsurface cavities. Due to the fast acquisition of the technique it is also quite good at doing combined interpretation using geoelectrical data (El Khammari et al. 2007) in regions with large amount of large cavities. Since interpretation of GPR can be hard in combination with microgravity, data can be used in regions of sinkholes and karstic features (Leucci and De Giorgi 2010). One of the new ways to use this technique now is to use multiple antennas and create a radio frequency tomography of the subsurface looking for tunnels (Lo Monte et al. 2010). This is a relatively new technique which uses diffraction scattering from the void and multiple antennas to look for shallow tunnels. The main disadvantage of using GPR techniques is mainly that the inversion depends completely on the conductivity of subsurface.

Another common type of geophysical technique which has been used quite extensively in the past is gravity. In general when looking for tunnels or near surface voids the technique is known as microgravity. A gravimeter is used to measure the relative value of gravity at the surface, so in situations of a near surface void the change in density can be seen in the gravity measurements and cause a gravity anomaly. More information on the processing and inversion can be seen in (Telford et al. 1990). Since microgravity looks at relative gravity measurements the technique is used quite extensively in geotechnical studies looking for buried voids (Debeglia and Dupont 2002) or any subsurface cavity (Butler 1984). The technique can also be used in karstic features in mining operations to increase safety by locating these voids (Bishop et al. 1997). The reason microgravity is so useful for looking for subsurface voids is that even if the void is filled with water or is air filled the large change in density, can cause a large gravity anomaly. Since gravity only looks at relative gravity changes it can be used with large efficiency without giving false artifacts. The problem associated with gravity is that in urban environments with large basements the change in density due to the buildings can mask the location of tunnel. To get around this a detailed structure model needs to be known of the region being surveyed and this sometimes cannot be known.

Electromagnetic methods (EM) are quite popular in near surface studies due to their high frequency content and ability to map large areas. The first type of EM

technique is known as frequency domain electromagnetic method (FDEM), which measures induced electromagnetic current. Measuring the induced current direct measurements can be calculated for a volume in the subsurface, and can be continuously measured for quick mapping of the subsurface. Since the volume of subsurface is gathered FDEM surveys generally have poor vertical resolution but can be used to obtain lateral changes such as produced by cavities (Sogade et al. 2004).

The second types of EM method is known as Time-domain electromagnetic methods (TDEM) and are a very common type of near surface technique used in hydro geological and geotechnical studies; which can also be used to look for tunnels. Time domain methods use induced electric current to create a magnetic field to induce a secondary electric current into the ground. The electric current then pulsates and in between the injection of electric current the time decay response is measured, which then can be related to electrical conductivity of the subsurface. Information about different types of TDEM methods can be seen in (Nabighian and Macnae 1991). TDEM in general is very useful to detect very conductive anomalies, but can be used to see changes in lithology and ground water (Legchenko et al. 2009). For tunnel detection TDEM is quite useful in detecting saline water filled voids or metal lined cavities. In general most tunnels are filled with air, but if not lined thethe water table may fill the cavity making and in regions of salty sands it may be able to detect the saline water in the tunnel. The main disadvantage of this method is that it is usually not possible to detect an air filled tunnel due to the surroundings being more conductive. While the advantage of this technique is to detect any tunnel that is water filled and or have a metal lining. The technique is not used as a staple for detecting clandestine tunnels but can be used secondarily to supplement other methods.

Similar to TDEM method, magnetic surveys can also be used to detect subsurface tunnels in certain situations. In most cases magnetic surveys can only detect those subsurface tunnels or voids lined with a metal exterior or otherwise containing a large amount of iron or steel metal. The main use for this technique has been to find larger tunnels which have cart tracks or concrete lined with rebar reinforcements. Due to the rapid acquisition of this technique it can be useful if

there is prior information about steel or iron in the tunnel but is usually not used in the field.

In near surface geophysics geoelectrical methods are one of the more common geophysical techniques. The reason for this is that resistivity changes in the subsurface can be related to changes in fluid, mineral content, porosity, water saturation, and salinity in rocks. Since the near surface physical properties of rocks can change drastically imaging both vertical and lateral changes is necessary. Electrical resistivity tomography (ERT) was developed to image the subsurface complex geology faster than the conventional sounding approach (Griffiths and Barker 1993, Zhou, Beck and Stephenson 2000) using a Wenner array geometry. Different arrays can also image complex geology such as the dipole-dipole array (Zhou et al. 2000) which specialize in lateral changes in the subsurface. ERT is quite useful in imaging the near surface and has widely been used to image sinkholes and karst geology (van Schoor 2002, Kruse et al. 2006, Leucci, Margiotta and Negri 2004, Dobecki and Upchurch 2006). Sinkholes in general will resemble collapse tunnels in geophysical images where the ground shows up as either a highly resistive or conductive anomaly depending on being water or air filed. Using the same methodology as tunnel detection ERT can be used to detect archeological targets by looking for tombs and graves (Negri, Leucci and Mazzone 2008, Papadopoulos et al. 2010, Cardarelli et al. 2010). When using ERT at archeological tombs the anomaly that is seen is a highly resistive block due to weak soils and air filled chambers. Since air is highly resistive ERT methods can be used for joint interpretation methods to limit uncertainty (Cardarelli et al. 2010, Piro, Tsourlos and Tsokas 2001). The main advantage compared to most other methods is that electrical methods work quite well in complex geology. Electrical methods can map the subsurface quickly and for fairly cheap due to the fast acquisition and easy interpretable results. The main disadvantage with ERT is that in very conductive soils the current may not penetrate deep enough to where a highly resistive anomaly may be, and thus not be imaged correctly. The method also only gives apparent resistivity values of the subsurface so the actual values cannot be directly interpreted for a given geological feature.

In the detection of clandestine tunnels both seismic refraction and reflection techniques are popular. The reason for this is that seismic methods can detect

contrasts in rigidity, compressibility and density of the subsurface. Since for a given void site fluid filled voids have a huge change in physical properties compared to the surrounding material. For all seismic methods the velocity of the subsurface is related back to the physical properties for interpretation. The main issue in most void sites is that the highest resolution usually available is on par or smaller than the given void.

Seismic modeling experiments were done to see if using seismic methods can be used (Grandjean and Leparoux 2004) to detect subsurface voids. What was seen was that both P-wave and Rayleigh waves are important to detect tunnels. The case study described how both direct and diffracted waves are attenuated and changed by the presence of a cavity in the subsurface. What is seen in the field that is in general due to the size of the void site seismic reflection is too small to treat a tunnel like a layer. So instead of reflecting off the void site the void acts as a secondary scatter and is treated as a second point source and is seen as a diffraction (Xia et al. 2007). Diffraction imaging is quite useful in detecting subsurface voids and have been used to back propagate locations of tunnels (Lee et al. 1989). Using similar technique but the diffractions can be stacked to look for small size voids (Belfer et al. 1998). A newer approach tries to image the subsurface using diffraction imaging, where you separate the diffraction by using a moveout function (Xia et al. 2007), or a display similar to semblance (Keydar, Pelman and Ezersky 2010) to find the anomaly. The reason for all different types of imaging using diffractions is that first diffractions arrive to the surface receiver at times similar to the surface waves. Further, the time-receiver offset trend of the diffractions look similar to reflections. And thus is processed similarly. Since diffractions can have a small amplitude, enhancement may be needed to remove the energy of other seismic waves by (Khaidukov, Landa and Moser 2004). This is exceptionally useful when there are numerous strong reflectors since most diffraction have significantly lower amplitude then the reflections. The main disadvantage of using diffraction imaging is that it is hard to discriminate a given diffraction caused by a void from that produced by a local heterogeneity or contrasting physical properties. To circumvent this problem, seismic tomography can also be carried out and the results between the two methods are correlated. The main advantage of this diffraction method

compared to some other seismic techniques is that the diffractor comes directly from the tunnel location so it is easy to locate the location for the void.

The seismic wave can also be used with the first arrival or the refracted wave to detect tunnels. The first arrival is the first wave that comes from the source to the sensors located on the ground. The larger the spread length of the sensors from the source point, the deeper and faster is the refracted wave generally. Since the P-wave velocity of air and water are quite a bit lower then sedimentary rocks the location of a void causes a delay in the arrival and in the energy of the seismic wave (Engelsfeld, Sumanovac and Pavin 2008). Just using travel time data alone allowed estimations of void locations underneath a concrete road by (Markiewicz and Rodriguez 1986).

Refraction tomography uses the first arrival travel time and uses the changes in arrival times to calculate the velocity structure of the subsurface. Due to the size of voids the velocity information estimated by refraction tomography is only slightly lower than the surround material (Sheehan, Doll and Mandel 2006a). The reason for this is that when inverting for the velocities using the travel times from direct arrivals the regularization in the inversion causes a smooth velocity change. The method uses ray tracing to calculate the velocity of the structure and do to the lower velocity less rays travel through the location of the tunnel (Hickey and Howard 2006). Since the tunnel has such a large contrast in physical properties, the rays bend around the tunnel because the seismic waves can travel through the surrounding rock (i.e., transmission of seismic energy into the air filled void is minimal). The velocity tomogram was still able to see a small decrease in velocity around the tunnel site. Another way to try and detect subsurface tunnels using refraction tomography is to use joint interpretation. Using the information from ERT surveys one can estimate a subsurface initial model for refraction tomography to increase the accuracy of tomogram and decrease false artifacts (Cardarelli et al. 2010). Multiple refraction tomography programs have been tested to see the effectiveness in characteristic near surface features (Sheehan, Doll and Mandell 2006b). Some of the limitations and disadvantages of using tomography were discussed by (Doll et al. 2006). Due to the decrease in cost of near surface seismic

studies a large amount of research is going into seeing how well seismic can characterize the near surface.

In a seismic study there is also surface bound waves that only travel near to the surface called surface waves the strongest surface wave is known as the Rayleigh wave that is also in geophysical jargon called ground roll. The Rayleigh wave is dispersive and loses amplitude very quickly at depth in the subsurface. The reason it is used in near surface studies is due to the high amplitude of the signal which can be used extensively in urban environments. The technique most associated with surface waves for near surface studies uses multichannel analysis of surface waves (MASW), which was a method developed by the Kansas geological survey (KGS) (Zhang, Chan and Xia 2004). The technique uses dispersion curves to estimate the velocity of subsurface and due to the nature of S-waves the presence of any fluid can detect near surface voids (Nasseri-Moghaddam et al. 2007). The technique can be applied quite well in busy urban environments where most techniques fail due because of high noise levels. (Karray and Lefebvre 2009) The study found cavities underneath pavement in an urban environment using surface waves. The key to characterize MASW techniques requires good spatial and frequency sampling. What this means is that both low and high frequencies need to be recovered well since the velocity image relies on the dispersive nature of the wave. Good spatial resolution is needed to detect narrow subsurface cavities, such as dipping cavities in abandoned mine shafts (Xu and Butt 2006). The history of MASW in the search for tunnels was described by (Miller et al. 2006) who suggests that MASW seems to have the largest possibility to find clandestine tunnels. The main disadvantage of using surface techniques is the fact that without low frequency geophones, which can be costly the depth of investigation is limited. The main limitation of this technique is that for now the inversion from the dispersive curve to velocity image is all 1D so large spatial sampling is needed to accurately image the subsurface.

Surface techniques for detecting subsurface tunnels are the most cost effective and but in general are always limited by the urban environment around them. Since surface techniques are also limited to estimate the initial subsurface model, artifacts and interpretation error can be prominent. One way to ameliorate

this problem can be to ground truth the geophysical data by carrying out additional measurements in shallow boreholes at the investigation site. This is quite common in oil and gas exploration to 'tie' seismic reflections to the real geology. Using boreholes one can place sensors in borehole and a source in the other and look at 1-Way travel times for seismic waves, this technique is known as cross-borehole tomography. The technique has been used quite effectively to detect tunnels due to the simplicity of the inversion and large effect a tunnel can have on higher frequency seismic waves that can be used in such environments (Vesecky et al. 1980). The tunnel can affect the seismic response two ways. First, the seismic wave must refract or diffract around the tunnel due to the air filled cavity retarding the travel time considerably. Second, the size of the tunnel changes the incoming amplitude of the seismic waveform (Rechtien, Greenfield and Ballard 1995). Drilling boreholes to gather information in the near surface is quite expensive and in general is not physically able to be done. The main advantage of using cross-borehole tomography is due to the simplicity of inversion and the fact that you are getting ground truth results. The disadvantage is that it is impractical to have boreholes at your survey site so can only be used in certain situations.

There are multiple methods to find and detect subsurface voids and in general in all depends on the site characteristics and what equipment is available. The goal of this research project is to look at how seismic methods can be used and what are some key features in tunnel detection. For seismic refraction tomography the university has two major program licenses, Raygui (Song and ten Brink 2004), and SeisOpt Pro™, (provided by Optim Software and Data Solutions, USA). Raygui is an open source ray tracing program used for imaging refraction tomography where the user manually creates the initial velocity model. SeisOpt uses a 2-D eikonal solver for the ray tracing and starts with a homogeneous layers and continues to forward the results until the lowest RMS is calculated using a Monte Carlo method. At the University of Mississippi they use Rayfract™ (Intelligent Resources Inc.) which updates the velocity model using the residual from synthetically figured out first breaks. Along with seismic the ERT uses a program called RES2DINV (Loke 2002) to invert the calculated apparent resistivity pseudosection in the subsurface, and also has its own forward modeling software, RES2DMOD (Loke 2002). In the

end GPR was not used for the reason that the soil at the tunnel sites of interest had a large amount of conductive clay rendering ineffective the GPR signal.

Technique	Advantages	Limitations
GPR	-Fast acquisition. -Good lateral and vertical resolution. -Can resolve very small anomalies. continuous profiling	-Depth of penetration depends on local geology -Need good contact with antennas to transmit and receive signal.
Passive Seismic	-Continuous measurements.	-Expensive to set up. -Need large amount of sensors to image tunnel.
Microgravity	-Very accurate. -Interpretation can give depth, size and type of anomaly. -Can be used on any terrain.	-Slow acquisition. -Sensitive to vibrations. - Basements in urban environments need to be modeled and post processed.
EM	-Good lateral resolution. -Fast acquisition, no ground contact.	-Limited vertical resolution. -Tough to use in urban environments.
Magnetics	-Fast measurement. -Very sensitive to conductors. -Non intrusive.	-If no conductors is useless. -Sensitive to any surface conductor.
ERT	-Vertical and lateral resolution. -Simple interpretation.	-Interference from any conductor. -Not as effective in very conductive regions.
Seismic reflection/ diffraction	-Gives information of depth and composition. -Good lateral resolution	-Sensitive to acoustic noise. -Extensive processing.
Seismic Refraction	-Good lateral resolution - Can resolve multiple layers	- Sensitive to acoustic noise. -Need large spread lengths.
MASW	-Not as sensitive to acoustic noise. -Fast acquisition.	-Very Frequency dependent. -Low resolution.
Borehole Seismic	-Gives ground truth. -Very accurate. -Limited processing.	-Site needs boreholes. -Impracticable to drill at test sites.

Table 2-1 Advantages and limitations of the common geophysical techniques used to detect tunnels and near surface voids.

2.4 TUNNEL CONSTRUCTION

In general when trying to find a clandestine tunnel, the construction of the tunnel was done long before the survey can be performed. The type of construction that is used though is hugely important to detect the tunnel itself. The construction for this study can be split into two major types ``cut and cover`` (Mouratidis, Lambropoulos and Sakoumpenta 2005) or mechanical excavation. The main difference between the two methods is that for mechanical excavation you excavate the ground by boring through the rock, while cut and cover causes you to just remove the top layer of earth and place the tunnel inside dug up zone. Now for most clandestine tunnels along the US-Mexico border some sort of mechanical excavation will be used since the tunnel is trying to be built without the knowledge of the US border patrol. The Tunnel is usually built from the Mexico side in a basement where the tunnel is built in a straight line to the basement of a location on the USA side. The method of excavation requires some sort of removal of the bored rock and generally causes the stress field around the excavation site to become fractured. Because of this some sort of support or casing can be created while construction, this is known as a shield. For some cases the clandestine tunnel will be completely cased in to keep water out and is usually built after the construction of the tunnel. For a cut and cover, the surrounding material is excavated from the ground and the reinforcement cased tunnel is placed. This method is usually done for urban environments where secrecy is not an issue due to the safety and the accuracy of building the tunnel. The reason these types of tunnels may need to be found is that in situations where the clandestine tunnel may bore into a service tunnel. Geologically speaking, a cut and cover tunnel will have its native material removed and reset, while a mechanical excavated tunnel will have the same native material around it.

2. 5 SUMMARY

In near surface geophysics characterizing near surface features are generally completely dependent on the local geology. Tunnel detection is characterized as a

subsurface void which is fluid filled and is generally lined with a competent material. The detection of clandestine tunnels is very important on the security on the US-Mexico border for illegal immigration, drugs, and terrorist activity. Detection of tunnels is a major issue and has had multiple conferences and workshops. The University of Alberta and University of Mississippi worked on a mutual collaboration for detecting tunnels using near surface seismic techniques. Along with seismic techniques ERT was performed to help classify geological information. The different geophysical techniques used for void detection and the advantages and limitations of each technique can be seen in table 2.1.

CHAPTER 3
3.0 DATA ACQUISITION AND EQUIPMENT

3.1 FIELD SITES

In general a tunnel can be described as a subsurface void, which in most cases is cased with a competent material to keep dirt and water from intruding into the air filled void. Many study sites can be used as a surrogate tunnel locations to help understand the physics of the tunnel and possible acquisition parameters. The issue with most geotechnical operations is that service tunnels are in fact underneath concrete roads and are used as service tunnels in urban environments. These tunnels also don't act suitable as a surrogate site due to being filled with electrical wiring running through them. These in fact will not represent a good replacement tunnel so other avenues had to be explored. Drainage tunnels acting as culverts share similar characteristics to a real subsurface clandestine tunnel. Culverts are used as surrogate tunnel sites to perfect acquisition and processing on pseudo tunnels in order to obtain a better idea of geophysical responses expected at a real clandestine tunnel site. Consequently, in this project there were two different study sites. The first site is in Oxford, MS where multiple surveys were gathered along an abandoned railway surface where culverts have been inserted to lessen erosion on the bank of the valley. This provided a wide range of depths and dimensions for testing. The second and main site is in Douglas, Arizona where an actual clandestine tunnel was discovered in 1990 and is now property of customs and border patrol for research purposes. Details about the field notes and basic information about each individual tunnel site can be seen in Appendix A

The first study site was performed from February 1-20 2009 in Oxford, MS, where seismic and ERT surveys were performed over multiple different tunnel sites, of varying depths and compositions. The study site is several kilometers from the main town district and is now used extensively as a walkway. The reason this study site was chosen was its varying depths and compositions but also its proximity to

NCPA compound where the equipment was being stored. The goal of this site was to experiment with varying acquisition parameters to see if there are pitfalls or limitations in detecting tunnels. Multiple sources were tested to see the effects on clipping and energy at the tunnel sites. The data was collected and was processed at at a later date by both the NCPA and University of Alberta, where Dr. Craig hickey performed refraction tomography at the NCPA.

The second study site was in Douglas, AZ and was collected on September 31-August 4 2009, similar to Oxford both seismic and ERT data was collected. This site is a known clandestine tunnel discovered in 1990 where cocaine was being smuggled in from Agua Prieta, MX through the tunnel into Douglas, AZ. The tunnel itself is approximately 70m long and on average about 10m deep. The tunnel is now used for research purposes and has had multiple small boreholes dug around the tunnel for cross bole hole tomography. The true purpose at this study site is to detect that a void exists, and to detect the possible thickness and depth of the void. To do this multiple surveys were performed at this site during the week of acquisition.

3.1.1 THE UNIVERSITY OF MISSISSIPPI TEST SITE

As described earlier, the data collected at Oxford, MS was to test and validate that geophysical methods could be used for tunnel detection. The site itself is an abandoned railway track just south of the University of Mississippi campus where it is used now extensively as a walking path. The site is approximately 2km from any major highway and the only real major source of error is pedestrian traffic. The abandoned railway track has multiple drainage culverts inserted into the side of structure and were probably installed during its construction 150 years ago. There are also metal culverts that were surveyed, which were probably installed after construction to deal with other local drainage issues. Seen in Table 3-1 the various tunnels sites with its distinct physical characteristics, the GPS of each tunnel is given. Figure 3-1 the Google earth image of the plan view of the approximate location of the tunnel sites projected onto surface.

Tunnel	Tunnel Casing	Depth (m)	Size (m)	Latitude (N)	Longitude (W)
Tunnel 1	Sandstone Block	9.0-10.0	1.5x1	34°20'11.04"N	89°33'34.14"W
Tunnel 2	Metal Pipe	5.5-6.0	1.25	34°20'42.06"N	89°32'58.80"W
Tunnel 3	Cast Iron Pipe	4.0	0.5	34°20'45.54"N	89°32'56.52"W
Tunnel 4	Sandstone Block	5.5	0.5x1	34°19'47.52"N	89°33'58.32"W
Tunnel 5	Small Concrete Pipe	2.0-2.5	0.75	34°20'3.00"N	89°33'48.12"W
Tunnel 6	Concrete Blocks	6.0	0.6x1	34°19'30.54"N	89°34'12.48"W
Tunnel 7	Concrete Pipe	1.5-2.0	0.5	34°20'18.96"N	89°33'19.68"W
Tunnel 8	Sandstone Block	5.5	0.9x0.9	34°19'29.19"N	89°34'14.64"W
Dam	Concrete pipe	4.0-6.0	0.6	34°21'5.45"N	89°33'21.96"W

Table 3-1 Basic tunnel properties for the surveys done at the University of Mississippi test site

The tunnels all varied in depth and size but in general the layout for most of the sites was similar. The acquisition had a similar layout at each test site due to the railway track only being 5-6m wide causing all survey sites to be surveyed perpendicular to the tunnel location. Most test sites here have similar subsurface structure and native material due to the closeness of each survey, all except the dam site. Looking at figure 3-1 there is the Google map image of the tunnel sites, as you can see the tunnel sites are quite far from most major roads, and in general most land near the sites is farm land. Due to the nature of the tunnel sites only using a hand held GPS was used to locate the tunnel sites, this was due to the dense tree coverage limiting access with the GPS. The general terrain showed very little change

in elevation so static corrections would not be needed in processing so handheld GPS data was sufficient.

Figure 3-1 Google earth image © 2011 Google of the plan view of the tunnel sites located in Oxford, MS. the university is north of highway 6.

The subsurface view of the each tunnel site varies slightly, but in general all tunnels followed a similar construction. In general the layout of a deeper tunnel can be seen in figure 3-2 where the subsurface view of the tunnel and an example surrogate tunnel can be seen. The figure shows what the tunnel looks like and the casing material of the tunnel, this is one of the original tunnels that were built during the construction of the railway. Most of the tunnel sites are similar to what is shown in figure 3-2 except the dam site. The dam site is made of mostly clay and silt and was still quite moist when the survey was performed. As seen in figure 3-2 most tunnels are completely air filled and very few were saturated in water.

A)

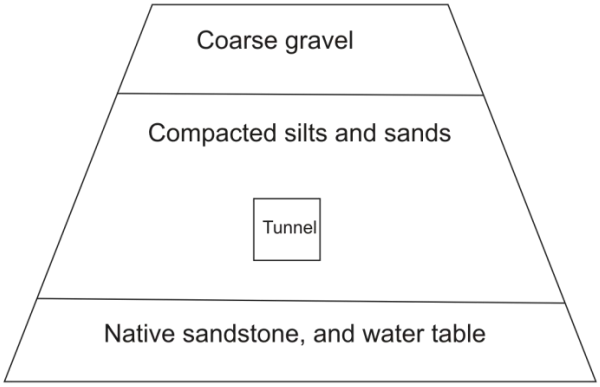

B)

Figure 3-2 A) this is the subsurface view for the general railway site. The tunnel casing changes on a site per site bases. B) This is a picture of the tunnel 1 in Oxford, MS can see a sandstone blocks as casing along with a geode spread through the tunnel.

3.1.2 DOUGLAS ARIZONA TEST SITE.

This test site is a known as a clandestine tunnel which goes from the across the US-Mexico border, the tunnel site is under the control of customs and border patrol (CBP). The purpose of this test facility is for research for the detection of tunnels. The tunnel itself is concrete lined and about 70m long coming from a basement on the Mexico side and to a warehouse in Douglas, AZ. The tunnel on average is around 5-10m deep and is generally filled with water unless it is pumped out. The site was drained prior to the acquisition. The geophysical surveys were performed on August 31-September 5, 2009 and were focused at this tunnel site. To

do this two different locations for both ERT and seismic were surveyed and will be referred to as the ditch data and the roadside data. The ditch data, as implied, is about 4m shallower to the tunnel in a ditch, while the roadside is along the road by the warehouse on the Douglas, AZ side.

These were the only two viable options for putting out over a 50m spread the tunnel site. Figure 3-3 displays the site layout for the Douglas, AZ, what can seen is the layout for both seismic and ERT surveys. Unlike the Oxford, MS test site there is a lot more surface heterogeneity and local culture interfering with the layouts. The ERT had both Wenner and dipole-dipole arrays surveyed while the seismic had multiple surveys using different sets of geophones. The roadside data also had a metal fence and road running nearby adding to noise to both surveys. The ditch data was comprised of unconsolidated loose sands making good contact with the surface difficult. The ditch itself was dug out to be used to slow down illegal immigration, and was in the process of being lined with concrete during the time of acquisition. Along the roadside there were also multiple boreholes which specially constructed for cross hole tomography. One of the surveys had 3 component geophones on the surface complemented with a gimbaled 3-C geophone package placed at the bottom of the borehole. Data was then simultaneously collected on the surface doing a refraction survey while this was giving a walkway VSP data at one common depth point.

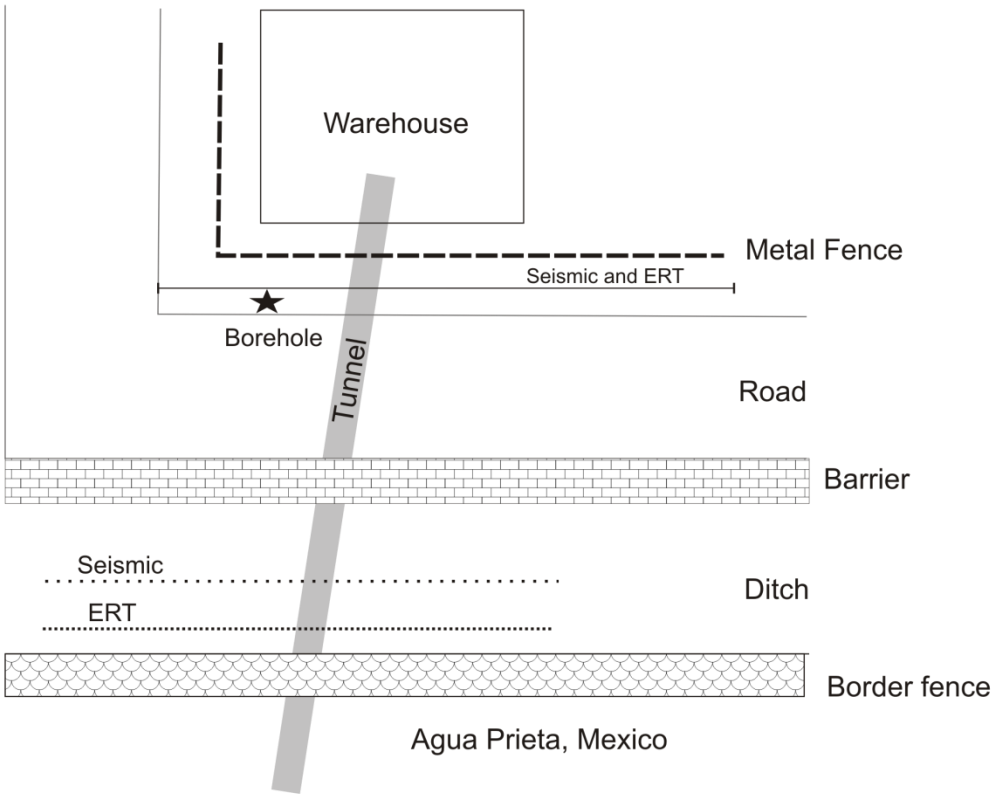

Figure 3-3 the figure above is the plan view of the Douglas, AZ test site. The tunnel itself varies from 8-10m depth along the road but changes to only 4-6 m deep in the ditch. The border fence is approximately 10m high and made of closely spaced steel square tubing.

The tunnel stretches from a warehouse on the Douglas, AZ side to a villa on the Mexico side. The tunnel is reinforced by a few cm of concrete and has electrical wiring with a ventilation system in place. In its heyday, the tunnel was operated from the Mexico side where the tunnels entrance +was disguised with a a hydraulic lift floor. The tunnel had evidence of dolly tracks to indicate some sort of tram being used for transportation of contraband though the tunnel. Because the tunnel depth is below the water table, the water was pumped out before acquisition. The tunnel itself is rectangular and approximately 1m tall and about 75cm wide. Due to the safety hazards associated with entering the tunnel no one was allowed to enter it and hence no sensors could be placed inside nor any photographs obtained. Looking at the ditch side wall there was loosely consolidated soils for first 2 meters of the

roadside data, and then laminations are evident on the bedrock showing more competent material near the location of the ditch surface.

3.2 FIELD EQUIPMENT

The geophysics department at the University of Alberta has an array of geophysical equipment used for near surface and monitoring studies. The grant proposal for this project was submitted by Dr. Craig Hickey where the University of Alberta was subcontracted out for equipment and near surface expertise. The joint cooperation was to use near surface seismic tomography and reflection profiling to detect tunnels. Since the UofA has other types of geophysical equipment additional techniques were used and tested to see which might benefit the study. In particular electrical resistivity tomography (ERT) was carried out due to its previous success in detecting subsurface voids (van Schoor 2002), (Griffiths and Barker 1993), (Kruse et al. 2006). Other techniques such as ground penetrating radar (GPR) have been used to detect tunnels (Benson 1995) but this was not attempted for various logistical and geophysical reasons. In the end only seismic and electrical methods were surveyed. For accurate locations, a differential GPS was employed at the Douglas, AZ test site.

3.2.1 SEISMIC EQUIPMENT

The seismic system used employs 'planted' geophone sensors on the surface to measure the ground displacement. During a measurement, the geophones transducer the ground surface particle velocity into an analog voltage signal to a digital converter which is then transferred to a computer using an ethernet cable. The geophones are activated by any acoustic or elastic wave energy that will displace the earth's surface; a source of elastic wave energy is required to provide a coherent signal for reception. This seismic energy travels through the earth and the time it takes to travel from the source to the sensor can be used to calculate the velocity of the subsurface. The University of Alberta achieves this by using a Geode™ (Geometrics Ltd., Santa Clara, CA) system which digitizes the geophone signal for

storage on a laptop directly. These data will be discussed in detail later. The seismic source generally consists of using a hammer or accelerated weight drop in these studies.

3.2.1.1 Sensors and Digitizer

A variety of geophone sensors were used for these studies site but in general the most common type was the GS-20DM 40Hz OYO and the GS-20M 14Hz OYO geophones (OYO Corp., USA). These are similar geophones with the difference being bandwidth of the frequencies the geophones can record. The 14Hz geophones will not record good signal below 14Hz and the 40Hz geophones will not record good signal below 40Hz. In general if you are in a region of high traffic noise then using a higher frequency geophone to limit the low frequency surface wave energy contaminating the site. In the Oxford, MS other 10Hz geophones were used at the end of the line during one of the surveys and this generally showed more surface wave energy.

The only different type of sensor used was the 3-C geophone which is a three component sensor which has different orientation to record energy coming from different directions. This geophone is encased in a plastic tube with a hydrometer attached to it and is used extensively for borehole studies. This was used in Douglas, AZ and was just placed at the bottom of the well, the orientation was not important since only travel time were used from this data.

The geophones are then connected to a takeout cable which can transfer the analog signal to be recorded to a digitizer. Each Geode records up to 24 geophones per box. A yellow Geode box can be seen in figure 3-2 which shows the etherent and trigger cable attached to it. The geode then is connected to an etherent cable which is then transferred to a computer where the information can be displayed. Multiple geodes can be used simultaneously for larger surveys. The geode options are controlled by a program called Seismic module controller where the data is stored. The Geode can handle one shot gather location at a time where stacking of the data can be done in field or after. The information is stored in SEG-2 format and can be directly transferred to most seismic processing programs. The program also uses a

real time noise monitoring so bad geophones or remnant acoustic energy can be seen. This is very useful on surveys in urban environments and high traffic areas.

3.2.1.2 Source

The source in seismic surveys can vary quite a bit but in general every source can be described by three types.

1) Force in the vertical direction
2) Force in the horizontal direction
3) Explosive force (i.e. in all directions)

These three types of forces indicate what type of energy you want forced into the ground. In general you want to use energy in the vertical direction for studies where you are looking at the P-wave velocities and use horizontal directional force for S-wave studies. Explosive forces direct energy in all directions and are the most common type of geophysical source in seismic studies. For the Oxford data site two types of surveys were performed, a manually hefted 5kg sledge hammer, and an accelerated weight drop.

The hammer system involves using a metal plate or strike pad and a hammer connected to some sort of trigger. The trigger is attached to the Geode and in this case a motion sensor trigger was used. When the hammer is swung towards the plate the Geode starts recording at a specified delay time before the impact happens. This is done to minimize data transfer and post field processing.

The accelerated weight drop runs off a similar system but instead of swinging a hammer now the hammer is forced down by the additional energy of a 2m long industrial elastic band. This system is attached to the hitch of a truck where the engine sits in the truck bed. To minimize noise the engine is placed on an inner tube to reduce vibration noise. This is operated by a hydraulic lift ran by a 5 hp Honda engine, which lifts the 90.7kg steel 'hammer' and tightens the elastic band. For additional force the band can be tighten around more turns to create higher elastic potential energy to give more force. Instead of a motion sensor triggera contact trigger was used. The strike pad has an electrical wire attached to it and the

weight drop has a wire attached to hit. When the two meet an electrical circuit is closed, the Geode senses this closure and commences digitization. In general the source used depends on spread length and accessibility, in Douglas, AZ only hammer seismic was done, the hammer can be seen in action and the accelerated weight drop in figure 3-4.

3.2.2 ELECTRICAL RESISTIVITY EQUIPMENT

DC electrical resistivity data was collected along similar or the same lines as the seismic data. The electrical system used was a Scintrex Ltd. (Toronto, CA) automated resistivity imaging system (SARIS™). The electrical system uses stainless steel electrodes, a smart cable and the SARIS recoding/activation module. The electrodes are attached to the smart cable using alligator clips which is connected to the SARIS unit. Each smart cable can handle up to 25 electrodes and the UofA has 2 cables. Both imaging and sounding surveys can be surveyed, but for this survey only imaging surveys were imaged. The two smart cables are attached to the SARIS unit which acts as the switchboard for the electrodes and also the computer to record the data. By changing the current potential electrode spacing you can obtain differing depths of penetration in the subsurface. However, the deeper the survey the greater the offsets required and hence the larger the electrical current must be. The system runs off of 24V battery power obtained usually from two car batteries in series to supplement the system's smaller internal battery. The system can handle up to 100 Watts and 1A of current. Different electrical arrays can be uploaded and to the system but most common array types are already on it. Wenner and dipole-dipole arrays were surveyed on most tunnel sites, not all locations were surveyed due to time constraints.

3.2.3 GPS

For the Oxford, MS test site only a handheld GPS was used since there were only very slight variations in terrain and the location of the surveys. For the Douglas, AZ test site a Trimble differential GPS was used to accurately determine where the

surveys were performed. The Trimble GPS system involves a base rover attached to a tripod which has a set elevation over a control point. Then the system is initialized over this control point and has real time data upload with the receiver unit. The mobile rover is attached to a 2m metal pole and used to get differential GPS from the base point. The control point in Douglas, AZ used was a borehole cover since accurate GPS data was known at this point. The data is collected and then can be post processed in for exact locations if the control points are given. The differential GPS should still have accuracy of about 1-3cm while the handheld GPS should be around 1-2m

A)

B)

Figure 3-4 A) Swinging the hammer along tunnel 6 in Oxford, MS, the resistivity can be seen on the right hand side of the walkway. The shotpoint locations are taken in-between each geophone. B) This is the accelerated weight drop; straps keep the weight drop vertical while in the hitch. The strike pad can be seen dragging along underneath the truck.

3.3 OVERVIEW

The two major test sites for this study came from Douglas, AZ and Oxford, MS. The Oxford, MS test site was used to test acquisition parameters and to understand some limitations seen in the field after processing the data. The Douglas, AZ test site was a location of a known clandestine tunnel and information gathered from Oxford, MS made it possible to get very good and accurate data. The large amount of data that was collected was used to see some limitations and advantages of using seismic and electrical methods to find subsurface voids. The equipment was from the University of Alberta and the surveys were performed as a collaboration with theUniversity of Alberta and University of Mississippi.

CHAPTER 4
SYNTHETIC MODELING

4.1 INTRODUCTION

It is prudent to carry out some sensitivity testing for the responses that may be encountered prior to carrying out field tests. Here, modeling of both seismic and electrical responses of hypothetical voids was carried out to see how these responses were changed and to assist in finding clues to the interpretation of real (complex) data. Seismic modeling was accomplished using the program FDVEPS_MPI while electrical modeling used RES2SMOD™. The seismic modeling is a parallel 2-D viscoelastic finite difference seismic modeling program (FDVEPS). Seismic modeling uses numerical computation to predict the seismic wavefields based off an initial model, imaging how the waves are affected by subsurface features. To model the subsurface resistivity the program used was RES2DMOD which is a finite difference or finite element forward modeling program. Which estimates the apparent resistivity map, called the pseudosection, from a given model grid constructed by the resistivity structure of the subsurface. The expected section can give details about which type of resistivity array should be used in the field and how the anomaly may look in real data. The synthetic modeling results will be shown to show what was estimated before the real surveys were performed.

The goal of using synthetic modeling programs in geoelectrical studies is to best define the most efficient array to interpret the geology of the subsurface. RES2DMOD™ is a forward modeling program used to test this using a finite difference/ finite element technique which will estimate the apparent resistivity of the subsurface given a user defined model. The estimated model is based off known resistivity values of what is expected to be seen in the subsurface based off previous studies or rock physics models. In the near surface the 2D model will consist of sedimentary rock containing an air filled cavity. Differing observational electrode arrays applied such as Wenner and dipole-dipole will be applied to show what affect

the air filled cavity will have on their responses. The array types are based on the work of (Edwards 1977) who describes some of the practical uses of multiple types of arrays. The results will then be used as a guideline for the acquisition of the field sites and resolve what type of survey spread is needed and surveys may best work. The criteria that is used for this study is; the depth of investigation, resolution and practicality. For more details about the theory of electrical methods can be found in Chapter 5

4.2 ELECTRICAL METHODS

The goal of modeling is to look at the theoretical electrical response of a clandestine tunnel at the approximate depth which would be see at the Douglas, AZ test site. The model incorporates values of resistivity and seismic compressional velocities obtained from the literature as found experimentally in laboratory and field measurements, this is given in Table 4-1. The same table also has the velocity values which are used for seismic modeling later in the chapter. The goal of the synthetic measurements was to see how the resistivity values in the subsurface change. An initial model is built to be representative of the underground tunnel and the surrounding material. After this then a detailed description of the forward modeling program operations will be given. The theory can be seen in detail in (Loke 2002). Once the initial model and theory have been described then the inversion results of the models will be interpreted with some of the conclusions used for acquisition. This modeling was done before the field measurements at the Oxford, MS test sites.

Material	**Resistivity (Ω.m)**	**Seismic Velocity (m/s)**
Sandstone	50-1000	1450-1650
Shale's	5-100	2200-4000
Conglomerates	1000-10000	2000-6000
Fresh Water	5-100	1480
Brine	0.25-1	1530
Sands (Unconsolidated)	600-10000	500-1000
Soil	5-25	180-450
Near surface rocks (average)	10-100	500-2000

Table 4-1: This is a table of basic rock resistivity's and velocities. The resistivity's are after (Palacky 1987) and the seismic velocities are (Marion et al. 1992).

4.2.1 INITIAL MODEL

Using hypothetical geological models allows for a basic understanding of the technology that is being applied and how this may be best used to limit poor aqusiition. The goal in the electrical modeling here was to assess what was the preferred geometry of the electrode array and to see what the limitations of the method would be. To do this multiple models were created using RES2DMOD a program used to first construct the 2D initial model, and from this forward model the apparent resistivity pseudosection from a given initial model. The different array geometries used can be tailored to detect different types of features in the subsurface. The applications and pitfalls of the different arrays used are discussed in detail by (Loke 2002).

Here, apparent resistivity pseudosections were calculated for both the Wenner figure 4-2 and the dipole-dipole arrays figure 4-2, and the reader is referred to Chapter 5 for more of the details on these.

In geophysical studies, every tunnel site is different; and unique difficulties with near surface heterogeneity will be encountered. However, in these models a homogeneous near surface was used in order to maximize the geophysical response of the tunnel itself and not confuse this with additional effects introduced by the heterogeneity of the earth. On the basis of experience, a value for the near surface of 25Ω.m is representative of simple sandstone rock. Further, it was assumed that the subsurface was fully water saturated in order to eliminate any vertical resistivity gradients. One complication was the air filled void space that in reality would have for practical purposes an infinite resistivity. However the modeling program does not allow for such numbers and a high unique value for air of 100000 Ω.m was used. A metal casing was also used in some of the modeling tests but the effects of high conductivity casings were otherwise ignored. The tests of high conductivity casing showed a low resistivity anomaly zone that was exaggerated in location and depth but was conclusive in detecting the anomaly. The test when applying a 0.5m cement casing of 100Ω.m was used and saw little to no difference compared to when just a 2x2m air filled void.

Effects of what casing can do to your resistivity data will be seen in chapter 5. The air filled cavity itself is 2x2m square block at 5.5m deep. The electrode spacing of 1m was used with 50m spread length, this value was used do to the inversion giving results of up to about 10m depth. The void was centered in the middle of the spread for these models, this was to ignore any edge effects seen in the modeling.

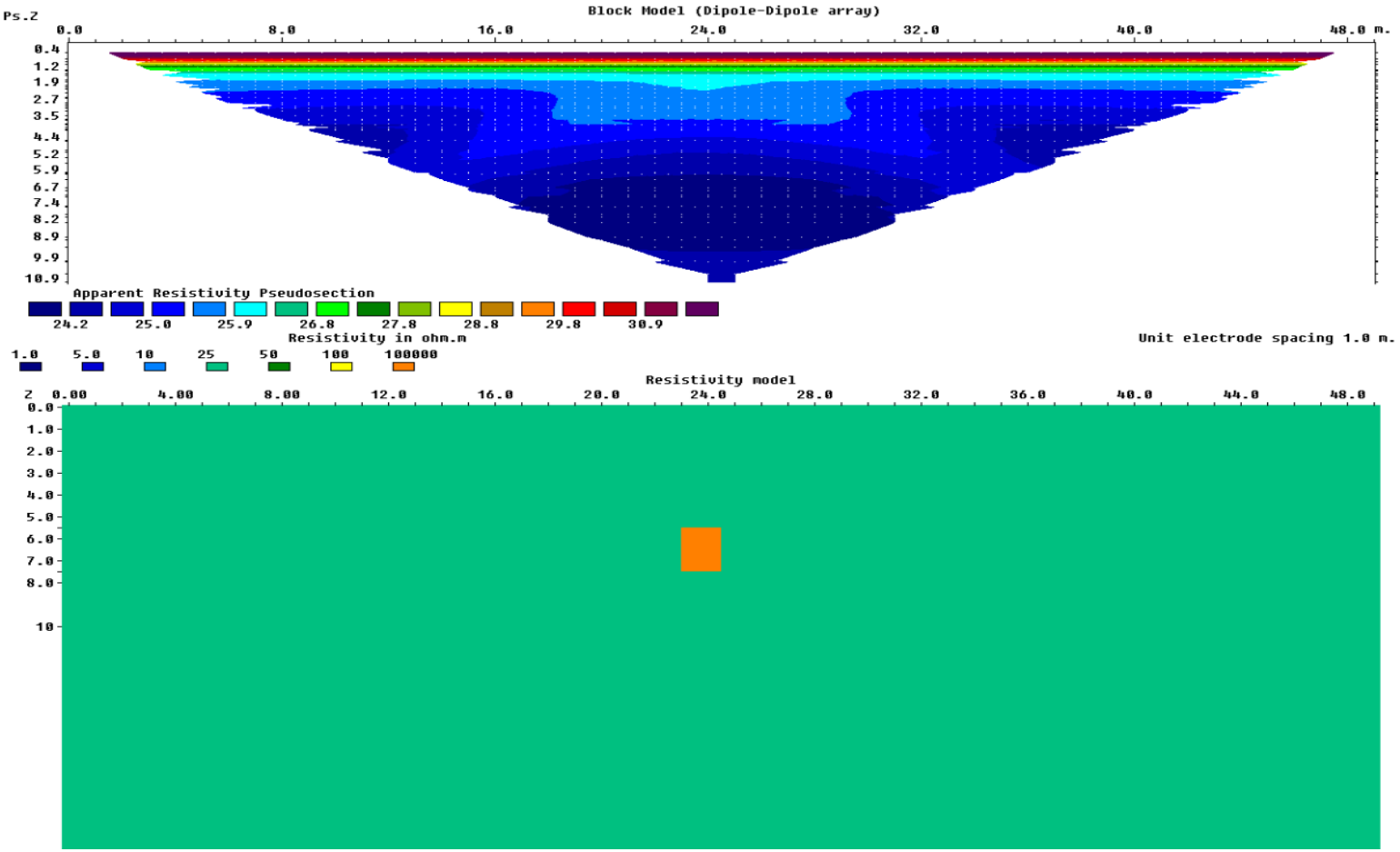

Figure 4-1 The initial model for an air filled void with homogeneous subsurface using a dipole-dipole array. Top; this is the apparent resistivity pseudosection created from the model. Bottom: this is the initial model where there is a a homogeneous subsurface at 25Ω.m and the air filled cavity of 100000Ω.m

.

Once the initial model was built in RES2DMOD the initial model is used as the inverse true apparent resistivity pseudosection, so basically what the desired result is. The program then forward models the electrical response using a finite element technique described by (Silvester and Ferrari 1990), which segments the resistivity structure into trapezoid blocks. The number of blocks controls the resolution applied and this depends on the mesh size; and for all resistivity. For the finer mesh a 0.25m block size was used in the horizontal direction. The vertical direction starts with 0.25m spacing and increases gradually every layer up to 2m at the bottom of the initial model. There is a maximum of 16 layers in the model and the highest sensitivity is near the surface. The model resolution can be seen in figure 4-5 which displays where the highest resolution for a given array. This follows what is seen in a resistivity array for real data, where there is more data in the near surface and has less and less data at deeper depths. Overall, there were 16 layers in the vertical direction where the last layer has a mesh size equal to 2m. Using finite element methods increases the compute time but the inversions are still completed in less than 1 minute. The initial model then fits the resistivity value into each trapezoid block and is placed in a measured apparent resistivity model section. This model resembles a given field data once put into a pseudosection. The first geometry used was the dipole-dipole array, this can be seen in figure 4-1, the model consists of just a homogeneous layer (light green) and an air filled void (orange) in the middle. A small resistivity change can be seen in figure 4-1 around the location of the tunnel but it's only on the order of a few Ωm above the void near the surface. The array is seeing a slight perturbation due to the anomaly but it is doubtful this could be detected in a real situation when noise is included.

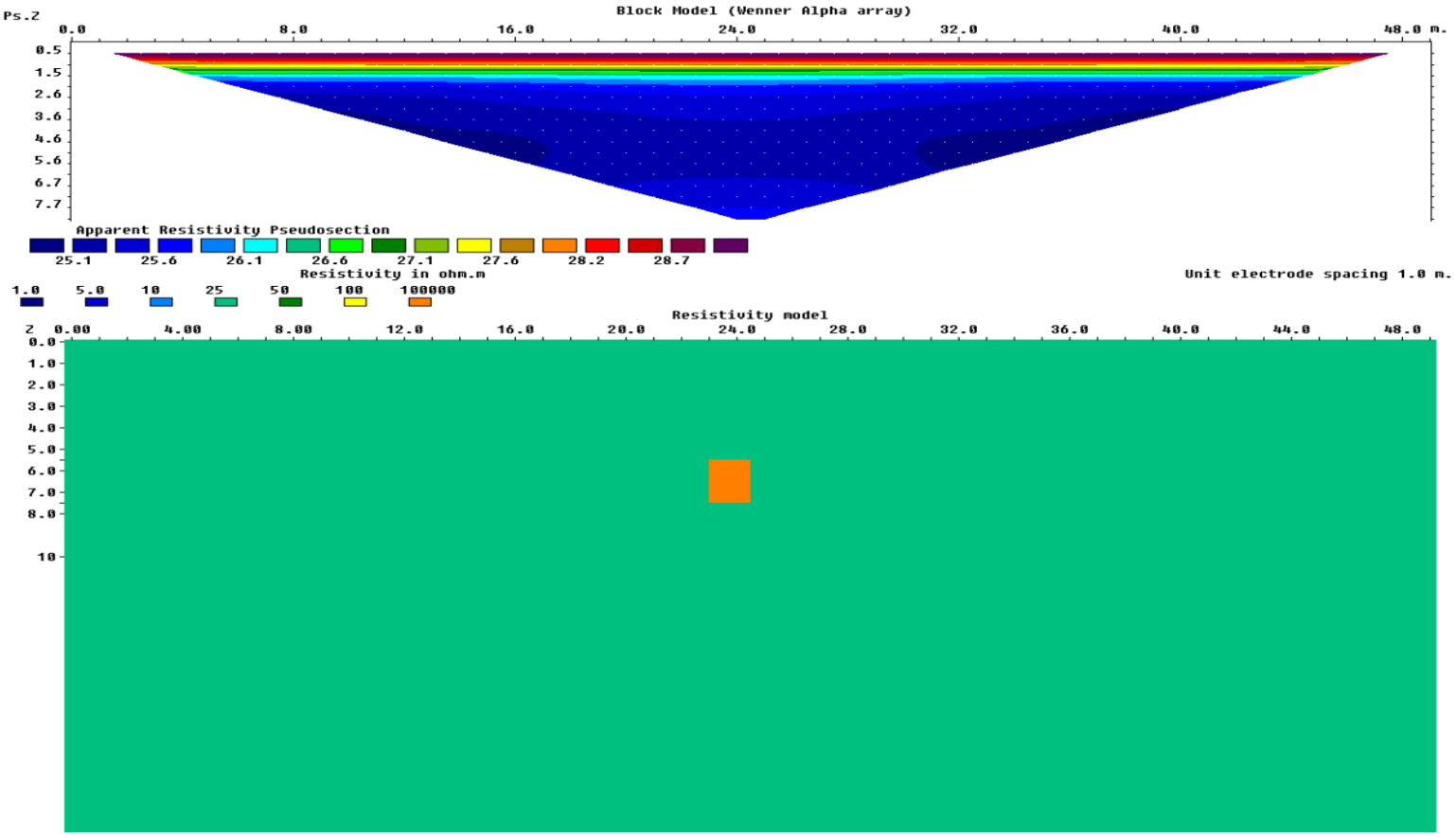

Figure 4-2 The initial model for a air filled void with homogeneous subsurface for the Wenner array. Top; this is the apparent resistivity pseudosection created from the mode. Bottom: this is the initial model where there is a homogeneous subsurface of 25Ω.m and the air filled cavity of 100000Ω.m.

The next model that was modeled was the Wenner array seen in figure 4-2; this is the same model parameters as the dipole-dipole array just different array geometry. The Wenner array is sensitive to vertical changes of resistivity in the ground. More information about electrical methods will be discussed in the next chapter but for now can just look at the relative affects of the tunnel. The main difference is that the apparent resistivity anomaly is even smoother. The anomaly is resolved even less then the dipole-dipole array and has resistivity greater than 25 around the surface, also a slightly higher resistivity diffuse through most the apparent resistivity pseudosection. The interpretation is that the due to the large resistivity contrast and the small size, the forward modeling causes a large area to have a relatively higher resistivity but not image the tunnel. Once the initial models are in the calculated resistivity form it can be used as the initial data set for the inversion to invert the model.

4.2.2 MODELS

The initial models are forward modeled to obtain the apparent resistivity section and then these are used for the inversion program known as RES2DINV. The program and how it works will be discussed in the next chapter about the electrical methods. The inversion works by modeling a calculated resistivity section and comparing it to the input data that inverts the residual between the models to update the inverse resistivity modeled section. If the inversion process was perfect, the final section should reproduce the initial model that was created. The inversion that was used was a finite element inversion using a fine mesh for largest horizontal resolution. The data when imported into RES2DINV had 1% Gaussian noise added to give it a somewhat practical data set.

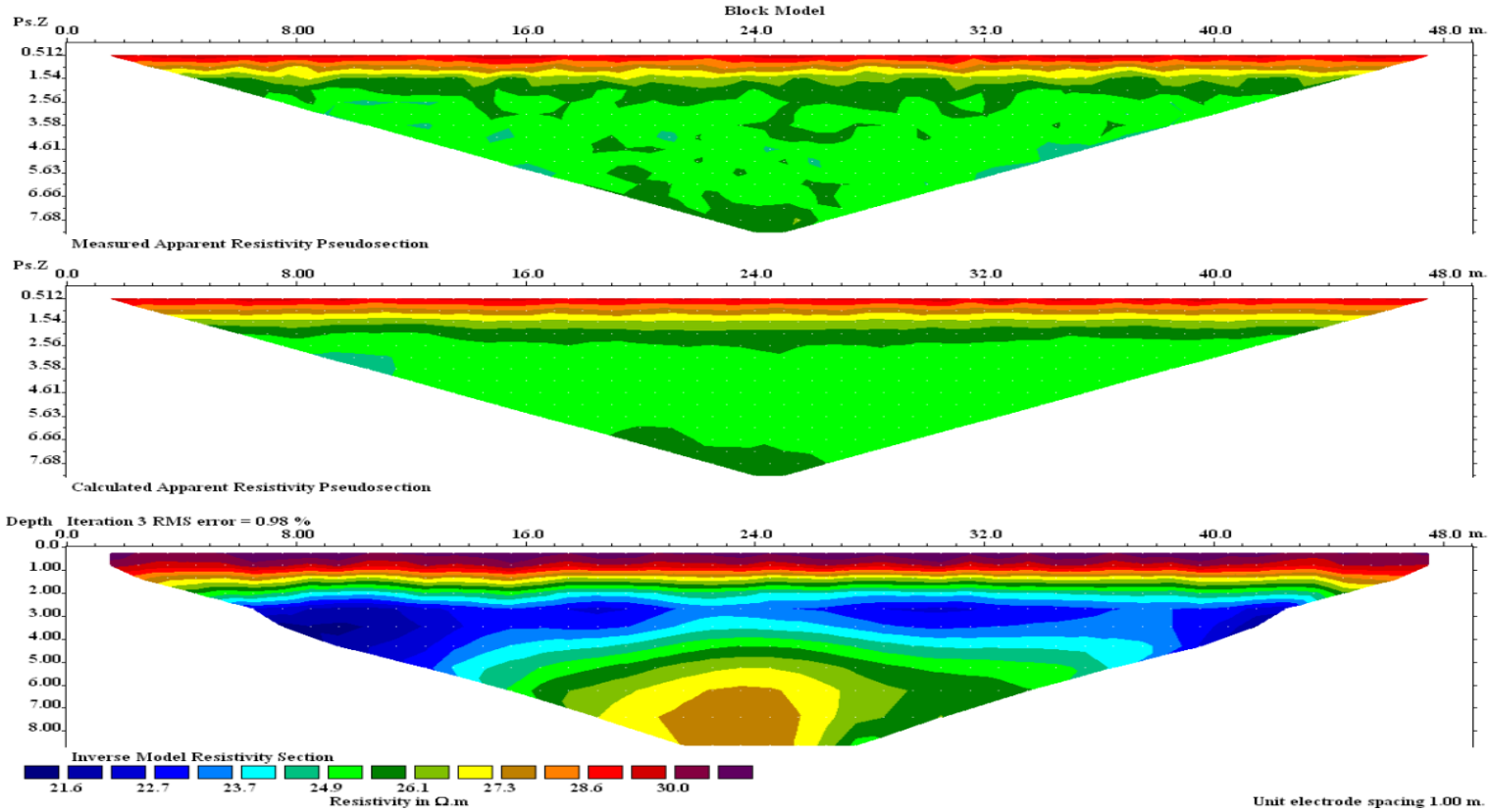

Figure 4-3 The Wenner array using the air filled void initial model with 392 data points. Top: This is the measured apparent resistivity pseudosection, there is 1% noise added to this. Middle: This is the calculated apparent resistivity pseudosection; this is the forward modeled result of the top picture for use of inversion. Bottom: This is the Inverse model resistivity section; this is the inverted result showing different layers of resistivity but no clear indication of the tunnel

The 1% noise added was found to be as much as the inversion could tolerate because the anomaly is so small that corresponding larger amounts of noise would overwhelm the response of the tunnel. Looking at figure 4-3 there is the Wenner array inverted section, since the Wenner array is very good at resolving vertical changes in the subsurface it treats the tunnel anomaly as a smeared layer. As such, the inversion of the Wenner array results in a layer like appearance with a conductive upper layer (blue) and a more resistively layer (yellow-brown) at the approximate location of the tunnel. The contrasts of the layers here are less than 5 Ωm. The inverted results come up with a 3 layer model but does not show any horizontal features resembling a tunnel. The model ended up converging after 3 iterations with only a 0.98% RMS error.

The dipole-dipole array forward modeled apparent resistivity plot is shown in figure 4-4 for the same case with the same 1% Gaussian noise added to it. The inverted section shows a localized zone with a ~ 7 Ω•m higher resistivity at the tunnel location. As seen with the Wenner array the inversion of the dipole-dipole geometry underestimates the resistivity of homogenous rock and the air filled void. The response of the tunnel itself also smoothed out over a larger region, and thus expands the general location of the tunnel anomaly. The reason the dipole-dipole data set looks so much noisier is that due to its survey design it obtains about 4-5 times the number of data points relative to the Wenner array.

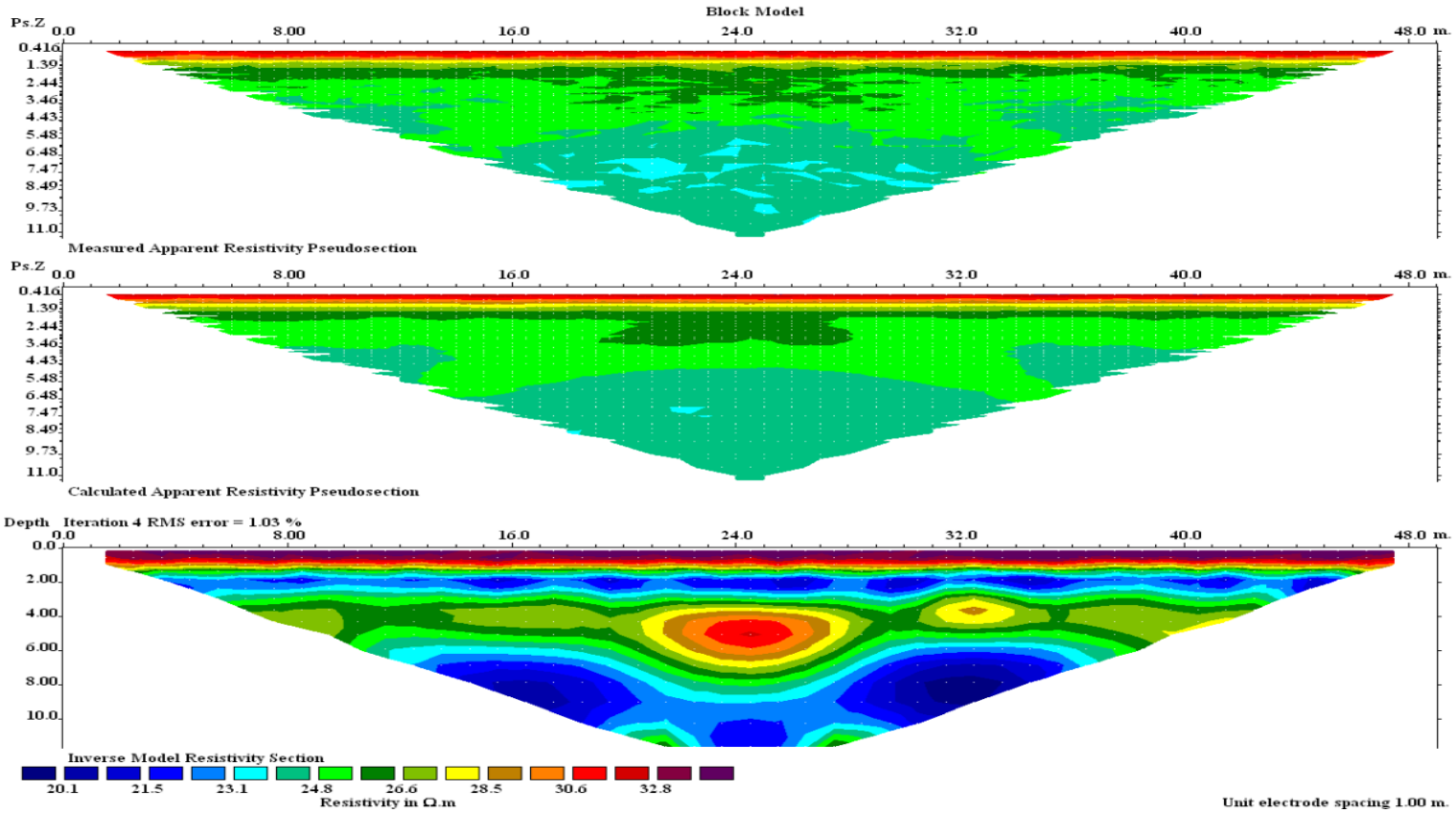

Figure 4-4 The dipole-dipole array using the air filled void initial model, there is 1594 data points. Top: This is the measured apparent resistivity pseudosection, there is 1% noise added to this. Middle: This is the calculated apparent resistivity pseudosection. Bottom: This is the Inverse model resistivity section, this is the inverted result, the result is showing that the anomaly is a hot spot of around 32Ω.m

.

4.2.3 RESOLUTION

The electrical resistivity array gives a continuous spectrum of apparent resistivity's through subsurface. The actual depth of penetration and the resolution of the array depends on the electrode spread length and electrode spacing respectively. In general the depth of penetration is approximately 1/4th the array spread length. A qualitative estimate for the depth of penetration can be imaged using a sensitivity function which is the Frechet derivative of the array (Edwards 1977, Loke 2002). The sensitivity function is calculated by measuring the change of potential at the surface as it goes though small horizontal layers. The sensitivity is calculated for the entire subsurface and then can be plotted as a pseudosection to give sensitivity map imaging the model resolution. The sensitivity of the Wenner and the dipole-dipole array can be seen in figure 4-5. What is seen for both models is that the highest resolution is near the surface but around the tunnel they act differently. The sensitivity function is normalized so the larger the value the larger the effect to influence the resistivity value of that model block. This is the reason why there is a smooth result and not a perfect inverted section (Loke 2002).Both Wenner and dipole-dipole arrays have the tunnel having little influence on the model. The dipole-dipole array does have stronger influence around the tunnel though possibly being why the dipole-dipole array images the tunnel anomaly slightly better.

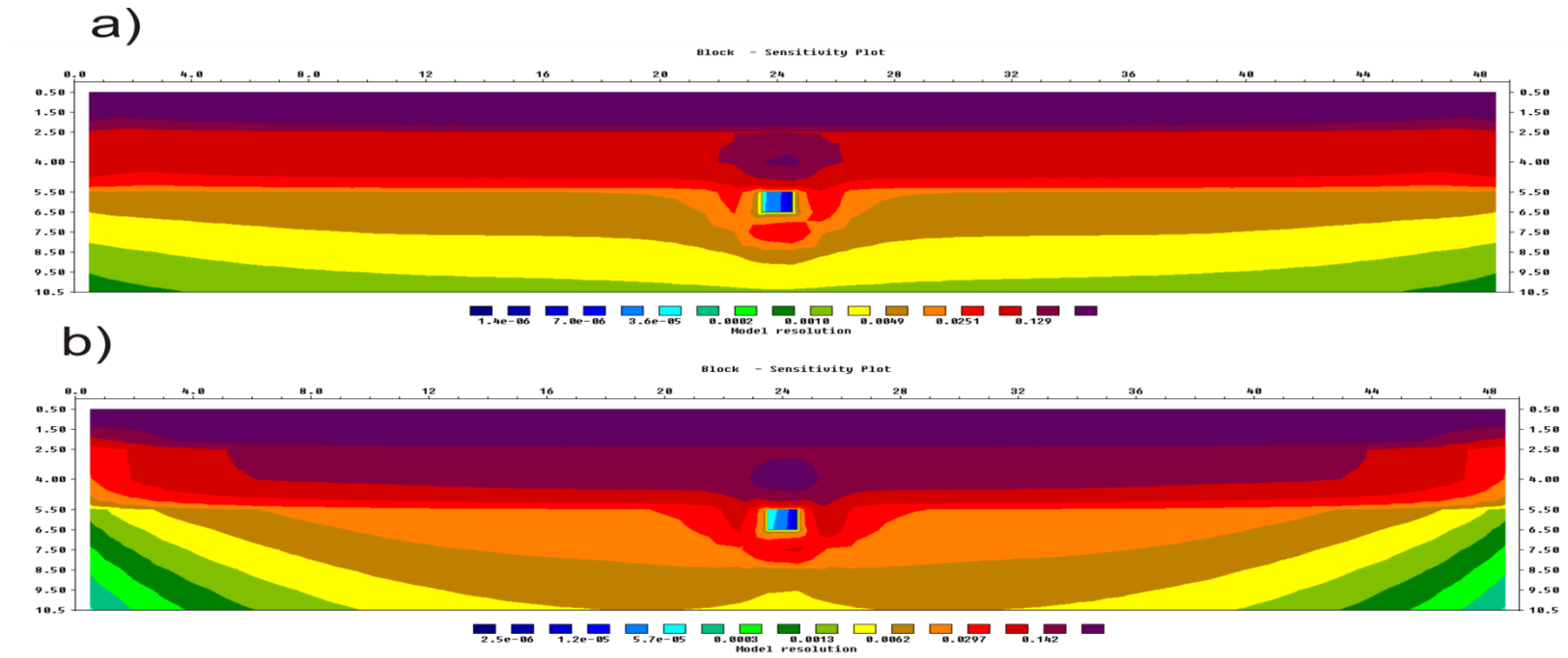

Figure 4. Sensitivity plot of the initial model displaying where the pseudosection has the highest model resolution. The darker the color the greater the model resolution with a) the Wenner array, highest resolution above the tunnel location b) is the dipole-dipole array sensitivity plot highest resolution around the tunnel and near the surface..

4.2.4 DISCUSSION

The use of synthetic modeling helps decide what type of electrical array should be used in the field, by looking at the practicality, cost, and depth of investigation. The models that were chosen to be used for modeling were the dipole-dipole array; which is sensitive to horizontal changes in the subsurface, and Wenner array; which is sensitive to vertical changes in the subsurface. The goal was to see how these models could be used what the limitations of each in regards to the detection of tunnels.

The Wenner array smoothed the tunnel resistivity laterally across the entire spread and could not properly detect the tunnel. This Wenner inversion is quickly computed. Although the Wenner array was not successful in detecting the tunnel when it perpendicularly crosses the array profile, could be a useful in cases where the tunnel may run at a small angle or parallel in detection.

The dipole-dipole array was also tested. What was found is that inversion of the dipole-dipole array does allow for detection of an anomaly coincident with the tunnel but it cannot 'resolve' the tunnel dimensions. Instead, the tunnel's high resistivity is smeared over a large area. A small disadvantage of the dipole-dipole geometry is that more data point are obtained and this requires an increase in computational time over the Wenner array buy about a factor of 10. In practical terms, however, this is still at most a few minutes of time on a ca. 2005 computer.

The results of the modeling indicated that the dipole-dipole geometry should be used in preference to the Wenner array. A decision was also made that if the tunnel was sufficiently small the electrode spacing would be reduced to enhance the lateral resolution (but at the cost of the overall coverage). The rule of thumb obtained from the experiences here was that for reasonably conductive (50 Ω.m) the depth of penetration is about 1/5 of the surface spread length. This means, for example, that the 50 electrode spread at a 1 m electrode spacing would reasonably sense to 10m depth.

Overall, this modeling study suggests that tunnels can be detected using ERT techniques, but their small size does not allow for their true resolution. Practitioners would instead look for anomalously high (for air filled voids) 'bulls-eye' type resistivity anomalies.

4.3 SEISMIC MODELING

The goal in modeling of the seismic response differs slightly from that for the ERT. The goal in the electrical modeling was to assess whether the tunnel could be detected at all, and if so, what technique would be most appropriate. In the seismic studies, the tunnel dimensions will be smaller than or on the same order as the interrogating seismic wavelengths; and hence before we start we realize the tunnel cannot be directly imaged. Instead, the goal is to determine the degree to which the wavefield will be disturbed and how this disruption might be used in tunnel detection.

How different seismic waves are affected by a subsurface tunnel will be investigate in detail in this chapter. A discussion of the theory of the different seismic waves will be discussed in more detail later in chapter 6. The finite difference algorithm used is FDVEPS which is a parallel 2-D elastic/ viscoelastic finite difference seismic modeling algorithm freely available to the academic community (Bohlen 2002). Below, in advance of presenting the modeling itself, a brief and basic introduction to the theory of finite difference calculations will be made. This will be followed by a description of the model and what was involved. Following this some examples of the modeling will be shown to see the effects of the tunnel on the seismic wave field.

THEORY 4.3.1

Finite difference modeling is in principle a method to give an analytical solution of the wave equation for an elastic wave. The reason forward modeling is

used is to understand the effects of complex media in the subsurface. The goal is to see if modeling the wavefield through a tunnel location causes a distortion in the seismic wave field. To do this some theory will be discussed about the method and some understanding of the parameters and why they were chosen for the modeling.

Finite difference (FD) calculations have been widely used to model wave propagation in the subsurface in both 2-D and 3-D elastic medium. Finite difference methods are popular because researchers are able to construct complex heterogeneous subsurface geological structures in terms of their seismic velocity and density. FD methods have been used to model complex tunnels to assist their construction (Jetschny, Bohlen and De Nil 2010) to determine what their effects on the seismic wavefield as measured at the surface might be (Kneib and Leykam 2004). The FD method used here is referred to as a 'formulated fourth-ordered staggered grid finite difference system' (Levander 1988, Virieux 1986) based on first-order coupled elastic equations using the seismic velocities and stresses as variables. Using finite difference to solve for stresses and velocities were developed to calculate synthetic seismograms for 2D elastic geometries; and as a result they cannot incorporate seismic anelasticity. This was later developed by (Robertsson, Blanch and Symes 1994) who replaced the elastic model with a viscoelastic rheology described by a generalized standard linear solid (GSLS) following the work of (Korn 1987). The new method which is used here is a viscoelastic staggered grid modeling program that can include both attenuation and seismic wave dispersion (Bohlen 2002).

The viscoelastic wave equation is a good way to model the subsurface but the main drawback is that the computational resources used for such FD methods can be quite intensive. Each of the calculated test shots shown require approximately 24 hours to run using a cluster of 6 Processors (ca. 2002). To do this the model is split up into multiple parts and ran in a parallel environment.

We avoid a discussion of the mechanics of the FD solution and the reader is directed to (Bohlen 2002, Robertsson et al. 1994) for the details. What is more important here is to present some practical limitations and important considerations required in using the modeling to assist in tunnel detection. The FD

method solves for the seismic wavefield at every time location the total seismogram and is a sum of all of these individual time steps. The propagation of each time step is saved as the seismic wave goes through the ground. The tunnel affects the wavefield if the time steps are small enough that the wavefield should be able to resolve the small lateral changes in the subsurface. To do this some considerations need to be taken into account; first discretization or how it is gridded. The second thing that FD methods can cause issues with numerical dispersion, where we look at how small of time sampling is needed to is need to sample the wave field,. The final consideration is the stability and how we handle the edge of the modeled data using boundary conditions.

The order of the FD determines how the wave field is calculated, the higher the order the more the model is broken down with partial derivatives and the better the solution should be. However, this of course comes at the expense of increased computing costs (i.e. time). THe 4^{th} ordered FD method provided acceptable results, and calculations at higher orders did not noticeably change the output, while the end product from the 2nd order calculations appeared substantially smoother. The discretization is how the data that is gridded from a continuous spectrum into continuous blocks. The main errors occurred in finite difference methods come from discretization from rounding errors and truncation errors. Since the finite difference method is in the form of a Taylor expansion the terms above the order are removed and thus you get truncation error. The analytical solution of a wavefield is technically an infinite order Taylor expansion of increasing orders of partial differential equations. The higher the orders of derivation show more detail of the higher frequency sampled. Generally only a few orders are needed to sample the wavefield but the truncation of the higher orders causes the truncation error. Rounding errors come from the computer cutting off the decimal of the solved quantities of the wave equation. These errors can cause small changes in the sampled wavefield but are generally quite small.

Conversely, problems with numerical stability and dispersion arise when the time steps are too long such that the proper wavefield cannot be resolved. In the program FDVEPS with 4^{th} ordered operations, the guidelines suggest that numerical dispersion is avoided when

$$DH \leq \frac{V_{s_{min}}}{2f_c N} \tag{4.1}$$

where DH is the grid size and $\frac{V_{s_{min}}}{2f_c}$ is the smallest wavelength propagating though the model, where $V_{s_{min}}$ is the smallest shear wave velocity in the model and $\mathbf{f_c}$ is the central frequency. Another consideration comes from sampling theory in that a minimum number of 8 grid points per the minimum wavelength that will be detected are also needed to avoid numerical dispersion. Hence, stability requires sufficiently short time stepping and spatial node sampling. A rule of thumb stability criterion for a 4th ordered staggered grid is

$$DT \leq \frac{6DH}{7\sqrt{D}v_{p\,max}} \tag{4.2}$$

where DT is the time sampling and DH is the horizontal gridding, D is the dimension of the model, for all the cases are 2D, and $v_{p_{\max}}$ is the maximum compressional velocity in the model. The program will not run unless the stability and dispersion issues are already met and so avoid making the mistake of an erroneous calculation from the perspective of numerical dispersions, but they limit some of the parameters for the modeling, such as extremely different velocities. This can be problematic when there is an air filled void. There will be some form of numerical dispersion but the error should be quite limited if the time stepping is low enough.

The boundary conditions applied to the geological model are the final consideration that must be taken into account. There are two types: a free surface boundary (at the top) and the side boundaries. At the top surface of the model, which is presumed to be exposed for the effective purpose to be a vacuum to not restrict its motion, no normal stresses (or equivalently one can allow the 'material' above the free boundary to zero wave speed). (Levander 1988) (Robertsson 1996). A similar boundary condition is often applied to the bottom surface of the model. The side boundaries are more complicated as they must present some kind of dissipative surface that can attenuate or absorb the seismic energy incident upon them. This is often done by multiplying weighting the stress and velocity field using a value less than 1 (Cerjan et al. 1985). The goal of this is just to dissipate all the seismic energy that hits the side in order to reduce the side reflections propagating

back into the model. Of course these side reflections will not exist in the real earth which can be considered for all effective purposes as a laterally infinite medium.

4.3.2 GEOLOGICAL MODEL

The geometry that is used in the synthetic modeling is given in figure 4-6, note that the dimensions of the entire geological model (constructed in terms of the seismic velocities) is substantially larger than of the area of interest where the responses are to be found. In the model the total length L of the survey detectors is 120m, a length larger than but comparable to that used in the field. The distance X is the distance to the tunnel from edge of the model, *T* is the thickness of the tunnel casing, and *W* is the tunnel width. These are varied during the modeling to assess the effects of size and depth on the observed wavefield. The width of the absorbing boundary changes for some surveys but generally is 20m. The initial model needs also; the density, Q factor for shear and compressional components, the compressional wave velocity and its shear velocity.

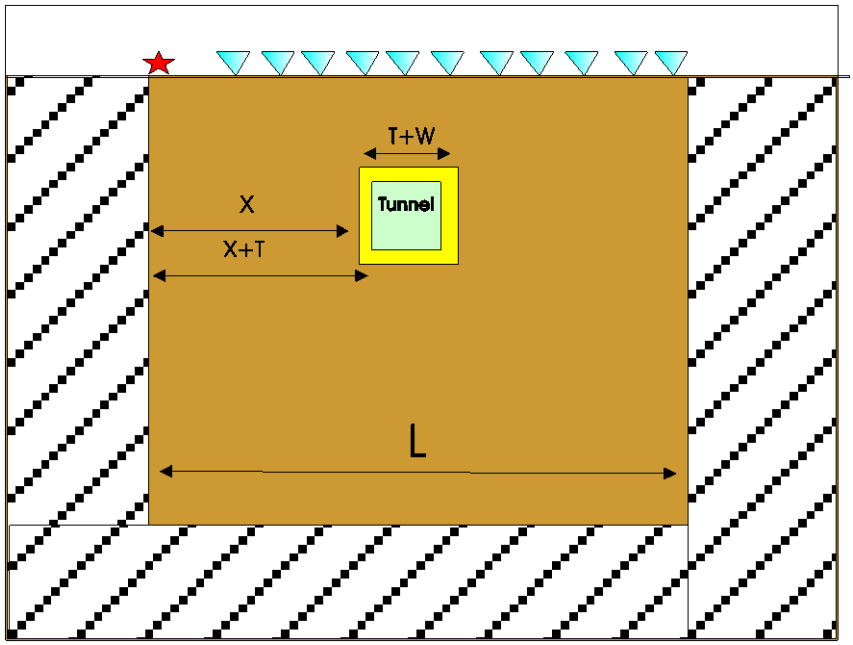

Figure 4-6 The subsurface model for the seismic modeling. The values that were used were for the brown or subsurface we have a velocity of 1000m/s. The Yellow is the casing and for this an assumption of concrete`s velocity is 2000m/s. The green middle is the tunnel which has with a compressional velocity of 343 m/s.

The initial model generated was to be similar to the Oxford Tunnel 1. The information that was known at the time was that the tunnel was approximately 10m deep and was constructed through a geological formation consisting of partly consolidated sands with lesser amounts of shale. The presumed material properties are given below in table 4-2

Material	**Vp (m/s)**	**Vs (m/s)**	**Density (kg/m^3)**	**Qp**	**Qs**
Surrounding rock	1500	750	2000	100	100
Tunnel casing	2000	1000	2000	100	100
Void	343	1E-6	2000	100	100

Table 4-2 These are the based parameters for the synthetic site for tunnel 1, the values for Q and density remain the same because we didn't want to worry about attenuation in this test.

4.3.3 SEISMIC MODELS

The synthetic models that were derived here only used 1 processor for both the y and x direction. The FD mesh typically had 400 and 250 grid points in the x and the y respectively, and was sampled at was 0.01s or 10ms, the calculations proceeded long enough to produce 0.250 s trace record. A symmetric 50 Hz Ricker wavelet, which is, the second derivative of the Gaussian function, was used as representative of the seismic pulse used. This parameter was default and was similar to what was seen in some sample test shots. The source duration was for only 0.002s (2 ms) and thus acts almost like an instantaneous explosive force. The source signal has all energy to propagate downwards, similar to that of a hammer swing. The absorbing boundary is 20m wide; both the particle velocities and stresses are decayed by 95% over this boundary (Cerjan et al. 1985). The receiver array is 120m long with the receivers spaced apart 1 m and buried at 10 cm from the free surface. The depth of 10cm must be used due to the fact that with the receivers at the free surface the energy would be zero and would see nothing. The attenuation for this array follows an approximation based off the GSLS factor and

with a simple case where re assume that there is only 1 relaxation frequency we have

$$Q \approx \frac{2}{\tau} \qquad (4.3)$$

Where Q is the seismic quality factor which is related inversely to the attenuation for a rock; τ is the stress relation time which is dimensionless. What this means is that we can give τ a value of 0.02 to give a Q approximation of 100. More information on empirical values of the seismic quality factors for different rocks can be seen in (Oconnell and Budiansky 1978). Using these parameters we did the synthetic test site for Douglas, AZ. More synthetic examples were also calculated and will be discussed but will not be shown.

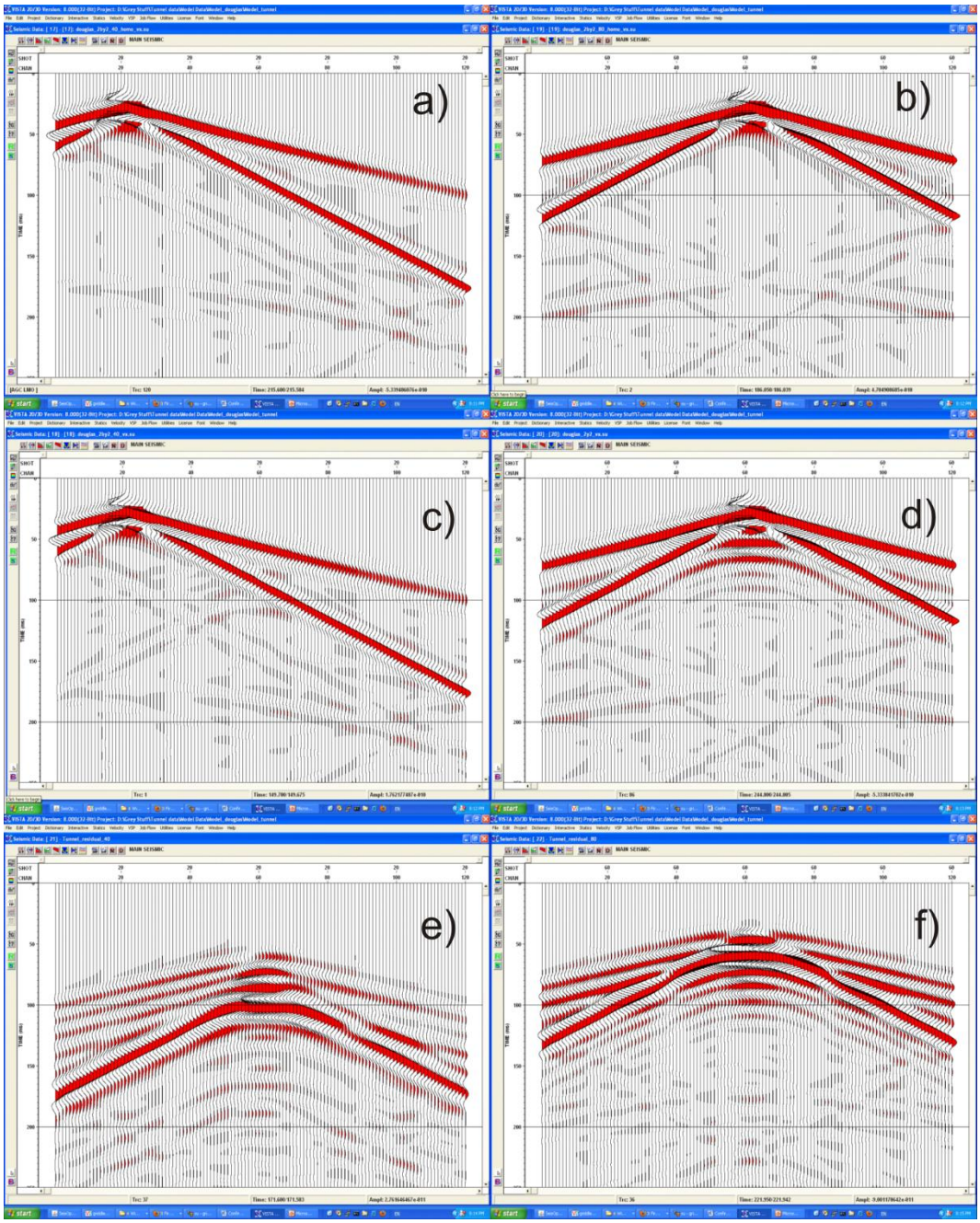

Figure 4-7 Examples of calculated shot gathers over the Oxford Tunnel 1 model. Shot gathers over a homogenous layer with no tunnel for a) shot point to the left of the model 40m from the center of the tunnel, and b) shot point at the centre of the model. Similar shot gathers but now the model contains in its centre a 2 m X 2 m tunnel at 9m depth for c) shot point to 40m left of the tunnel d) shot point at the centered over the tunnel. The data was then subtracted differences between the homogeneous and tunnel model e) shot gathers c)- a) giving the residual. f) is the residual d)-b). Panels e) and f) highlight the perturbations of the seismic wavefield introduced by the tunnel.

Looking at figure 4-7 we have the synthetic results for the Oxford, MS tunnel 1 test site. The calculations for two models that differ only in that those on the right are calculated in the same velocity structure as those on the left but they contain the 2x2m tunnel. Both near and a far offset shot gathers were modeled. The reason for this is that to see if being closer to the tunnel and closer to being perpendicular had any effect.

In figure 4-7, despite the application of the absorbing boundary conditions the side boundary reflections were not completely eliminated. This was one of the constraints imposed by the models because although to make the models even wider such that the side reflections would arrive much later, this would have increased the computational time considerably such that the modeling would not have been possible with the computational resources available. The side boundary reflections do add noise, but taking the simple difference between the model with a tunnel and the(Figure 4-7 e) and f))yields the wave effects of the tunnel itself. What can be seen is that there are 2 hyperbolic waves that are being displayed in the residuals and with that there multiples. These multiples are caused by the constant reflections going back from surface and the tunnel creating more than 1 anomaly. The true anomaly is the first one. There is also some aliasing in the waves around where there are two sets of hyperbolic waves; this is due to wave overlap of the two different diffractions with different velocities causing a situation of where both diffractions are present for a certain time until the seismic wavefield can detect the presence of both diffractions.

As will be seen later, the seismic refraction tomography (SRT) uses as input the travel times of the refracted waves. These are the first arrivals in the shot gathers shown in Fig. 4-7 a)-d) and they follow a linear 'moveout' from the source. Unfortunately, for the Tunnel 1 model, there is no noticeable change in this arrival and as such the tunnel cannot be detected as it is too deep to properly influence the waves using just the direct arrival. In the real world there would also be the situation of multiple layers causing the seismic wave to refract and change speeds in more than one area of the model. When the test was done with using a 5x5m tunnel the direct arrival did change and caused the direct wave to move significantly. The

other problem that is not shown is that we don't forward model the ray coverage map which can also be used as an indicator for the tunnel

Of more interest to tunnel detection perhaps is the diffractions produced by the tunnel, these are the only anomalous arrivals between, say, Fig. 4-7a and Fig. 4-7c. Looking at figure 4.7 we have the same tunnel as (figure 4-7 d)) with both the first arrival and the surface wave; but also the two diffractions that were seen in the residual. By fitting a hyperbolic curve to the seismogram by relating the travel time to the offset of the seismic wave the velocity can be calculated by fitting an hyperbolic curve. This can be seen in figure 4-8. These velocities are 1500m/s and 1000m/s. The first diffraction of 1500m/s resembles that of a diffraction of the P-wave, and the 1000m/s gives the value of a P-SV wave diffraction. How this happens is that the wave field hits the tunnel and reflects both the P-wave but also a shear component which is detected at the surface. The reason this is significant is that the wave comes in at speeds less similar to the surface wave and will most likely be able to be detected in real data.

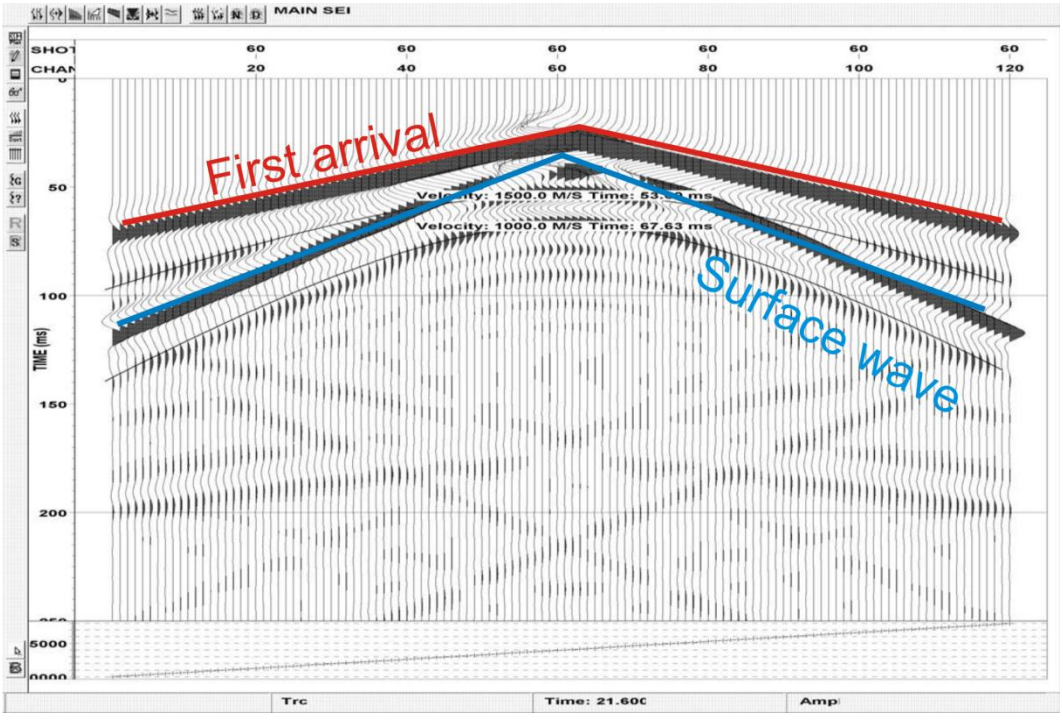

Figure 4-8 Looking at the same data set directly over the tunnel site with 2 types of diffractions present. There are two that are highlighted, the first is 1500m/s and the other is 1000m/s. These diffractions resemble that of a P-wave diffraction and a P-SV wave. The diffractions

happen when the compressional wave approaches the tunnel, hits it, then both a primary wave is reflected back and a SV wave is reflected back. These phenomena will be discussed in chapter 7.

4.3.4 DISCUSSION

The calculated shot gathers illustrated that using the homogenous velocity model with a tunnel does not easily allow a tunnel to be detected in the first seismic arrivals. The tunnel did not significantly influence the first arriving waves until it reach a large size of 5x5m. .Conversely, the modeling does show that diffracted wave arrivals do appear centered at the approximate locations of the tunnels and that both a P and an P-SV diffractions are produced. The data is used as a prerequisite for what was done for Oxford, MS and Douglas, AZ and used as some of the acquisition parameters. The synthetic data assumes a viscoelastic surface but has no changes in the compressional and shear wave attenuation and distortion. There is no anisotropy that is assumed, this is done since there is not enough information known before the acquisition of the field sites. The seismic modeling showed that there is very little to no change in the first arrival wave field but conversely seismic refraction methods have been used to detect small scale tunnel features(Hickey and Howard 2006). This test site only had a small metal pipe that had water flowing through the tunnel causing the tunnel to degradation around the small metal pipe, making it possible to detect the tunnel.

4.4 CONCLUSION

Full elastic wavefield modeling is useful to carry out before the acquisition of data in order to get an idea of the proper parameters for a given target site. The modeling that was shown here was done prior to the acquisition of the data in Oxford, MS and was used as an acquisition aid. The results show that for electrical methods a tunnel using a dipole-dipole array can be sensed, in the seismic methods the tunnels have some of the energy diffracted back toward the surface indicating the tunnel is a diffractor point source. The main thing that was not considered in

seismic methods was noise and a more realistic and heterogeneous subsurface. Similarly in the electrical methods some Gaussian noise was added but no add any near surface heterogeneity.

CHAPTER 5
5.0 ELECTRICAL RESISTIVITY TOMOGRAPHY

In the following geophysical technique known as electrical resistivity tomography (ERT) will be described. A brief introduction of the uses of the technique in general will be followed by theory and method to describe the common applications of geoelectrical methods. To do this Wenner and dipole-dipole arrays will be described in more detail for better understanding. Following this the data collected from Oxford, MS and Douglas, AZ will be shown to show the uses and what is seen in the application of imaging subsurface voids. At the end some discussions about the technique will be described to try and enhance the application in tunnel detection.

5.1 INTRODUCTION

The goal of any geophysical method is to understand the structure of subsurface and try to calculate some physical property that can be related to the actual properties of the rocks. In geoelectrical methods this is done by injecting current into the ground from one surface electrode and measuring the potential at the other. The current and potential can then give you an idea of the resistivity of the subsurface which can be related to subsurface materials. Electrical resistivity is a unit of measure of the degree to which a material opposes the flow of current be it electronic, or particularly in the earth, ionic conduction. By comparing the apparent resistivity values of common material to rocks, we can constrain the dominant rock properties of the zone we are measuring. This comparison was first started in the 1960's by comparing 1D sounding curves to analytical sounding curves from empirical data (Keller and Frischknecht 1966). Electrical methods then advanced further with the invention of high speed computers and then the idea of combining tomography methods and electrical sounding curves started the technique known as electrical resistivity tomography (ERT). This method first was developed in the laboratory measuring core using electrical tomography to compare water transport

through a rock sample (Daily, Lin and Buscheck 1987). The idea was then expanded to surface acquisition using automated switch and multiplexer for faster deployment and was used for monitoring a steam injection site (Ramirez et al. 1993). For more information on history and electrical resistivity systems you can look at (Daily et al. 2005) and (Loke 2002). Loke's algorithms are widely used in near surface geophysical studies.

In vadose zones we generally have all three types of conduction occurring changing the resistivity of rocks quite drastically which is why most rocks have a large range of resistivity's. In the context of the near surface studies here, the most difficult aspect when classifying an electrical (or any geophysical anomaly) in the near surface is to understand its geological history and to know if there has been any earlier disruptive urban construction in the region. If the history of site is not well known careful consideration of interpretation has to be done in urban environments. Even if the history is known, careful consideration of how the subsurface void was created also has to be taken into account.

After the methodology and theory are set in place the ERT data collected from Oxford, MS and Douglas, AZ will be presented. The data presented will not be all that was collected since a substantial volume of data was collected in Oxford, MS but will show most the important surveys that definitively show that a tunnel was found, and for the sake of comparison some of the situations where the tunnel was not detected.

5.2 THEORY

In the following section a discussion on some basic resistivity theory and some physical processes of how electrons or ions move through materials will be analyzed. Understanding these basic processes leads to a discussion of the ERT method and the electrical survey designs used for tunnel detection. This is then followed up by a description of how electrical data is formatted to forward model problems and how the data is inverted to get a pseudosection of the subsurface.

5.2.1 BASIC RESISTIVITY THEORY

Ohms law relates the relationship between an applied electric field $\vec{E}$ to the displacement of charged particles creating a electric current density $\vec{J}$ with:

$$J = \frac{1}{\rho} E \tag{5.1}$$

where the resistivity ρ defines how the material opposes the flow of electrons. The electric field applied to any material spreads out evenly over a three dimensional space and the intensity decreases with distance from the source. Resistivity is in units of ohm-meters and the geometry of an object influences its resistance; assuming homogeneous material the resistivity can be related by the resistance R to the cross sectional area of the material A, and Length L.

$$R = \rho \frac{L}{A} \tag{5.2}$$

In a porous rock which is not homogeneous then we can assume similar relationship but instead of the length of the material we use the tortuosity of the material, τ. The tortuosity simply can be calculated by comparing the length of the actual length of the travel path of the charge carrier through a material, L. to the straight length through the material C.

$$\tau = \frac{L}{C} \tag{5.3}$$

The L path will depend on numerous factors such as the material porosity and the pore geometry. Although recent modeling of microscopic structures has shown promise towards the calculation of porous media resistivity, actually describing L can be difficult. As a result this is usually empirically reported using Archie's Law.

The key assumption made in this is that the electrical current will always travel through the path of least resistance. In the vadose zone (the region between the water table and ground surface), generally we have partially saturated unconsolidated material which implies high porosity and a mixture of air and water

in rock pores. The electrical resistivity of water has a large difference ranging from brine saturated of 0.5 Ωm to fresh water 100Ω.m (Palacky 1987), while air has a resistivity of nearly 10^9 Ω.m which for practical purposes is an insulator. Near surface rocks also have a fairly low resistance in the range of 10-100Ω.m this depends on the clay content and water saturation levels. With these resistivity values one can assume that the subsurface void being hunted for will be a highly resistive feature unless it is filled with brine saturated water. This has been seen in location of subsurface voids in the past (van Schoor 2002), where highly resistive zones were interpreted as subsurface cavities.

The movement of electrical current through a rock moves through via either electronic or ionic conduction.

Electronic conduction is the means by which metals conduct electricity; the basis is due to movement of electrons from partially filled electron bands to higher conduction bands of energy. This process creates a drift velocity for the electric field through the electron band. This causes for fast movement of electric current through a metal and thus makes it a very good electric conductor. For insulators there are no available bands for the electrons to go so no drift velocity is created between the bands. Electronic conduction is actually relatively rare in earth materials except for some base metal ores and graphite deposits.

Ionic conduction is predominant in most sedimentary and near surface rocks. The ions (e.g., Na^+, Cl^-) are displaced through the pore fluid solution or along clay mineral surface by the applied electric field and create a diffusional flux resulting in a transport of ions through the material. In general water is not very conductive, but as soon as there are any salts present the complete dissociation of salts in water creates an easy path for electric current to move through. It is well known that even a small amount of salts causes water to be ionically conductive (Palacky 1987). More information about how electric current can move through rocks can be found in (Knight and Endres 2005), (Telford et al. 1990).

5.2.2 METHOD:

As described above we can relate ohm's law to how electric field moves from a point source in a three dimensional fashion. The potential for one electrode array is given below, where V is the potential, ρ is the resistivity of the subsurface, and r is the distance from any point in the ground to the electrode. To measure the potential of the subsurface a current is injected into the subsurface and is evenly distributed throughout the ground dissipating in energy the farther it gets from the source. The potential is measured at a given electrode measuring the potential created by the injected current.

$$V = \frac{\rho I}{2\pi r} \tag{5.4}$$

In general instead of gathering a direct potential measurement most surveys gather the potential difference between two electrodes to give information about the apparent resistivity at a given point given between them. To do this a 4 electrode system is used with two potential electrodes across which the voltage is measured and two current electrodes across which an input current is applied. This can be seen in figure (5.1) where C1, and C2 are the current electrodes and P1 and, P2 are the potential electrodes. Detailed information about how these equations are setup can be found at (Loke 2002) but for this geometry: The current is injected into the subsurface from the current electrodes. The current travels though the ground and the potential difference measured from the injected current.

$$\Delta V = \frac{\rho I}{2\pi}\left(\frac{1}{r_{C1P1}} - \frac{1}{r_{C2P1}} - \frac{1}{r_{C1P2}} + \frac{1}{r_{C2P2}}\right) \tag{5.5}$$

Where ΔV is the potential difference between the potential electrodes and the difference between the points is related between each electrode and described by the various r. This is generally further simplified so we try to calculate the apparent resistivity, ρ_a and also use a new variable known as the geometric factor. The geometric factor k combines the difference in radius from current and potential electrodes and 2π. This changes for different survey spreads but then the calculation of apparent resistivity is the same for all surveys with

$$\rho_a = k\frac{\Delta V}{I} \qquad \text{where,} \qquad k = \frac{2\pi}{\left(\frac{1}{r_{C1P1}} - \frac{1}{r_{C2P1}} - \frac{1}{r_{C1P2}} + \frac{1}{r_{C2P2}}\right)} \tag{5.6}$$

The main thing that has to be remembered here is that since we use a potential difference between the electrodes we then only have an apparent resistivity unless the earth is completely homogeneous (a rather uninteresting hypothetical situation). To obtain the true resistivity structure, numerous observations of *V* must be made for a large variety of differing geometries must be inverted (Loke 2002)

The resolution of the survey required (horizontally and vertically) and data collection configuration depend on what the type of electrode array used and what on the kind of survey carried out. There are three main types of resistivity measurement geometries employed in near surface investigations:.

1) Sounding surveys (1-D)
2) Imaging surveys (2-D, or 3-D)
3) Borehole surveys

Borehole arrays gather information about the resistivity between the surface and a borehole or between two boreholes. In general the use of a borehole for tunnel detection is not feasible unless the borehole is in the immediate vicinity of the tunnel. Hence, covering a large area is not feasible at an early stage in the hunt for the tunnel.

Sounding arrays are 1-D depth soundings that produce a single apparent resistivity versus depth curve centered at the midpoint of the current and potential electrode. The data collected is all situated around a common point and the electrodes are symmetrically placed away from the centre of the spread in order to give data directly underneath the middle of the spread. Such types of soundings have long been employed, This was the first type of technique used and even though it gives good vertical resolution it provides no information on lateral heterogeneities (Koefoed 1979). The 1-D surveys require only 4 electrodes: 2 current and 2 potential that are moved separately for each station for each measurement. The depth of penetration depends on the electrode separation. As the electrodes are moved farther apart the depth of investigation increases although more current

must be injected into the ground in order that a sufficient voltage to be recorded across the potential electrodes.

Similar to this method there is also induced polarized (IP), or spectral induced polarization (SIP) resistivity surveys which use alternating current. These methods are useful for detecting conductive materials but in general require a large amount of current.

2D imaging. surveys build on the 1D approach and which were first introduced to in order to obtain information on lateral variations of the electrical resistivity. Such systems only came about with advances in digital data collection and instrument control as to be practical this a new type of system was needed to acquire a large amount of data in a short amount of time. This was done by using multiple electrodes and takeouts attached to a computer and a multiplexer to switch the electrodes for each measurement. This idea was first tested by (Griffiths and Barker 1993),(Ramirez et al. 1993). The system just requires the electrodes to be connected to a 'smart' cable which has multiple takeouts which is then attached to a computer. Once attached to a computer a survey design is implemented to evenly sample the subsurface. The survey design used depends on the expected structure of the target.

In the field the goal is to try and sample a uniform spread of information to display the gathered data into a pseudosection. The pseudosection is the data plotted along a transverse line showing the apparent resistivity as calculated and measured immediately in the field (Edwards 1977). The data seen is not the true resistivity and cannot be directly interpreted for geology since the each type of resistivity array changes the way the resistivity contours react. What a pseudosection does give though is the general trend in changes in the subsurface and can be used to eliminate bad data (Loke 2002). Since there are multiple types of arrays only the arrays used in modeling discussed in detail. The two types of surveys used were the Wenner array, which is more sensitive to vertical changes in the subsurface, and the dipole-dipole survey which is more sensitive to lateral changes in the subsurface.

The Wenner array is the most popular type of resistivity imaging geometry. This survey requires two current electrodes and two potential electrodes. The current electrodes are the outermost electrodes and are used to inject the current; the inner two electrodes then receive the current and measure the potential which is then digitally recorded. Figure 5-1 shows the layout of a Wenner array and how the measurement will change if the electrode locations are varied. In the Wenner array all 4 electrodes are evenly spaced apart. Hence, for each station level we just move over 1 electrode, thus instead of electrode 1,2,3,4 being used we have 2,3,4,5. This is done until the electrodes hit the end of the array spread when the electrodes 22,23,24,25 are sued. After this there is an increase in separation distance to 2a, thus using electrodes 1,3,5,7 and continue until 19,21,23,25. This procedure is iterated until there is no equal separation to fit all 4 electrodes on a spread cable. This can be seen in figure 5-1 looking at station 23 we can see what electrodes are used to obtain the data point. This process is continued until there the distance between the electrodes is greater than that of the electrode spread. The Wenner array gives a trapezoidal array of data of the subsurface. At the largest electrode separation we then have the largest depth of penetration but the lowest lateral resolution. The depth of penetration depends on the electrode spacing and the electrical conductivity, and since conductivity cannot be changed only spread length can change how deep the survey is. The reason Wenner arrays are sensitive to vertical changes in the subsurface is due to the sensitivity of how the electrodes react. Since the spacing between the electrodes are the same, the injection of current at the first electrode, the potential measured at the first potential electrode has an horizontal sensitivity contour. Injection at the second current electrode shows the same response at the second potential electrode. Since the current travels through the ground horizontally at each measurement any horizontal feature is averaged out and looks like vertical changes in a pseudosection.

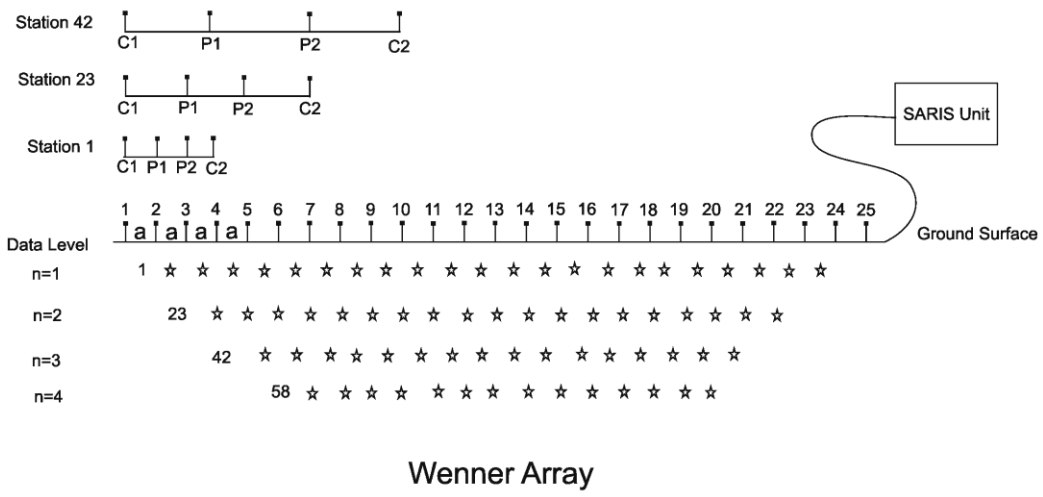

Figure 5-1 Wenner array configuration and arrangement of the data points gathered in the subsurface. A trapezoidal shape which progressively gets thinner at larger depths is produced with larger electrode spacing's. The resistivity system above used is a Scintrex SARIS ERT imaging system using a 25 electrode smart cable. Surveys obtained in the field used either 25 or 50 electrodes.

In contrast to the Wenner array that is sensitive to vertical variations in the electrical resistivity, dipole-dipole surveys are sensitive to lateral changes in the subsurface. As for most geoelectrical surveys, the dipole-dipole array uses four electrodes, again two current and two potential. The main difference is that the two current electrodes are adjacent to one another as are the potential electrodes. For example, in an a imaging survey the current electrodes start as 1,2 and the potential as 3,4, as seen in figure 5-2. For a dipole-dipole survey each level of measurements maintains the same electrode spacing while the separation between the current and potential electrode pairs is varied. Continuing the example, the second measurement would have current electrodes at 1,2 with the potential electrodes shift to positions 4,5. If enough current can be put into the ground this will continue until at the end of the spread which can be seen at figure 5-2 where the current electrodes are at positions 1,2 and potential at 24,25. The next data level then increases the electrode spacing and the same process is repeated. Unlike the Wenner array a large amount of data can be collected doing this method so a higher sampling rate of the subsurface is measured. The key aspect to remember, however, is that since the electrodes are so far apart a large amount of current needed for the potential to be measurable at the far end of the spread is quite large. As stated before the dipole-dipole array is sensitive to lateral changes in the subsurface. This

happens due to the spacing between the current and potential electrodes. The current that is received is detected by going through vertical changes in the subsurface. The sensitivity contours at larger offsets then average the vertical changes that go thought the subsurface and as a result changes in vertical direction such as layering are averaged out and not detected. The large amount of measurements gathered with the dipole-dipole array leads to better sampling of the subsurface and giving ideas of local lateral heterogeneity better then the Wenner array. For more information about sensitivity functions and graphs on geoelectrical methods a good reference is (Furman, Ferre and Warrick 2003)

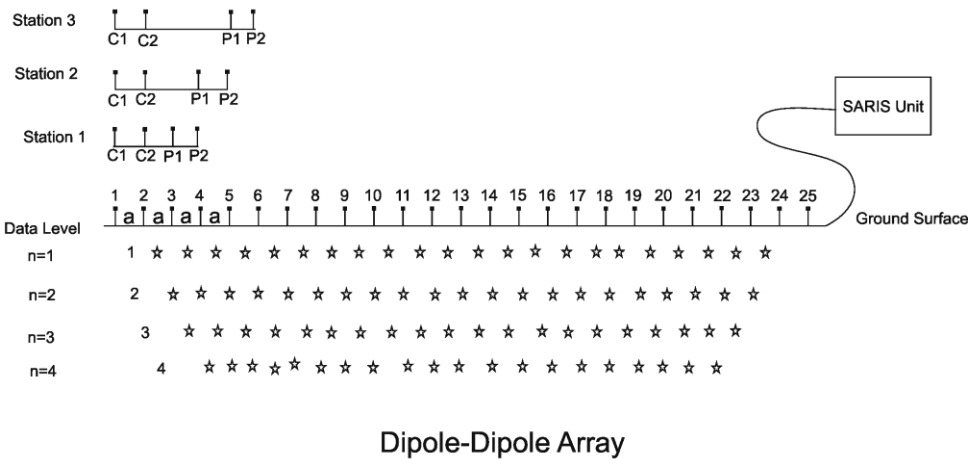

Figure 5-2 Geometry of a Dipole-Dipole array showing the locations of the measured apparent resistivity values in the subsurface. The three data points are give above the diagram to show what electrodes were used to get measurements. The resistivity system above used is a Scintrex SARIS ERT imaging system using a 25 electrode smart cable. Surveys calculated in the field used either 25 or 50 electrodes.

5.3 INVERSION

The inversion of electrical data takes the measured apparent resistivity and puts the data into blocks of calculated apparent resistivity. Once this is done the image can be viewed as a 2D grid and displayed as a 'pseudosection'. Geophysical inversion inverts the observed apparent resistivities in the field into a mapping of the variations in resistivity of the subsurface. This is done by defining a set of model parameters we will want to obtain from the measured data, the model response is

the synthetic data calculated from mathematical relationships to resemble the subsurface. The model data and the response is related in the software RES2DINV™ using a finite difference technique (Dey and Morrison 1979) or for higher accuracy a finite element method (Silvester and Ferrari 1990). The forward modeling of the model and model response solves for apparent resistivity values in cell blocks which can be related to the observed measured resistivity data. The measured apparent resistivity values gathered from our imaging survey can be put into column format and described as **y**. The model response, **f,** is a similar column vector as the observed values and is calculated from forward modeling. The difference between the measurements is the relative error of the measurements and is given by the discrepancy vector g.

$$\boldsymbol{g} = \boldsymbol{y} - \mathbf{f} \tag{5.7}$$

This discrepancy vector **g** then can be minimized to best fit the subsurface by summing the square of the discrepancy vector g

$$G = \boldsymbol{g}^{\boldsymbol{t}}\boldsymbol{g} = \sum_{i=1}^{n} \mathbf{g}_{\mathrm{i}}^{2} \tag{5.8}$$

By solving for the square of the discrepancy vector you can minimize the RMS error by iteratively updating the model to attempt to fit the real data. The initial model is changed to minimize for these errors and after the iteration if the error is worse the previous model it will be rejected. The more iterations done on the inverse problem the closer the inversion becomes to the real subsurface model. To reduce error a Gauss-Newton equation is used to solve for the inversion in order to limit the least squares error (Lines and Treitel 1984).

$$\mathbf{J}^{\mathbf{T}}\mathbf{J}\Delta\mathbf{q}_{\mathbf{i}} = \mathbf{J}^{\mathbf{T}}\mathbf{g} \tag{5.9}$$

Where,

$$\boldsymbol{J}_{\boldsymbol{ij}} = \frac{\boldsymbol{\partial f_i}}{\boldsymbol{\partial q_j}} \tag{5.10}$$

J is the Jacobian of partial derivative relating the model response to the model parameters. The vector $\boldsymbol{q}$ holds the model resistivity values known as the model parameters. The model parameters update after each iteration and the vector $\boldsymbol{q}_{\mathrm{i}}$ is

the model perturbation vector, this acts as a kick in the inversion to change the model values and find the optimum model.

More details about the inversion of such electrical data can be found in (Loke 2002). However, it is worth commenting on some aspects of the inversion. Equation (5.9) is known as a basic least squares inversion and is useful for 'well posed' inversions but in general it is not practical for use in real cases. The reason for this is that problems can arise when the solution of the Jacobian vector is singular or nearly singular making it impossible to solve for the model perturbation vector accurately. This happens when the initial model that is used is far from what the optimal model. To solve for this generally a identity matrix is added to the data creating a smoothing function to create a well defined inversion, this is done by adding a damping/Marquardt factor (Lines and Treitel 1984). Without this the inversion can create sharp inversion artifacts. RES2DINV™ uses a similar type of damping parameter but the damping parameters can change for both horizontal and vertical values can change. The inversion is known as a smoothness-constrained least squares method and is shown in equation (5.11) (Sasaki 1992).

$$(\boldsymbol{J}^T\boldsymbol{J} + \mu\boldsymbol{F})\Delta\mathbf{q}_i = \boldsymbol{J}^T\boldsymbol{g} \quad \text{Where,} \quad \boldsymbol{F} = \boldsymbol{f}_x\boldsymbol{f}_x{}^T + \boldsymbol{f}_z\boldsymbol{f}_z{}^T \tag{5.11}$$

The value $\boldsymbol{f}_x$ is known as the horizontal flatness filter and $\boldsymbol{f}_z$ is the vertical flatness filter. These values make it possible to change application of the damping to the inversion process giving more ability to adjust for different surveys. The inversion parameters can be changed in the program but for information about the inversion or how the parameters change the inversion process you can look at the resistivity tutorial notes (Loke 2002).

The inversion of the apparent resistivity data takes the observed data and forward models to look similar to the measured results which then can be inverted for the true apparent resistivity. The first step is to divide the subsurface into rectangular blocks (for finite differences) or trapezoids (for the finite elements) within which the observed values are assigned. The blocks of data then are forward modeled to look similar to the original data. This is done to get a continuous spectrum of resistivity data and not just blocks of resistivity values which would

give spiky inversion results. Once a continuous spectrum of a 2-D pseudosection can be calculated this value will be inverted for true apparent resistivity. This is done by looking at the difference of the calculated and measured apparent resistivity. The residual between these measurements is used to update the inverted resistivity pseudosection. How close the apparent resistivity is to the modeled resistivity gives you the RMS error of the inversion. Lower the RMS error the closer the modeled data is to the original data. This inversion process is iterated and is continually updating the model until the RMS error stops decreasing, if the RMS error starts increasing you then start creating over inversions and false anomalies in your data. The ERT tomograms shown below will only have the original data set and the inverted true apparent resistivity section. The forward modeled resistivity section is useful to QC your results but is not mandatory for interpretation.

5.5 OXFORD, MS

The field sites in Oxford, MS are described in detail in appendix A, since there are multiple sites with similar characteristics not all tunnel sites will be discussed. The goal with this study is to see if first, could tunnels be detected with resistivity tomography and second, what were some limitations and weakness in the method. The data will be split up into individual test sites and information about the test site and the resistivity image shown will be discussed in detail. The voids could not be detected at all of the sites tested, and this provides useful experience for the limitations of the technique towards detection of a clandestine tunnel in the Arizona test site. The data gathered in Oxford was all post processed in Edmonton so no further surveys could be performed after the initial surveys.

This was the most unique test site compared to the rest of the surveys known as the Dam site; this had different subsurface geology and probably the most competent surface soils. The site also was largely comprised of rich clay soils. The test site was an earthen man-made dam which is just off the University of Mississippi campus. The dam was constructed in order to control excess water run-

off from a dam up river. The culvert in the dam was placed using a cut and cover technique, and the surrounding material is a brownish clay which was water saturated at the surface. The clay helps create a cap to limit water infiltration through the dam. The electrical surveys performed on this site employed a 25m,50, and 100m electrode dipole-dipole array. The survey included 1m, 2m, and 4m electrode spacing's all centered around the 13th electrode that was placed directly over the middle of the tunnel location. The 2m electrode spacing dipole-dipole array can be seen in figure 5-3 and the 4m electrode spacing dipole-dipole survey can be seen in figure 5-4. The reuslts show a strongly conductive anonomaly.

The electrical data shown in figure 5-3 show a low resistivity anomaly around 8m depth and 24m offset. The inversion has 3.3% RMS error with 5 iterations. The first thing that was considered was that the anomaly was related to the ground going from the cut and fill native laminated sandstones. The main issue with this assumption is that in figure 5-4 is the resistivity increase past 12m depth. In figure 5-4 we have a 4m electrode spacing dipole-dipole array which is inverted with 5 iterations and a 1.26% RMS error. The anomalies seen on the edge of the data in figure 5-4 are due to over inversion and are in no way part of the subsurface. When the data is iterated over time the edge effects are extenuated and cause false artifacts and are known as edge effects (Loke and Barker 1996). The approximate locations of the tunnels are shown in on figure 5-3 and figure 5-4, the tunnel is over estimated and is seen at 7m in both figures this is due to the resistive surface with a conductive anomaly. What was shown in chapter 4 with the synthetic data was that the high resistivity anomaly of air should give a small resistive zone seen in data. In the case of the dam site we have a large amount of low resistivity soils and the concrete pipe which has had water infiltrate from the stagnant water in the dam. The water transfers through the pipe and gives electrical current a fast way to transfer. along with this there is water traveling through the culvert.

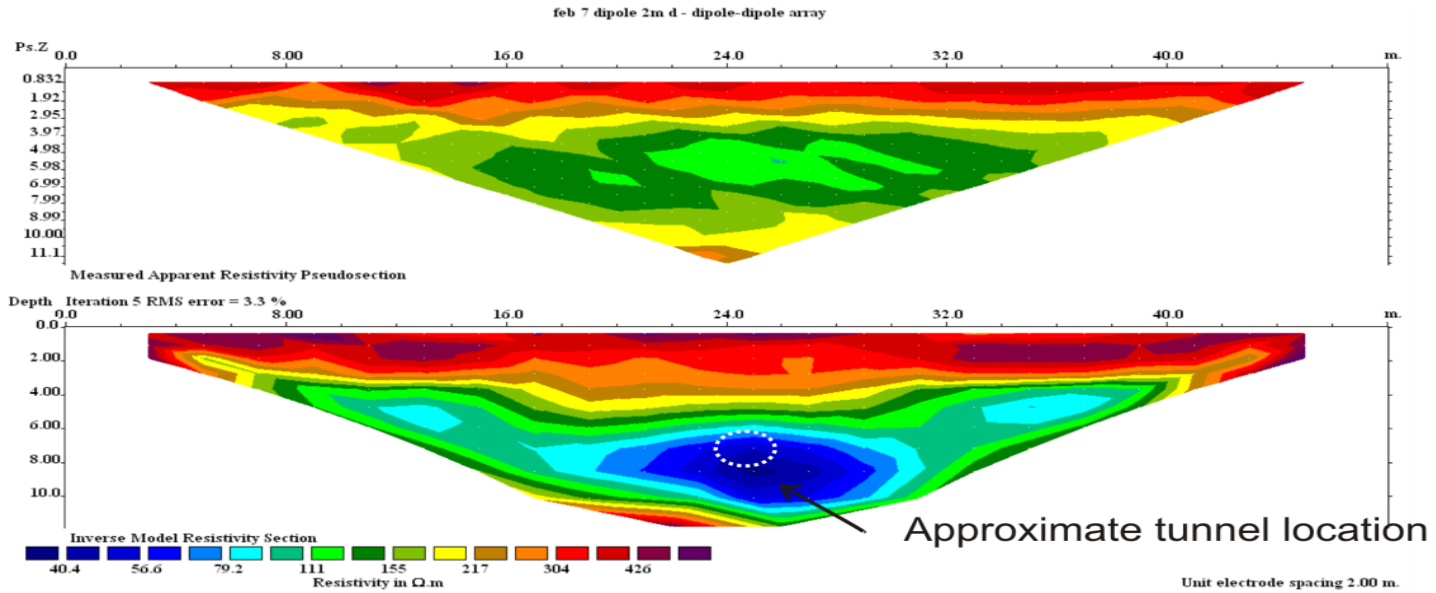

Figure 5-3: Top: This is the pseudosection for the apparent resistivity section. The dipole-dipole array has 2m electrode spacing. Bottom: This is the inverted apparent resistivity pseudosection, around 26m offset and 8m depth there is a low conductivity zone. The final section has 3.3% RMS after 5 iterations. The estimated location of the tunnel was around position 24m and at 6.5m depth. In the top section we can see the high conductivity anomaly around 5-7m depth and 22-27m offset, the inversion causes the high conductivity anomaly to be estimated deeper then what it should. The low conductivity is associated with water infiltration around the concrete acting like a salt double layer.

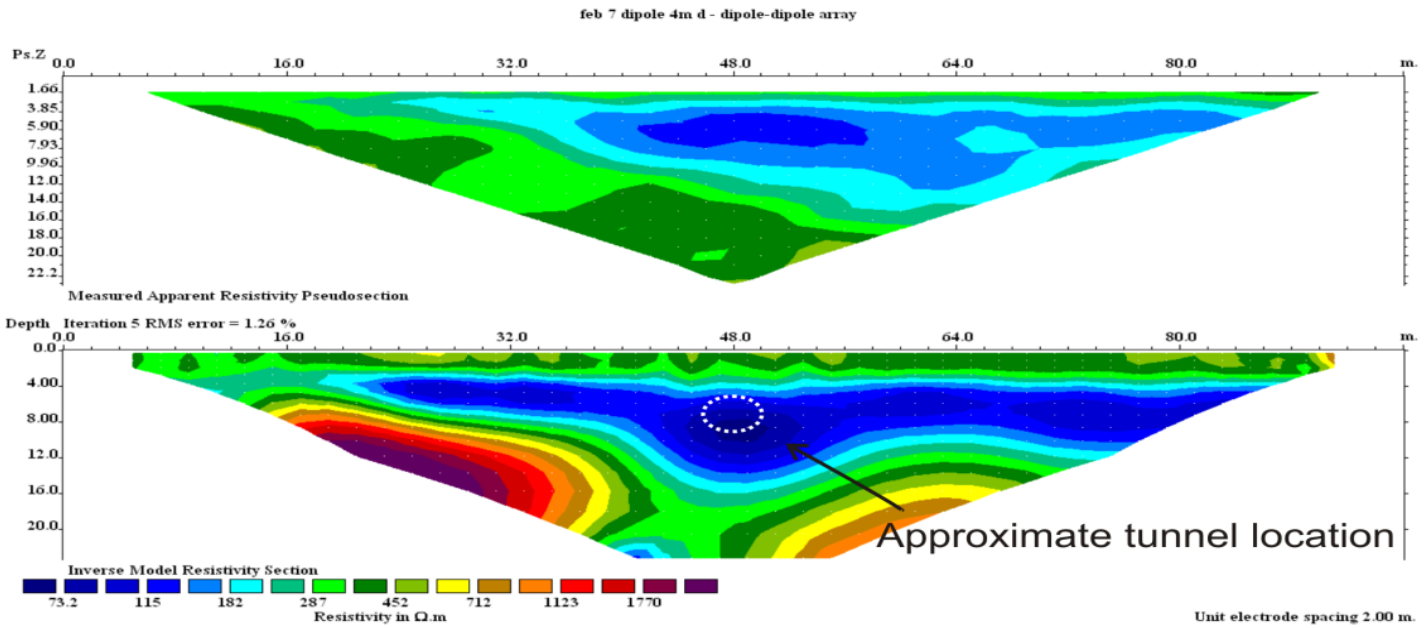

Figure 5-4 Top: This is the pseudosection for the apparent resistivity section. The dipole-dipole array has 4m electrode spacing. Bottom: This is the inverted apparent resistivity pseudosection, around 48m offset and 8m depth there is a low conductivity zone. The final section has a 1.26% RMS error after 5 iterations. The estimated tunnel location is higher then what is seen in the inverted section. What can be seen is that the low conductivity zone is at the region of where the tunnel should be and is where the water is infiltrating into the subsurface. Looking at the top section we can see a concentration of low resistance around the location of the tunnel.

Similar to what was seen in the Dam site the tunnel site 3 shows a conductive anomaly, but unlike the dam site this was a metal pipe culvert. The Metal culvert was estimated from 4-5m deep, and approximately only 0.5m wide, the survey collected a 190 data points over a 50m dipole-dipole array with 2m electrode spacing. The inversion included a finite element forward model with trapezoid grid blocks, due to some very large standard deviation differences some data was removed from the edge of the survey and some of the bottom layers. The 2 resistive edge anomalies have been over inverted creating a layering effect which could lead to incorrect interpretation. Looking at the measured apparent resistivity pseudosection in figure 5-5 we see a boundary of quite low resistivity values imprinted by a resistive region. This region is most likely the location of where they cut to place the tunnel into the subsurface. The overall quality of the data is still fairly good since after 5 iterations there was a 15.7% RMS error which was nearly all associated with the edge anomalies. The culvert in this case was not directly seen in the spread but evidence of changes in the natural rock can be seen. To get more accurate results a tighter spread length would be needed to be used.

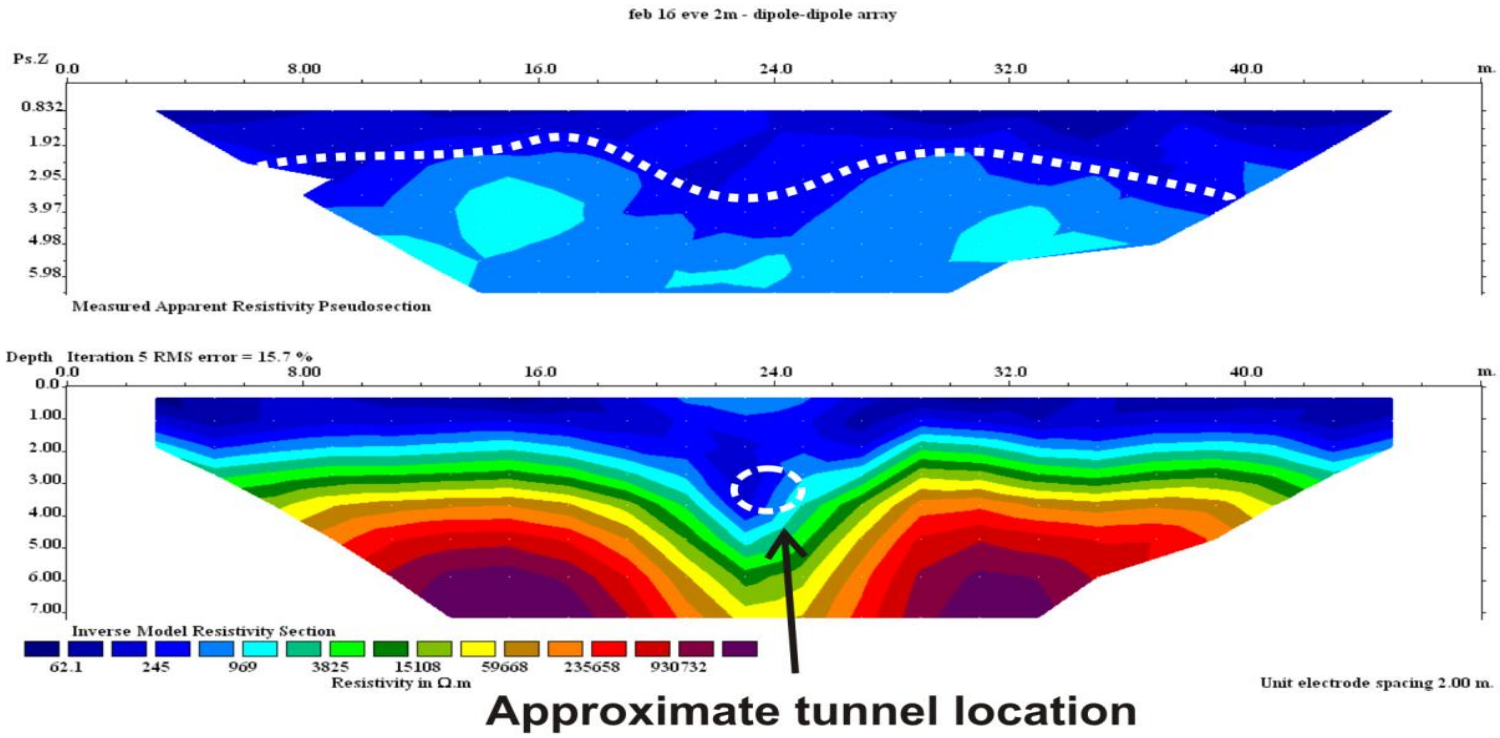

Figure 5-5 Top: The measured apparent resistivity section of a 50m dipole-dipole array over the Oxford, MS tunnel 3 site, the electrode spacing is 2m. A finite element with trapezoid blocks were used for inversion, the only editing done was to remove a bad data point on the edge of the data. The data needs to be removed due to the inversion causing unrealistic values. Bottom: This is the inverse model resistivity section, what is seen is a slight dip down at 24m offset. This drop down is above the approximate location of tunnel. The RMS error is 15.7%, after 5 iterations, the large resistive edge anomalies are inversion related anomalies and have nothing to do with the data.

To the most extent for detection of clandestine tunnels, if the tunnel is deep enough it will be impossible to detect due to the resolution of the technique. The reason for this is that the source signal will eventually be smoothed out making it no longer possible to detect the void. In other cases, a high degree of heterogeneity in the near surface can cause the electrical conductivity results in too much scattering of the electrical paths and this can also make it difficult to detect the tunnel.

Iin Oxford, MS we tried doing both electrical and seismic arrays on tunnels as shallow as 1-2m. In figure 5-6 we have a shallow concrete culvert which is only about 2-3m deep and approximately 0.4x0.4m wide. This survey used 1m electrode spacing on a 25m dipole-dipole spread. What can be seen is at the near the surface at approximately 1m depth a resistive zone at 12m offset is seen. This zone spreads from 8-14m offset and 1-3m depth and is similar to what was seen in chapter 4 where synthetic models of resistive anomalies were expanded. The inversion took 5 iterations and the RMS % error was only 3.8%, the error that was associated was fitting the conductive subsurface underneath the resistive anomaly. The dipole-dipole array has 232 data points with some of the data removed at the bottom layers (i.e. farthest offsets) with a lack of current strength causing false artifacts. The Inversion shows 2 strong anomalies and the approximate tunnel location is indicated on the figure. What can be seen is that though the resistive zone is spread over the tunnel, the location of the air filled tunnel is still overestimated in location and looks a lot larger in the inversion the depth is also not estimated correctly.

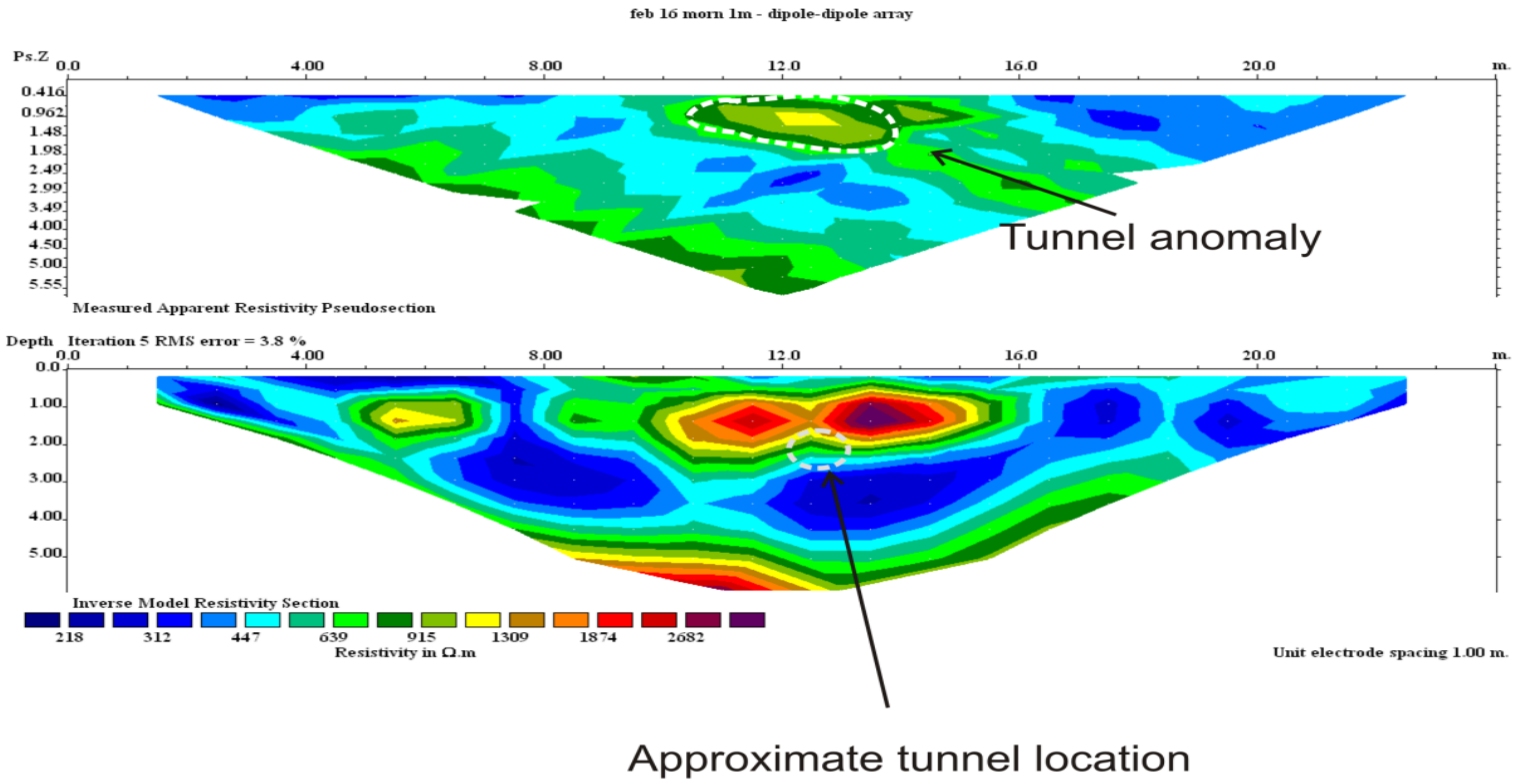

Figure 5-6 This is tunnel 5 of the Oxford, MS test site culverts; the tunnel is approximately 2-3m deep and 0.4x0.4m in dimensions. Top: The measured apparent resistivity pseudosection, there is 232 data points on a 25m dipole-dipole array with 1m electrode spacing. The section had some very minor editing done on the bottom few layers; these were removed due to masking some of the signal closer to the surface due to being so resistive. Bottom: this is the inverse model resistivity section of, where the approximate location of the tunnel is indicated.

The following tunnels of larger depth and size resembled what was expected at Douglas, AZ. Tunnel 6 was an interesting test site because the depth was approximately 8-10m deep and the culvert walls were made up of concrete blocks and not solid concrete. This change causes the way water drains in the tunnel as the blocks do not act as barriers for the water. In contrast metal pipes and solid concrete culverts can fully restrict the movement of the water. A dipole-dipole survey was performed with 4m electrode spacing with 100m spread length. The day this survey was performed was very windy causing the seismic data to be quite bad making it hard for to compare the results. The noise resulting from wind in resistivity is little to none, only the movement of the wires can cause a small distortion. Since the tunnel was so deep the goal of the survey was to see if the anomaly could be seen with such a large electrode spread, since using smaller electrode spacing would not give enough depth penetration. The data was processed using a finite element and trapezoid block forward model configuration giving the inverted resistivity pseudosection a 4.1% RMS error after 7 iterations with no editing on the data. Looking at figure 5-7 we can see that the inversion hints at the estimated location by a local increase in the resistivity. The inversion appears to further suggest that the tunnel lies in between two geological layers of differing electrical conductivity. The actual apparent resistiivity indicates that the most conductive zone is still somewhat resistive near 60Ω·m giving an indication of sedimentary rocks. The resistive zone above this region is a higher around 500-1000Ω·m giving the impression of either very loosely packed gravel with little to no water saturation. Though this anomaly does not give a defined location of the tunnel it reasons to be that the tunnel should be able to be detected at lower electrode spacing and with similar spread length. Since this site only had a 4m electrode spacing.

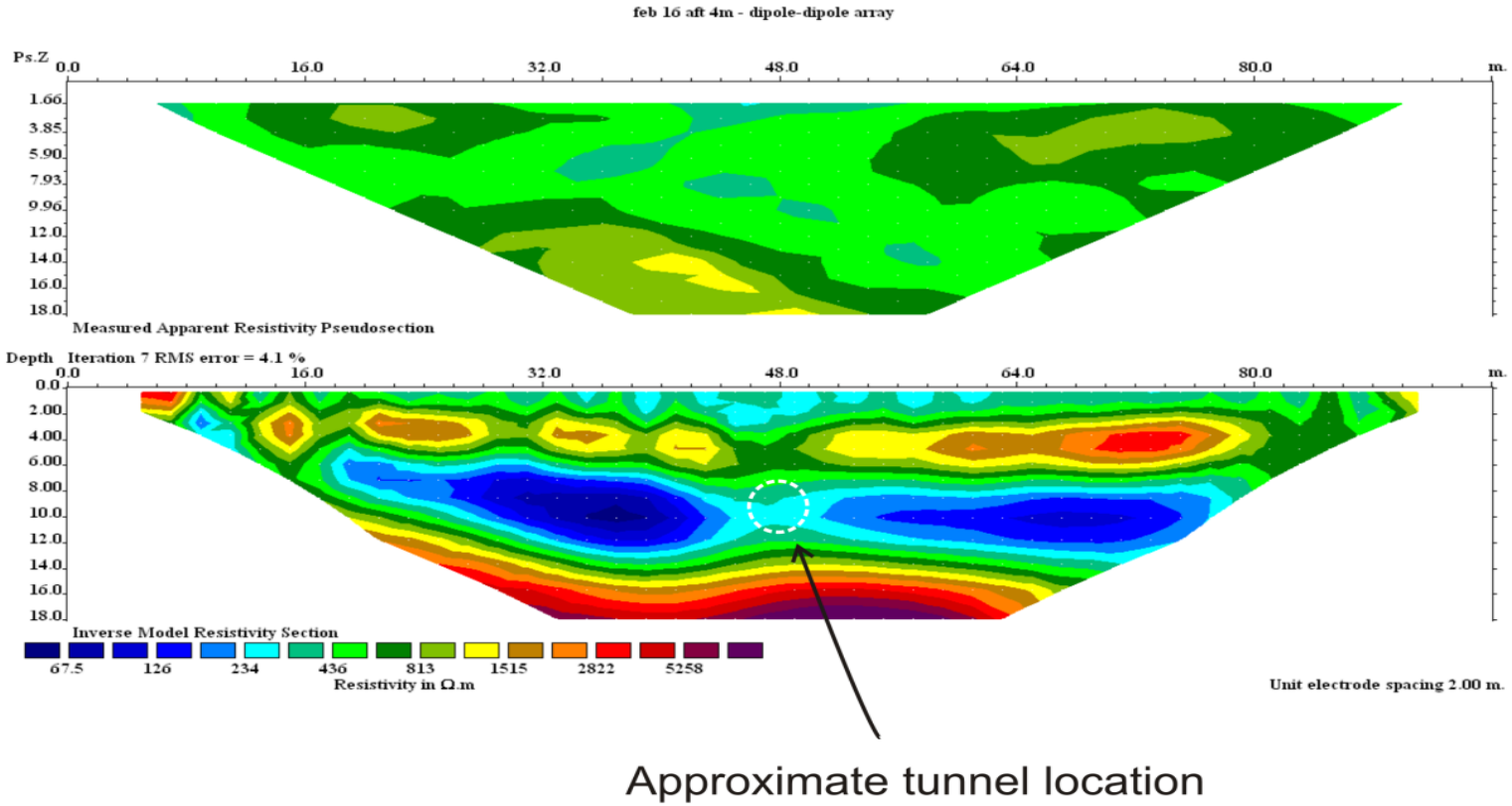

Figure 5-7 This is tunnel 6 of the Oxford, MS test site culverts; the tunnel is approximately 8-10m deep and approximately 1m wide and 0.5m tall. Top: The measured apparent resistivity pseudosection, there is 232 data points on a 100m dipole-dipole array with 4m electrode spacing. Bottom: This is the inverse model resistivity section; the approximate location of the tunnel is indicated. The tunnel site is not detected by the electrical array, most likely due to the large electrode spacing and smoothing of the pseudosection. The data is of excellent quality as, after 7 iterations only a 4.1% RMS error was found.

The first survey examined the deepest but also the largest tunnel site. There were two surveys that were performed over this site, both a Wenner and a dipole-dipole array. The dipole survey that was performed had a power outage so the last few data points were not obtained, this data does not constitute anything to the final interpretation. The dipole-dipole survey that was performed had 2m electrode spacing and a 96m spread length. This is a longer spread length due to the depth of the tunnel. The tunnel was constructed of concrete blocks and was used as a drainage culvert. Looking at figure 5-8 we have the resistivity pseudosection. The approximate location of the tunnel is approximately halfway through the spread around 10-12m depth. The tunnel is anomaly is not seen very well on the pseudosection and is believe to be due to the fact that the tunnel due to the large amount of heterogeneity above the tunnel location. We do see a slight perturbation on above the tunnel location but nothing that is detectable. The inversion ran with 4 iterations but still had 19.7% RMS error, thus the layering and near surface effects are related to inversion related artifacts.

The other ERT survey that was performed was a Wenner array. The goal of this survey was to see if doing a Wenner array would give any indication of the tunnel site. What was noticed is that during the inversion and in after interpretation is that the low resistivity zone seen in figure 5-9 shows a possibility of where the railway track may have got destroyed and needed to be replaced with other material. This is important in the next chapter where we see a similar anomaly causing none of the seismic energy to go to image properly.

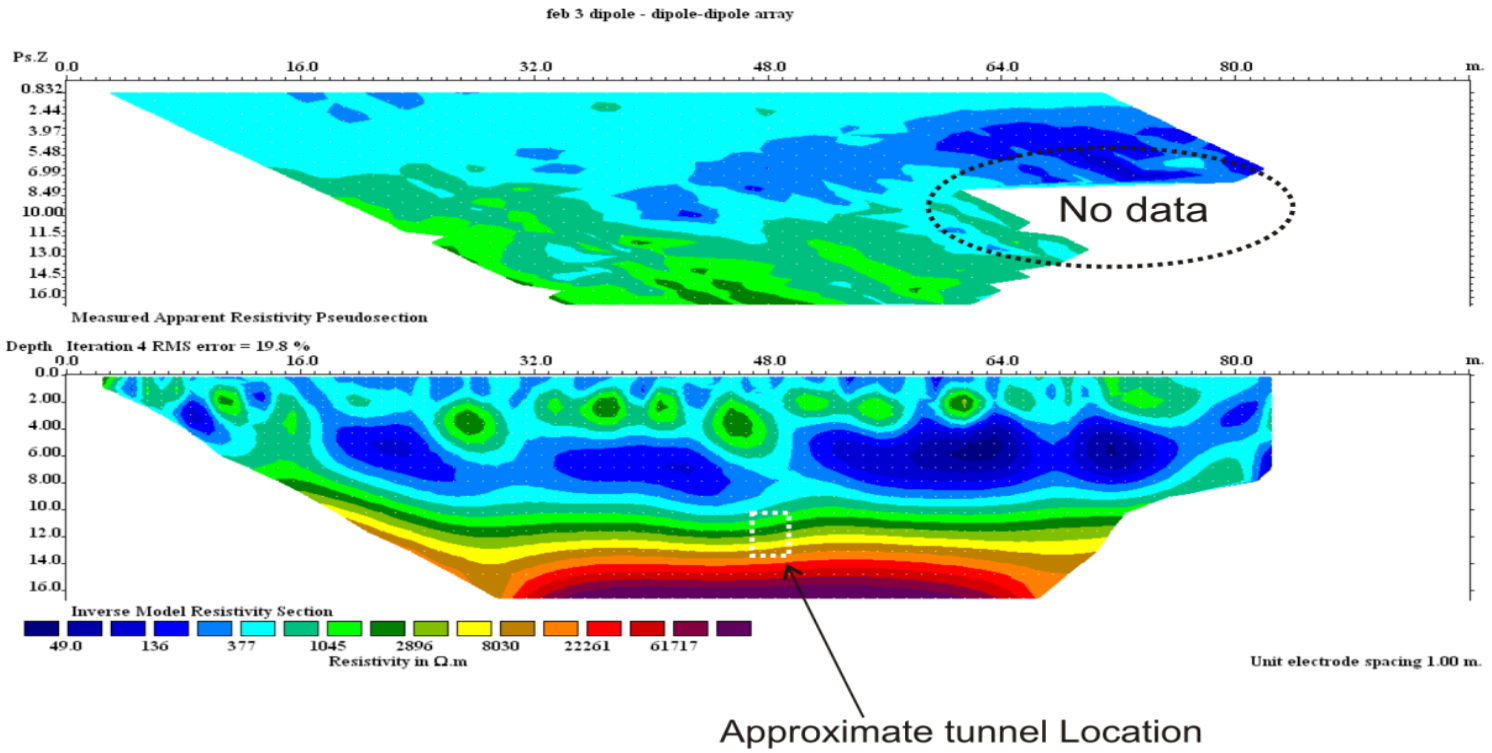

Figure 5-8 This was the first survey site performed in Oxford, MS and was also the largest. The survey has 2m electrode spacing with 100m dipole-dipole array. The survey was not completely finished due to power shortage while running. There is 753 data points with large amount of poor data points removed. Top: This is the raw collected data gathered over the first tunnel site, The tunnel is approximately 12m deep. Bottom: This is the inverted pseudosection for true apparent resistivity. The approximate location of the tunnel is displayed. There is a 96m spread length with 2m electrode spacing the inversion iterated 4 times and had an RMS error of 19.7.

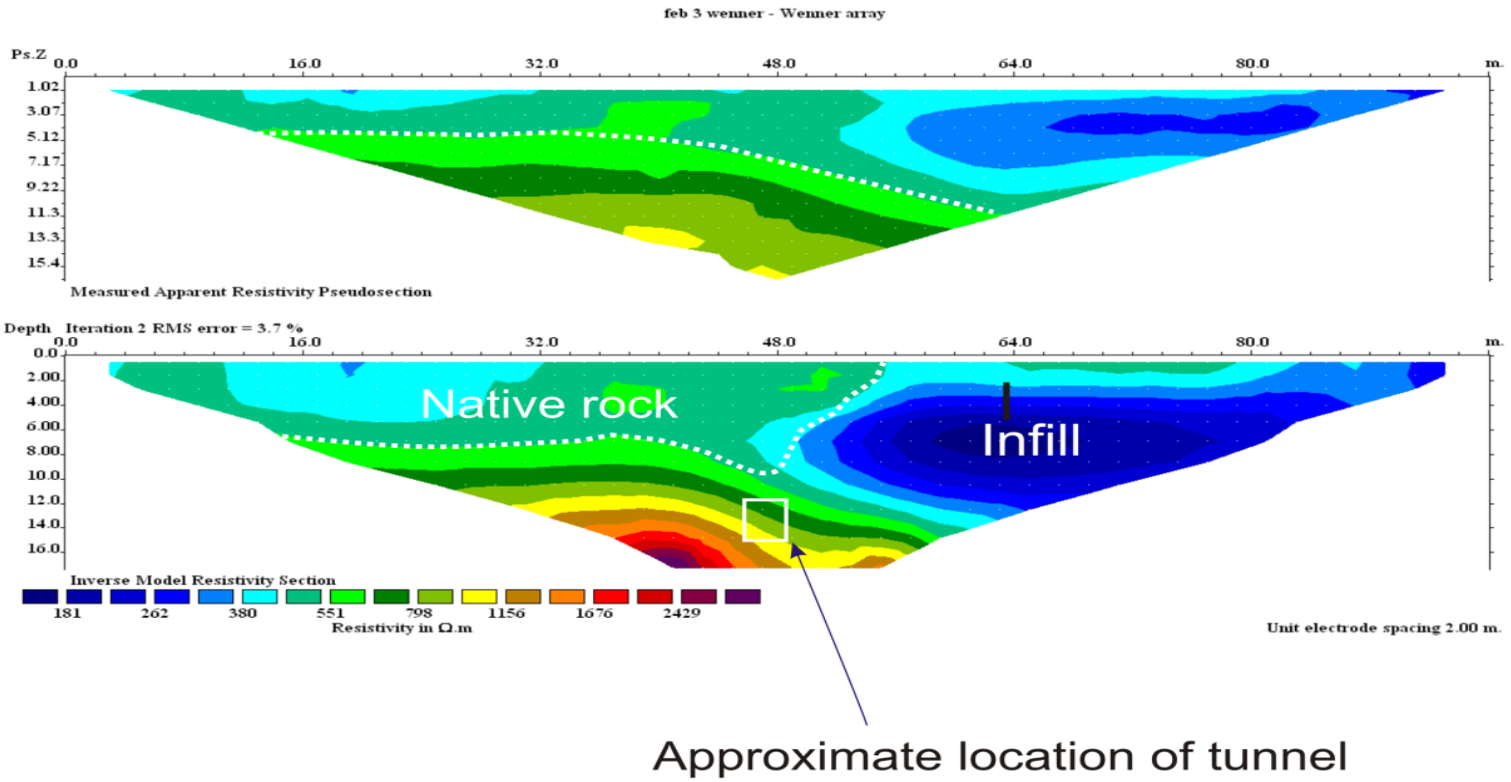

Figure 5-9 This was the first survey performed site in Oxford, MS and was also the largest. The survey has 2m electrode spacing with 100m Wenner array. Top: This is the raw collected data gathered over the first tunnel site, The tunnel is approximately 12m deep. There is 375 data points with 16 data levels, with 1 data point removed. Very severe edge effects were applied. Bottom: This is the inverted pseudosection for true apparent resistivity. The approximate location of the tunnel is displayed. There is a 96m spread length with 2m electrode spacing the inversion iterated 2 times and had an RMS error of 3.7.

5.6 DOUGLAS, AZ

The Douglas, AZ test site had two surveys performed but due to a large amount of surface heterogeneity and a metal fence only one of these produced reliable results. The data will be shown with little to no processing done figure 5.10 then some editing done to improve both the RMS error and also limit the false resistivity values seen figure 5-11. Since there is a large amount of RMS error very little parameter changes are done to the inversion. The modeled apparent resistivity section is also shown in figure 5-11 to show the effects of the large RMS error and how the random error can compound the error. Looking at figure 5-10 we can see the two high resistivity anomalies which are described as E1 and E2 in the approximate location of the tunnel. Since the tunnel was built at the level of the water table and there was no water in the tunnel itself we can expect a higher resistivity anomaly for the tunnel then surrounding materials. There was a large amount of surface heterogeneity but the actual subsurface should be fairly homogeneous, this assumption is based off the side wall in the ditch.

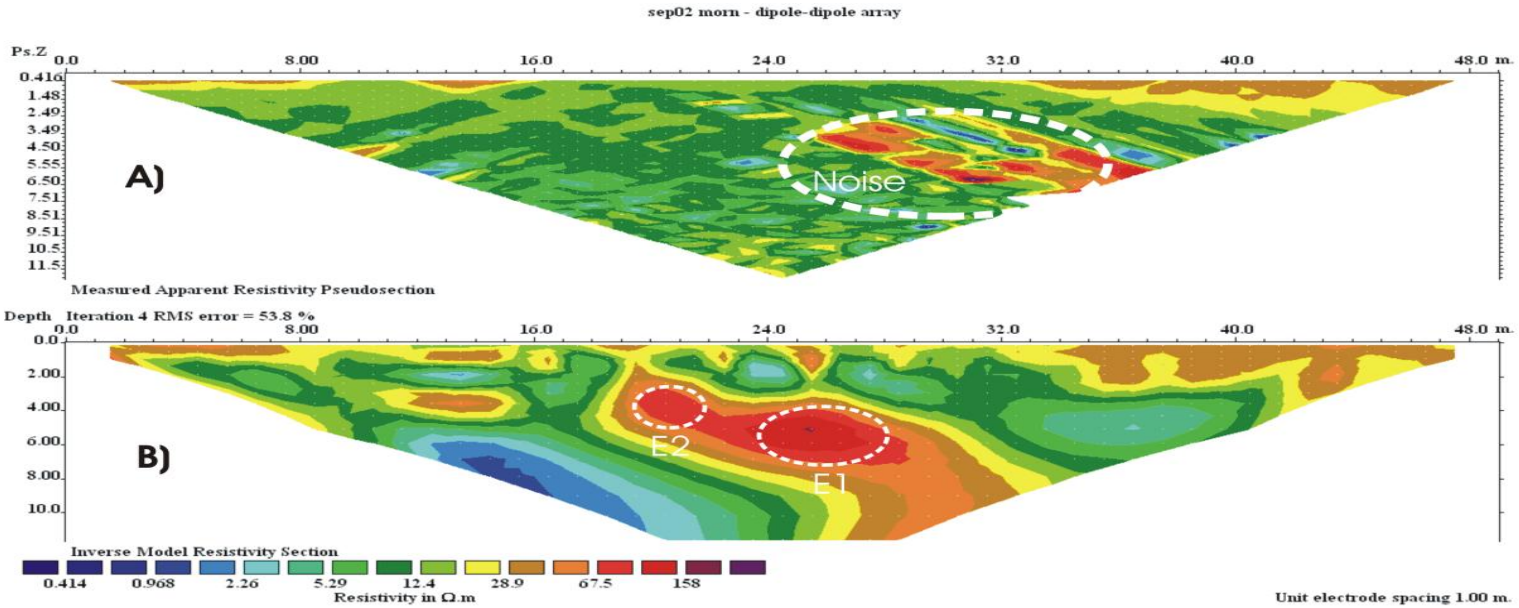

Figure 5-10 This is the electrical resistivity tomography of the ditch data in Douglas, AZ. The data has a 1m electrode spacing with a 50m dipole-dipole spread. The tunnel location is approximately 6m deep where the tunnel was approximated to be in the center of the spread. There are only 3 data points removed with a finite element inversion used. Top: This is the raw data set gathered, the data has over 1000 data points The data has a large amount of noise in the circle area. Bottom: This is the inverse modeled resistivity section, the data set has 2 anomalies put on the section showing the possible location of where the tunnel is. There was 4 iterations with a still large 53.8% RMS error.

The data was then further processed to try and enhance the anomaly and also to try and decrease the RMS errors. The first thing to do this was remove some of the noisy data on the far end of the spread. Since the contacts were loose the and the electrodes with in dry sand, at larger electrode offsets the current was not enough to measure the resistivity of the subsurface. Second, the model spacing's were halved in an attempt to increase lateral resolution. This usually increases lateral resolution but can also result in additional inversion anomalies (Loke 2002). When looking at figure 5-11 the calculated apparent resistivity section shows lineation's and sporadic noise getting compounded. This is the cause of the large amount of the RMS error. To resolve this problem, higher voltages are needed to be injected during the survey. The anomaly that is seen in the apparent resistivity is split into 2 anomalies around the estimated location of the tunnel. The RMS error for the newer inversion is 45.0% which is still high, this was after 2 iterations, and all iterations after this just enhanced the lineations in the calculated apparent resistivity section compounding the sporadic noise more. The survey was in loose sand where water was used to increase coupling with the ground. But by the end of the survey water had dried up. The ground in this region had a resistivity of around 15Ωm and the inverted anomaly for the tunnel only has around 80Ωm. At the roadside site the second resistivity survey was parallel to a metal fence essentially short-circuited the measurements.

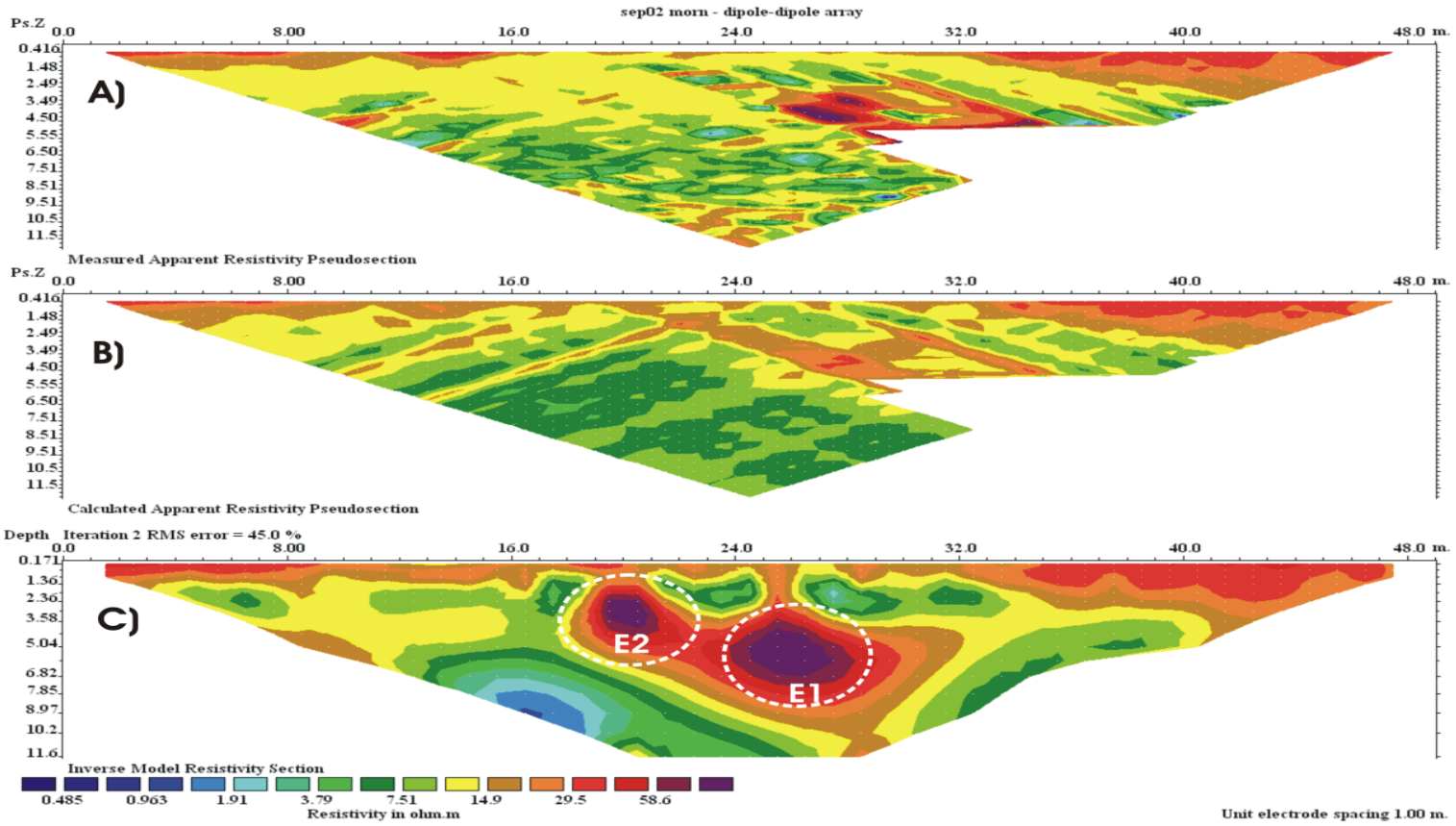

Figure 5-11 This is the electrical resistivity tomography of the ditch data in Douglas, AZ. The data has a 1m electrode spacing with a 50m dipole-dipole spread. The tunnel location is approximately 6m deep and is approximately 1m wide, rectangular shape. Top: This is the apparent resistivity section with large amount of data points removed. Middle: This is the calculated apparent resistivity pseudosection the lineation's are indicative of low voltage in the Bottom: This is the inverse modeled resistivity section, the data set has 2 anomalies put on the section showing the possible location of where the tunnel is. There were 4 iterations and still 53.8% RMS error.

5.7 DISCUSSION

The goal of using electrical methods for finding subsurface tunnels had mixed results. In general a survey can detect a tunnel if the tunnel is fairly shallow and you have enough injected current capacity to produce measureable electrical potentials. The main problem with using electrical methods is that in urban environments there is a large amount of near surface culture that diverts the current through man-made conductive near surface features. What was described was some basic theory on electrical methods and how these methods were used for detecting tunnels. the experiences gained here appears to suggest that natural and/or cultural heterogeneity in the subsurface will change drastically the interpretation. In the Oxford, MS test sites the expected anomaly was detected at only four of the possible eight sites surveyed.

This disappointingly low success rate included those surveys that suffered from poor injected current. Consequently, the electrode-ground coupling was taken more seriously at the Douglas, AZ sites so less current was dissipated at the near surface. Despite this, the tunnel was detected in only the survey carried out in the ditch at Douglas. Again, the roadside site had a large metal fence beside it so when acquiring the data little hope of detection was expected.

In Oxford, MS some of the sites displayed resistive anomalies such as tunnel 5 while others had were conductive such as the Dam site, and tunnel 3. This suggests that some care must be taken towards the interpretation of the tomograms; a tunnel need not necessarily be associated with a highly resistive anomaly in the tomogram.

During the synthetic modeling of the surveys, we felt that the casing around the tunnel would not affect the resistivity and the air would be such a large resistivity contrast. What was seen is that the casing could make it possible for water to have an area of easier flow, and thus actually cause the anomaly to be conductive. The Douglas, AZ test site showed to have a large amount of surface heterogeneity caused acquisition problems but in the subsurface only an issue of

getting enough current into the electrodes was holding us back. Due to having an increasing resistivity with depth some of the current was getting trapped in near the surface due to it being easier to move. This caused some data at larger depths to have poor signal and the noise could be quite large. In general using electrical methods to detect tunnels can be used but due to the uncertainty seen we believe that it has to be done with other techniques to ratify the results. Other studies believe that finding near surface voids can be detected, but due to the large amount of surface changes in urban environments we have seen mixed results. Only the tunnel anomaly was seen in 4 out of 8 possible tunnel locations in Oxford, MS, and 1 out of 2 locations in Douglas, AZ.

CHAPTER 6
6.0 SEISMIC REFRACTION TOMOGRAPHY

The goal of this chapter is to show how using seismic first arrivals and refracted waves can be used to image the subsurface in terms of its seismic velocities. This is done by first giving a brief overview of some of the basic seismic principles and following this with theory on refraction modeling and ray tracing. With this background, some practical aspects of data preparation, first arrival time picking, and theory of the refraction inversion are presented. The chapter concludes with data examples from both Oxford, MS and Douglas, AZ.

6.1 SEISMIC OVERVIEW

6.1.1 SEISMIC WAVES

A seismic wave is an elastic wave that is caused by an excitation or source that causes the elastic energy to propagate through the earth. The energy transfer depends on the type of particle motion which can be either parallel (longitudinal) or perpendicular (transverse) to the wave's propagation direction, with these two waves (in isotropic media) called the P- and S-waves, respectively. In most refraction studies we will be focusing on these two body waves. Surface waves also play a part in near surface studies and must be discussed because they always exist and cause problems for the analysis of the body wave refractions because of their strength.

There are two main types of body waves; P- (or also compressional, longitudinal, primary) waves or S- (or also transverse, shear, and secondary) waves. The body wave travels through the earth and the speed of transmission depends on the density and the stiffness (i.e. elastic moduli) of the material it travels through. The shear wave depends on the rigidity on the rock, if the rock is a fluid and has no rigidity, then there is no shear wave propagation is allowed as is the case for all

fluids. The velocities of the body waves can be described then for an isotropic media as

$$Vp = \sqrt{\frac{\left(k+\frac{4}{3}\mu\right)}{\rho}} \qquad (6.1)$$

And,

$$Vs = \sqrt{\frac{\mu}{\rho}} \qquad (6.2)$$

where Vp is the compressional velocity or P-wave, and Vs is the shear velocity or S-wave. The parameters k and μ are the effective bulk and shear moduli, respectively, and ρ is the density. The bulk modulus is a measure of the compressibility of a rock that is the degree to which the material changes volume under a change in the applied hydrostatic pressure. The shear modulus, or also the rigidity, is the measure of the distortion produced by the application of a constant shear stress also known as the rigidity. A major difference between the bulk and shear moduli is that there is no change in shape with the former (only volume) and only change in shape (no volume) for the latter. A compressional wave travels though the rock with the particle motion in the same direction as the direction of the wave. Shear waves travel through the rock with the particle motion perpendicular to that of the direction of the wave. The body waves are faster than the surface waves and the primary wave is faster than the shear waves as may be seen easily by examination of Eqn. 6.2.

Surface waves travel in the top layer along the surface, there are multiple types of surface waves but for this study I will only considered only Rayleigh waves. The Rayleigh wave is made of both compression and transverse waves and it depends of the same elastic parameters and density. The speed of the Rayleigh wave is slower than the shear wave and for a Poisson solid (when shear and compressional modulus are the same) can be estimated as $v_{rayleigh} \approx 0.91 v_s$ (Sheriff and Geldart 1985). Rayleigh waves travel along the surface in a retrograde elliptical motion. In practice they can be considered as low frequency low speed waves that travel in the top layer of the earth. In the context of the current study, surface waves are essentially noise and often called “ground roll” in most seismic surveys. Using spectral analysis and transferring the seismic signal into frequency ray parameter domain the Rayleigh wave can be used as a signal for some near surface studies

(Park, Miller and Xia 1999) and in tunnel detection (Miller et al. 2006). We did not use surface wave techniques in this study because we did not have geophones sensitive to low enough frequencies to image enough of the fundamental mode that will penetrate to sufficient depth (Xia, Miller and Park 1999).

When the elastic wave energy is propagates from the source into the subsurface and intersects a boundary of changing impedance, then the seismic waves will reflect or, depending on the angle of incidence, critically refract. The acoustic impedance is defined as a product of the velocity and the density for a given material. The transmission and reflection of elastic waves through a boundary depends on the contrast in impedance across it. The ray paths that the wave follow are described by Snell`s law where $\theta_1$is the angle of incidence,θ_2 is the angle of refraction; the angles depend on the ratio of the velocities between the layers $\frac{v_1}{v_2}$:

$$\frac{\sin\theta_1}{\sin\theta_2} = \frac{v_1}{v_2}. \qquad (6.3)$$

as known from elementary physics principles, the angle of refraction depends on the angle of incidence and is controlled by the differences in the wave speeds between the two media. Further, Snell's law states that a certain incidence angle the wave will critically refract at a refraction angle of 90°. At this point the wave follows along the boundary and as it goes leaks back up to the surface. Looking at figure 6-1 we can see the transmission of a wave through the subsurface, and the different situations possible. The blue ray highlights the situation where the incident wave is incident at critical angle of refraction; the subsequent blue paths show it following along the boundary interface and radiating energy back toward the surface as it goes. The red ray shows the situation when the wave energy transfers transmits through the first boundary being again refracted within the third layer. The red ray path shows a true primary reflection that reflects back to surface. For this study we are looking at how the seismic wave gets affected by a subsurface void and in figure 6-1 we see that a possible tunnel location that is air filled reflects back due to its slow speed. The energy around it goes to the surface leaving a blackout zone of no rays going through. This will give a zone of low coverage and can be used as an indicator for a low velocity zone. Using Snell`s law we also need to realize that as the

seismic wave travels through the subsurface the angle that it travels depends on the velocity of the material it is traveling through. This means that eventually the energy will either attenuate or it will reach the surface to be detected.

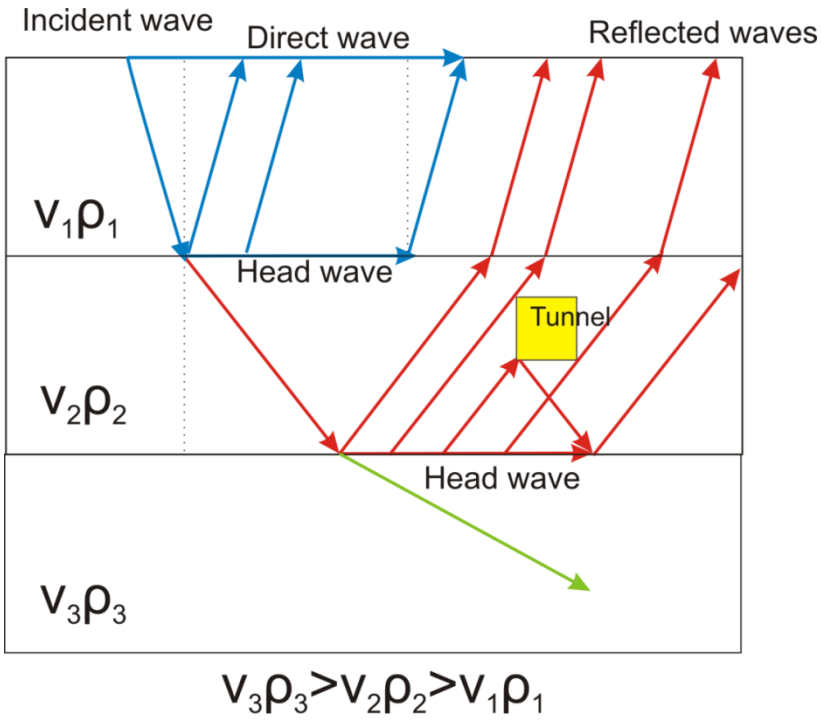

Figure 6-1 This is a display of how seismic waves travel through the subsurface through a 3 layer model with increasing impedance. There is also a tunnel in there to show how an air filled void of small velocity is displayed.

In a seismic survey we have a 'controlled' source, which in our case is either a sledgehammer or an accelerated weight drop. The seismic waves are detected with an array of receivers laid out in a straight line radiating from the source. We consider the location of the source to be a point from which energy radiates equally in every direction. The receivers, in our case, geophones, are sensitive to the vertical component of the particle velocity of the ground surface as the wave passes; the geophone transduces this particle velocity to an analog voltage time series. In modern practice, this time series is digitally recorded; and in geophysical practice the record of the particle motions commences with the triggering by the source and continues for a set period of time (usually influenced by instrumental sampling rates and memory). This record is called a 'trace' and the surface distance between each

geophone and the source is called the 'offset'. The offset-ordered ensemble of all the traces of a given shot is called a field record or a common shot gather (CSG).

The collection the various shot gathers with the source at different locations is the basic data collected in a seismic survey. To record a seismic survey we start recording the receivers' analog output as the sledgehammer hits the ground. The shot gather is displayed as offset vs. time where the offset is just the relative distance from the shot to the receiver. An example of a CSG can be seen in figure 6-2, the figure shows how surface waves and primary waves are displayed, the reflections are much weaker and are masked due to the large amount of energy of the surface waves and the first refraction. To increase the energy and limit the random noise, multiple field records will be recorded at a given location and stacked (summed) to increase the signal to noise ratio (S/N). The field record should be the same if at the same location and gives the results repeatability, this has been tested(Knapp and Steeples 1986). Stacking at a single location should just decrease the random noise encountered in a survey. Noise is anything that is not considered as signal, this can range to other types of seismic waves, random noise, or correlated noise (random noise is noise that is varies on a field record to field record basis; an example is a footstep or wind blowing on the receivers. Correlated noise is noise that is seen in all shots and is stacked when stacking different field records, examples are other seismic waves, or engine running on the accelerated weight drop.

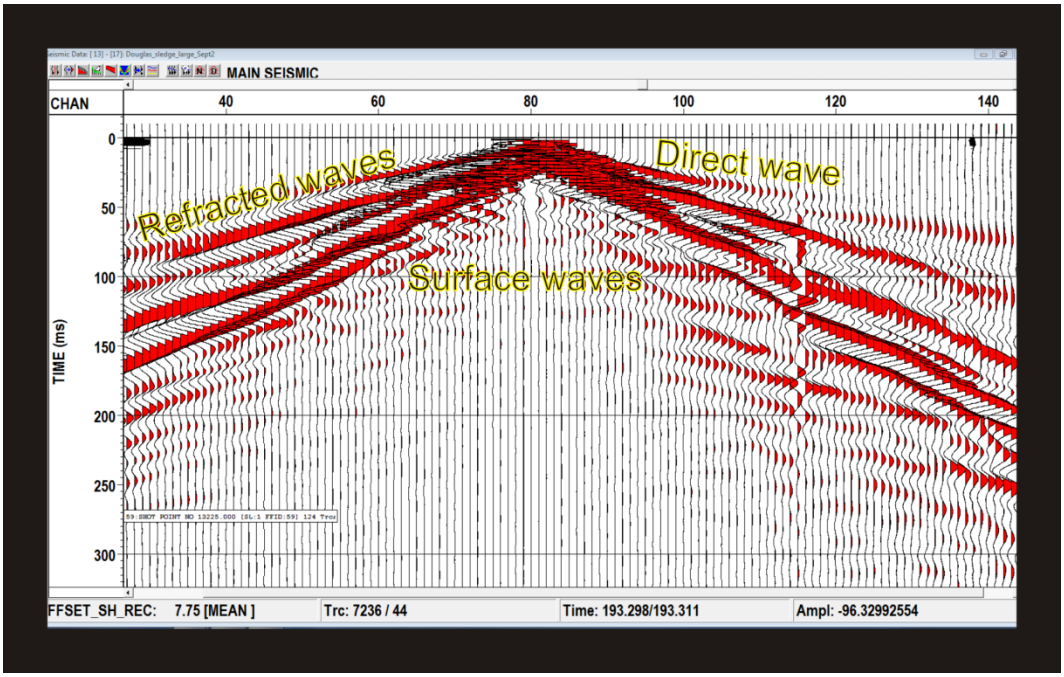

Figure 6-2 Example ensemble of seismograms (a common shot gather) from the Douglas, AZ. The direct, refracted, and surface waves are shown.

The other type of survey that can be acquired in the near surface employs a downhole geophone package; in this case the travel times of the down going waves from the surface can be directly measured. This type of data acquisition is known as vertical seismic profiling (VSP). The main difference is that since the receiver is down in the ground the seismic waves that travel towards it are one-way and direct thus giving exact velocity information for what they traveled through. This survey was only carried out at 1 survey site but can be useful in getting exact velocities in the subsurface.

6.1.2 Resolution

Before we can go into detail about the modeling of the seismic wave field for tunnel detection we first need to be familiar with the concepts of seismic resolution, although to some degree this remains difficult to quantify. Classically, resolution limits are defined as being the minimum distance apart that two independent

objects can be such that they can still both be individually identified. These limits depend on the wavelengths involved and Rayleigh considered ¼ wavelength separation to be the limit. Of course, this concept becomes less clear once we deal with real seismic pulses that have a broad range of wavelengths.

When dealing with tunnel detection the main concern is that that for acquisition we are setting up a survey that will theoretically has a chance to be able to image the tunnel. Resolution can be split up into that for either vertical or for horizontal. Vertical resolution mainly depends with the wavelength of the incoming wave and the ability to discriminate individual layering and horizontal structures. Horizontal (or lateral) resolution depends on the dominant incoming frequency of the wave field and the depth of the target. These values determine the size of the Fresnel volume which is a circular zone that controls the area from which an observed anomaly will come. Advanced processing techniques such as deconvolution and migration can help increase both vertical and horizontal resolution (Yilmaz 2001), but for this chapter we will focus on the effects on the unprocessed seismic wave.

As stated above the vertical resolution is how close two objects can be placed to be distinguished separately. The oncoming wave has a dominant wave length in which anything smaller than this wavelength will cause tuning and not image each feature independently. The dominant wavelength, **λ** can be calculated from the velocity of the wave **v** and the dominant frequency of that wave **f**.

$$\lambda = \frac{\vec{v}}{f} \qquad (6.3)$$

For the case of tunnel detection we can assume that the first arrival wave speed should be in the range of 600-2000m/s and the dominant frequencies produced by a sledge hammer or the weight drop striking a plate on the ground are on the order of 20-60Hz. Given that the wave speeds in the near surface are on the order of 300 to 2000m/s the seismic wavelengths will range of 5-100 m, which is drastically greater than the dimensions of the tunnel. For most cases you can still resolve an anomaly on the range of λ/4 this depends on the S/N ratio, and in some cases up to λ/8 (Widess 1973), where constructive interference occurs between the top and the

bottom of the reflector. These considerations are for seismic thin beds but the theory also applies to small anomalies.

Horizontal resolution is the ability to see two separate laterally offset events and distinguish each independently. For a wave field to adequately detect the presence of the tunnel we then need to be able to resolve a single object. What we will assume is that the only way to distinguish a horizontal object is that it must be larger than that of half of the Fresnel zone width (Yilmaz 2001). The Fresnel volume width is the region over which a reflected wave (as considered to be will interfere constructively and thus not see two independent events. The size of the Fresnel zone depends on the frequency and velocity of the incoming wave and also the velocity and depth of the reflector.

In tunnel detection it is generally assumed that we are just trying to image only one structure and that is the void of the tunnel itself; but in reality the 'tunnel' is probably more than this. The first item is of course the void in the ground that is filled with water or air. The second part that needs to be remembered is the tunnel casing; this can just be the native rock surrounding material, wood planks, concrete, or other support mechanisms. This is usually just a thin layer. The final zone that has usually not been discussed the damage zone in the vicinity of the tunnel. In weak soils this could be produced by some aspects of the tunnel boring itself and also by the stresses concentrated in the vicinity of the void. When considering all of this and taking vertical resolution into account we need to figure out what the seismic wave field is seeing when entering a possible tunnel location.

6.1.3 Ray Limit Approximation

The other main focus on resolution can be related to that of ray limit theory. The limit of resolution in travel time tomography are based off the ray approximation where we can assume that the ray tracing will generally break down when the scale of the anomaly is on a similar size as the wavelength (Williamson 1991).

$$r_{min} \approx \sqrt{L\lambda} \qquad (6.4)$$

where r_{min} is the radius of the first Fresnel volume, L is the propagation distance and λ is the wavelength of the seismic wave. What this means is that with higher frequencies we get higher resolution while longer wave propagation lowers the resolution. The resolution of travel time tomography also depends on ray tracing theory and how reliable ray tracing actually is in image sharp contrasts or dealing with diffractions and post-critical wave behaviors. Studies using ray tracing programs have been performed to see how sharp boundaries are handled. The ray tracing programs assume constant velocity in the vertical direction generally and thus smear sharp boundary into a gradient or an area (Sheehan et al. 2006b). The reasoning for this is that the wave resolution and the regularization algorithms used assume constant velocity distributions in the horizontal which cause the smear.

6.2 REFRACTION THEORY

Seismic refraction tomography is a method of imaging the subsurface that inverts the observed travel-times of the first arrivals of the direct and the refracted waves to produce accurate velocity structure of the subsurface. This is done by inverting the travel time data for both the refracted and direct arrival P-waves, into a 2D grid whose cells are to be populated with the wave speeds. Since in most refraction methods we are finding out a velocity for a single source receiver pair the image that is gathered can change laterally as well as horizontally.

Refraction methods in the past were used to find the base of weathering layer, this information is important when correcting for the near surface effects (static corrections) in reflection seismic imaging. There are a number of differing methods to carry out such analyses that include the intercept-time method (Edge and Laby 1931), delay time or Gardner method (Gardner 1939), plus-minus method (Hagedoorn 1959), and the generalized reciprocal method (Palmer 1981). These techniques all assume rather simple geometries of the near surface materials and as they are based on systems of linear equations they are able to solve for vertical changes in the subsurface but will not be able to distinguish horizontal features. The

goal of linear methods is to image the base of weathering and apply that in static corrections when NMO corrected seismic reflection data.

A linear inversion for that inversion of ray locations was first developed by (Hampson and Russell 1984) which is known as generalized linear inversion (GLI). This method is a layered base method that inverts the subsurface as continuous layers and does not truly model horizontal variations. This method works by ray-tracing through an initial model, constructed either using prior knowledge of the subsurface or by educated 'guessing', to provide a series of traveltimes that are compared to those picked (observed) in the seismograms. GLI assumes that the seismic velocity within the layer is constant and thus with this the depths of the refractors can be calculated. However, this method too suffers from not being able to truly distinguish lateral variations in the seismic wave speeds.

The basic premise for tomographic inversion is similar to GLI methods except now the velocity model is now gridded into a 2D mesh instead of layered. Ray tracing methods require four major things: 1) an initial model to begin the calculations, 2) a forward model solver for the ray paths in order to obtain theoretical traveltimes (synthetic picks), 3) a regularization scheme, and 4) an inversion method to solve for both velocity and depth. The initial model that is needed does not have to be indicated of the true geological model, but can help reduce the number of iterations that are needed, the modeling should eventually give comparable results (Lanz, Maurer and Green 1998). This being said using a completely wrong geological model can lead to a bias in the inverted model (Kissling et al. 1994) The forward modeling program needs to be able to create synthetic picks, and br able to compare to the original picks. The inversion needs to be able to calculate the difference between the first arrivals and update the velocity model accordingly to the residual of the travel time file. The inversion then iterates this procedure until a predetermined stopping criterion. The inversion must converge to comparable results despite using different initial models.

6.2.1 Refraction Inversion

There were two tomographic modeling programs that were used in this study. The first is Rayfract™ (Intelligent Resources Inc.) this program uses a wavepath eikonal travel time inversion based off of the work of (Schuster and Quintusbosz 1993). The other program used was SeisOpt® Pro™ software (provided by Optim Software and Data Solutions, USA) this is a generalized simulated annealing approach based of the work of (Pullammanappallil and Louie 1993). Both programs were used for inverting the tunnel data but due to the large computational cost of simulating annealing, SeisOpt Pro was not employed at all the tunnel sites. The Rayfract software license resides at the University of Mississippi in Oxford, MS and the tomographic calculations were done by our collaborators with Dr. Craig Hickey and his associates. The two inversion programs will be described briefly below. The two tomographic programs both use a finite difference approach to solve for solving the ray path location but the inversion and updates of the velocity model differ significantly. The results of the tomography are then displayed with Depth on the y-axis, surface location on the x-axis, the velocity is displayed as a color bar and each grid location is filled in with a color that designate its velocity. A smoothing is applied to the data to make the model look continuous.

6.2.1.1 Rayfract

The program Rayfract™ (Intelligent Resources Inc.) is a wavepath eikonal travel time tomography (WET) based off (Schuster and Quintusbosz 1993) which models rays using a finite difference back propagation method. The finite difference modeling program is based off back propagating the rays and calculating the travel times (Vidale 1988), these travels times then are used to solve the wave eikonal equation (Qin et al. 1992). This inversion was then made faster and just as accurate using the WET technique by (Schuster and Quintusbosz 1993). This back propagation technique uses Fresnel volume approach which incorporates the finite wavelength of the real waves and the influence of adjacent ray paths up to half of the period of the fastest waveform. This program works by

1) Picking the first arrival travel times from the seismograms. Either the refracted of the direct wave

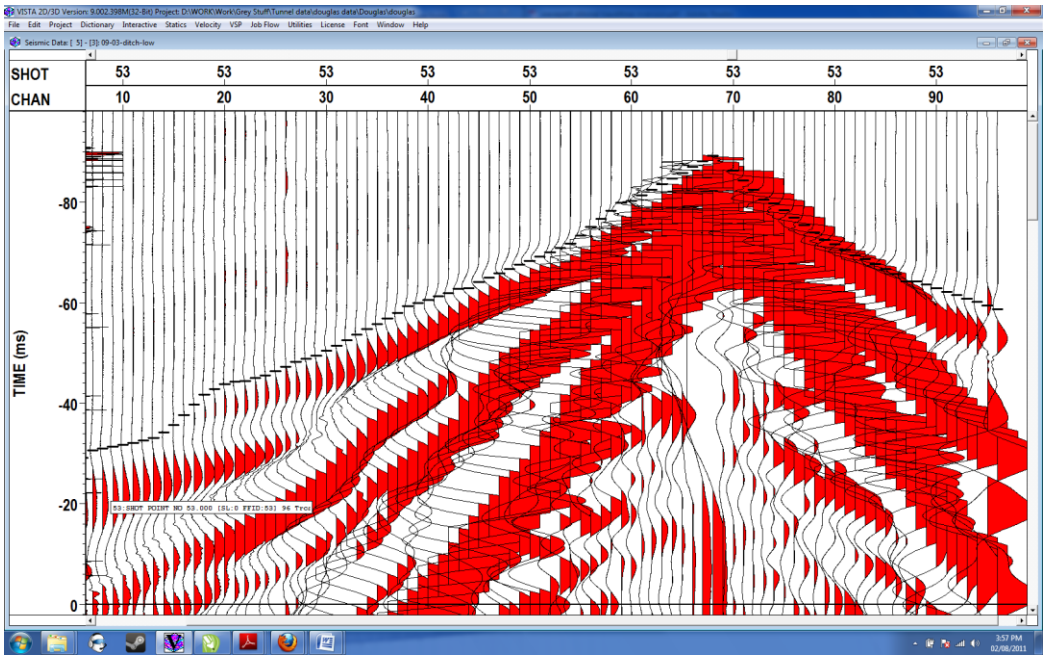

Figure 6-3 Seismogram with first arrivals displayed in black, amplitudes are normalized using a mean scale. This was a 96m spread length

2) The initial velocity model is proposed, and for our case a 1D gradient model is used. The eikonal equation is solved using a finite difference method proposed by (Qin et al. 1992), to obtain the finite difference travel times. The travel time residual is calculated by subtracting the observed first arrival travel times and finite difference calculated travel times.

3) A weighting function is solved for all points in the model to give a source misfit value. This misfit is a function related to the slowness which is used as the velocity update.

4) The slowness model is updated and these steps are iterated until convergence. This scheme can be seen in more detail at (Schuster and Quintusbosz 1993).

6.2.1.2 SeisOpt

The other program used for calculating velocity tomograms was SeisOpt® Pro™ software (provided by Optim Software and Data Solutions, USA). The algorithm is based off inverting the first arrival travel times using a nonlinear optimization technique called generalized simulated annealing (Pullammanappallil and Louie 1993), the technique uses a simple simulated annealing and does not go into major details of statistical measures. The program has the subsurface split up into numerous rectangular blocks which all have the same size where the dimensions that are used are user dependent. The smaller the grid blocks the higher the resolution but the larger the cost of computation. The travel times have the ray tracing calculated by finite difference modeling based off the work of (Vidale 1988). The simulated annealing approach is a method that tries to determine an optimized model by using a statistical approach by trying to find the global minimum least squares error. The algorithm proposed by seismic imaging (Pullammanappallil and Louie 1993) can be seen below.

1) Pick the first arrivals in the observed data set

2) Using finite difference modeling the synthetic first arrivals are picked for the proposed initial model.

3) An error function is calculated comparing the observed travel times and the calculated first arrival times, using a least squares approach. This can be seen in the equation below

$$E_i = \frac{1}{n}\left(\sum_{j=1}^{n} \left(t_j^{obs} - t_j^{cal}\right)^2\right) \qquad (6.5)$$

where E is the error function and n is the amount of travel times per shot record location, j is the actual travel time, and t^{obs} and t^{cal} are the observed and calculated travel times respectively.

4) The current model velocity field is perturbed by randomly adding constant velocities in different neighbouring boxes in the model. This procedure is statistically random and the change can be any velocity within a range that is given. The new model has new travel times calculated and thus a new error calculation, E1. The purpose of this step is to attempt to avoid local minima of error Eqn 6.5.

5) The new model is accepted if the error is less than that of the previous model $E_1 \leq E_0$, and when $E_1 > E_0$ is accepted sometimes when the model is accepted provisionally bases off a annealing probability cooling function (Pullammanappallil and Louie 1993). The reason for this probability is to use it as a kick function to not have the model stop in local minima in the search for the global minima. The probability can be seen below:

$$P_c = \exp\left(\frac{(E_{min}-E_1)^q \Delta E}{T}\right) \qquad (6.6)$$

where $\Delta E = E_0 - E_1$the change in error, T is the temperature for annealing, q is an empirical parameter, and E_{min} is the least squares error at the global minimum, usually close to 0. This probability has the ability for the inversion to 'kick out' of local minima, but at later iterations and when the model approaches the global minimum it decreases the probability to accept a new model. The rate of cooling is the process of decreasing the value T, T starts at the beginning as quite a large number to help get to a good model. This large T helps increasing the probability of accepting a new model even though the RMS error is high to help kick the model out of local minima's. As the iterations increase the value of T is lowered as it approaches a global minimum and eventually is lowered until eventually it can't accept a new model (Pullammanappallil and Louie 1993).

6) This process is iterated until the inversion reaches a predetermined error criterion. The convergence conditions require the difference in the least square model between consecutive models to be minimal and that the probability has a very little chance of accepting a new model.

6.2.2 METHOD

The data that was collected in the field went through a similar processing scheme for refraction tomography for both types of refraction tomography programs. The first thing that need to be considered is that since the data was being processed at two difference locations a common processing scheme was used

1) The Shot gathers that are in SEG-2 format are imported as a single project with all the shot gathers that were used for inversion. To do this vertical stacking at each shot location of common shots needs to be done to get unique shot records or only 1 shot gather at each location is inserted.

2) The shot-receiver geometry is checked and additional header info is inserted for each case. Since the geometry is only inserted for shot records additional information such as source receiver offset, field station numbers etc. is needed to see the seismic data in other domains. The geometry is then gone through a QC stage where the headers and seismic data are compared to field record notes. Data has bad traces killed and traces that can't be properly picked are removed so as not to contaminate the solution.

3) The first arrivals are initially picked automatically as can be seen in figure 6-3 to do this an amplitude gain is applied and ranged from 0-12dB in order to boost the visibility of the attenuated arrival at far offsets relative to those on traces near the source. A general mean normalization is done also to get consistent wave fields for easier picking. No AGC or other processing is performed during the first break arrival process.

4) First breaks are checked for consistency and picked manually if they are bad. If no energy of the first arrival can be seen then it is ignored (i.e. not included in the calculation of error).

5) These picked first arrival times are then inverted for the velocity tomogram using one of the algorithms seen above. Most models were done with Rayfract™ due to time constraints but some done with SeisOpt® Pro™. The initial models used as a 1D gradient model for Rayfract™ and a homogeneous layer for SeisOpt® Pro™. The parameters used generally are the default and run for 20 iterations for Rayfract™, and for SeisOpt™ around 50000 corresponding to about 10 minutes and 4 days, respectively.

6) The velocity and ray tracing image are then displayed. The ray tracing is compared to the velocity model to check for consistency and geological accurate results. The number of iterations could either be increased if the RMS error still

showed substantial decay, or decreased if the model was too smooth and not resolving horizontal features.

6.3 OXFORD, MS

Seismic data was first collected over the tunnel sites in Oxford, MS, where we tried to detect the presence of culverts on an abandoned railway tunnel. The test sites that are going to be shown use the program Rayfract™ (Intelligent Resources Inc.) and both the refraction tomogram and ray tracing coverage will be shown. The refraction tomography that uses Rayfract™ was done by Dr. Craig Hickey and his colleagues in the National Center of Physical Acoustics (NCPA). Similar to what was seen in electrical studies the ray tracing gives us an idea of the forward modeling and how well the inversion will be able to resolve the features. The ray tracing and velocity image of the subsurface have changes due to differences of elastic parameters (Baker 2002). The elasticity of the soil is dependent on the cohesion, degree of cementation, and water content. These parameters are what are considered when interpreting the subsurface. The seismic surveys carried out in Oxford, MS had refraction tomography applied to the first arrivals of the seismic waves. As will be seen below, an velocity and/or ray density anomaly at the location of the tunnel was detected in six out of the nine surveys conducted. Below, the results from only 3 tunnels will be shown to illustrate cases in which the tunnel was not detected (failure), the tunnel was detected easily, and additional processing was needed for the tunnel to be located.

6.3.1 Tunnel 4

Tunnel 4 is constructed of small concrete blocks and is approximately 5-6m in depth. The tunnel site had loose gravel on the surface but most geophones could get good contact. The seismic spread laid out had a 1m geophone spacing and was 96m in length roughly centred on the tunnel. The shot spacing was 1m. The source was the accelerated weight drop 1.5m laterally offset from the line of geophones and so was within 2 geophone intervals. The general rule of thumb is that the shot has to be within 2 geophone spacing in order that one may still safely assume that the ray

paths fall within a vertical plane and 3D effects can be ignored. There was only an elevation difference of 0.6m of elevation from the start to the end of the line so a horizontal datum was assumed. The first arrivals from the weight drop produced enough energy that all first arrivals could be picked in the spread. In refraction tomography the depth of investigation is approximately ¼ the size of the spread length. We can see in figure 6-4 that the tomogram images down to about 40m (i.e. that is how deep the ray paths interrogate the earth) but the good data is seen only up to about 25m, we see this since very few rays are going past the 25m mark. The spread length was 96m so the data is getting down to 1/3rd the depth vs. spread length ratio. The only anomalies that are considered are the ones that should be within the Fresnel volume of the rays and anything outside the ray coverage of most rays will be ignored.

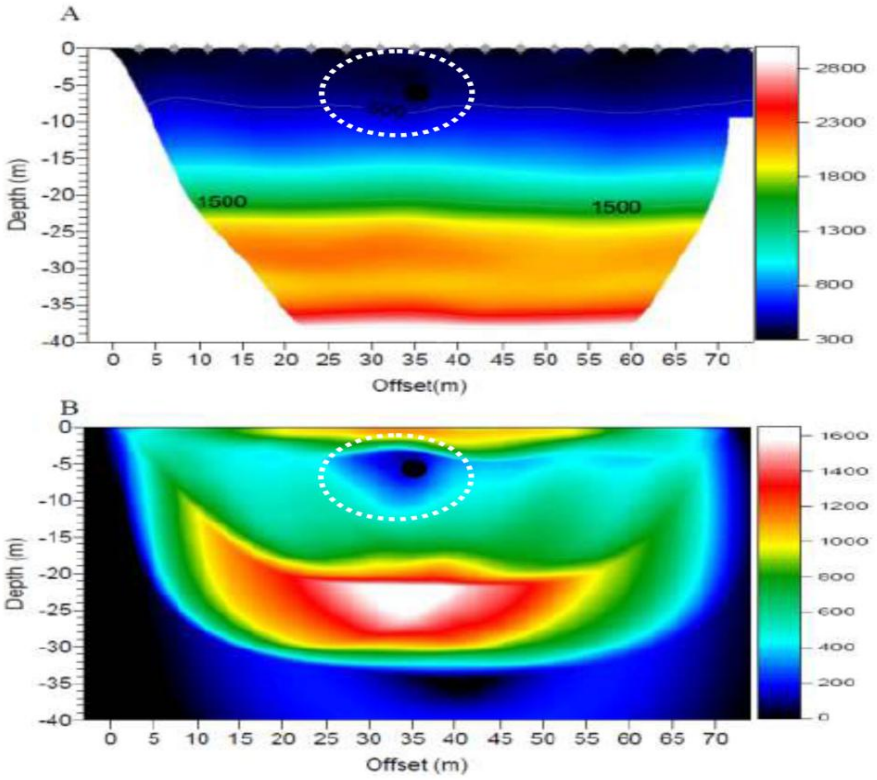

Figure 6-4 This is the seismic refraction result for tunnel 4 where Top) Refraction velocity image. Bottom) This is the ray coverage map. The black dots are the approximate location of the tunnel. The highlighted region highlights the anomaly. The inversion used a 1D gradient initial model and 20 iterations

The first arrivals had all data inverted for the entire data set where we had approximately 7000 rays for this region. The high resolution spread was then inverted with 20 iterations using the (WET) tomography from Rayfract™ where we assumed a vertical gradient mode. The initial model is based off the Linear move out velocity (LMO) which is the velocity taken to flatten the first arrivals, this is just the arrival speed of the direct wave. The gradient model is a vertical change in velocity that assumes constant horizontal velocity. Looking at figure 6-4 we can see both the velocity tomogram and the ray density coverage from the finite difference modeling. Looking at the velocity structure we can see some perturbations and some long wavelength changes in the horizontal direction but only a slight drop down in the velocity structure. This is similarly to what was seen in other subsurface void test sites, such as (Cardarelli et al. 2010, Belfer et al. 1998, Karaman and Karadayilar 2004), and realistically it is difficult to show the existence of the tunnel from this tomogram alone. What is more interesting, however, is the ray density coverage image that has a region of low ray coverage in the vicinity of the tunnel. This is anticipated because, as discussed in the earlier theoretical sections, the velocity of the air in the tunnel (~343 m/s) is substantially lower than that of the surrounding earth materials (~600 m/s), and as such the first arriving rays cannot pass through the tunnel. The low ray coverage does give an indication of the tunnel. However, similar to what was seen by (Sheehan et al. 2006b), the region sensed in the tomogram is actually much larger than the tunnel itself likely due to its disruptive influence caused by the regularization prgoram.

6.3.2 Tunnel 6

Tunnel 6 at a depth of 6.5 m, had similar dimensions and construction to Tunnel 4 above, but was not detected a tunnel with the initial survey geometry and processing. The reason for this is that the spread length used the same as for Tunnel 4, was 96m with 1 m geophone spacing but in this case because of the differing velocity conditions most of the rays penetrated at least to 15 m which is below the level of the tunnel. The tunnel anomaly is technically there but due to the masking of velocities by the color map the small change in velocity and ray coverage made it not possible to see the tunnel at first glance. To get around this the tomography only

used stations 32-72 and with the corresponding shots. This was just a perception issue and used to be able to be see the tunnel anomaly with the naked eye. We can see this in figure 6-5 where we have the refraction tomography for tunnel 6 and the ray coverage. If we take the rule of thumb of ¼ the spread length is equal to the depth of investigation then the data is still good to 10m and the tunnel location is 6m. Figure 6-5 shows that the velocity anomaly has a significant drop down in velocity to the other layer and the surface seismic velocities are on the order of 400m/s. This makes sense as to why we don't see the tunnel in a clear fashion since the surrounding rocks have a similar velocity and looking at the ray tracing map we can see that there are vanishingly few traces going through the approximate location of the void while the rays bend around it both on top and below. Therefore both refraction and ray coverage show a presence of a slower velocity and thus an indicator for a tunnel.

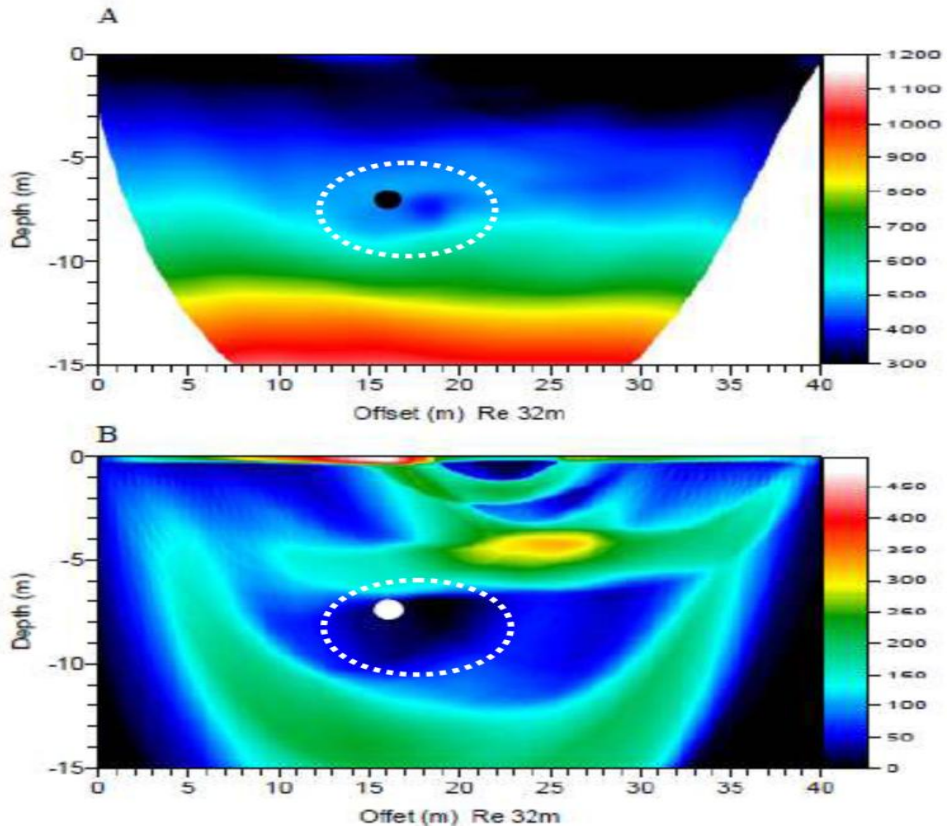

Figure 6-5 This is the refraction tomography of tunnel 6 where Top: is the refraction tomogram and Bottom: this is the ray coverage of the plot. The tomography has had its spread shortened to zoom in on the site and since most rays were going in past 15m so the spread is shortened from

station 32-72. The white and black circles are the approximate location of the tunnel. The inversion used a 1D gradient initial model and 20 iterations

6.3.3 Tunnel 1

Tunnel 1 site was the deepest and also one of the largest tunnels at Oxford, MS. The spread length that was used was 120m with a 1m geophone spacing and 1m shot spacing. The accelerated weight drop was used in this survey and had enough energy to produce acceptable first arrivals across the entire spread with just application of a low gain applied. The first arrivals were clean and only a minor batch of bad geophones had to be killed for the tomography. In figure 6.6 we can see the approximate velocity tomogram and the ray coverage plot for this tunnel location, the black dots are indicative of the approximate location of the tunnel. What we can see is that around the location of the tunnel there is no significant drops down in velocity, and in the ray tracing, a large amount of rays are actually traveling through the location of the tunnel. The near surface velocities range from 400-800m/s which is still faster than that of air and the rays that trace nearly all go at least 15m deep. Looking at the ray coverage we can see that we have and a reliable inversion down to about 30m and an acceptable solution all the way to 45m in some parts. This test shows that the seismic image here has past the ray limits for this survey site and was not able to detect the tunnel. The velocity model just shows some slight horizontal variations, but mostly only a general increase in velocity with depth is calculated. With post processing the same result was found when trying to lower the spread size since the rays around the tunnel are indicating that there is a faster anomaly there and not a slower one. The interpretation here is that the resolution of the seismic wave cannot detect the presence of a tunnel; this tunnel is just too deep to be detected in this environment. The combination of loose gravel and slow near surface materials results in steeply propagating waves that travel to deeper depths with the result that the ray path coverage through the tunnel is limited. The data collected was good and the first arrivals that were used were consistent and had very few poor picks.

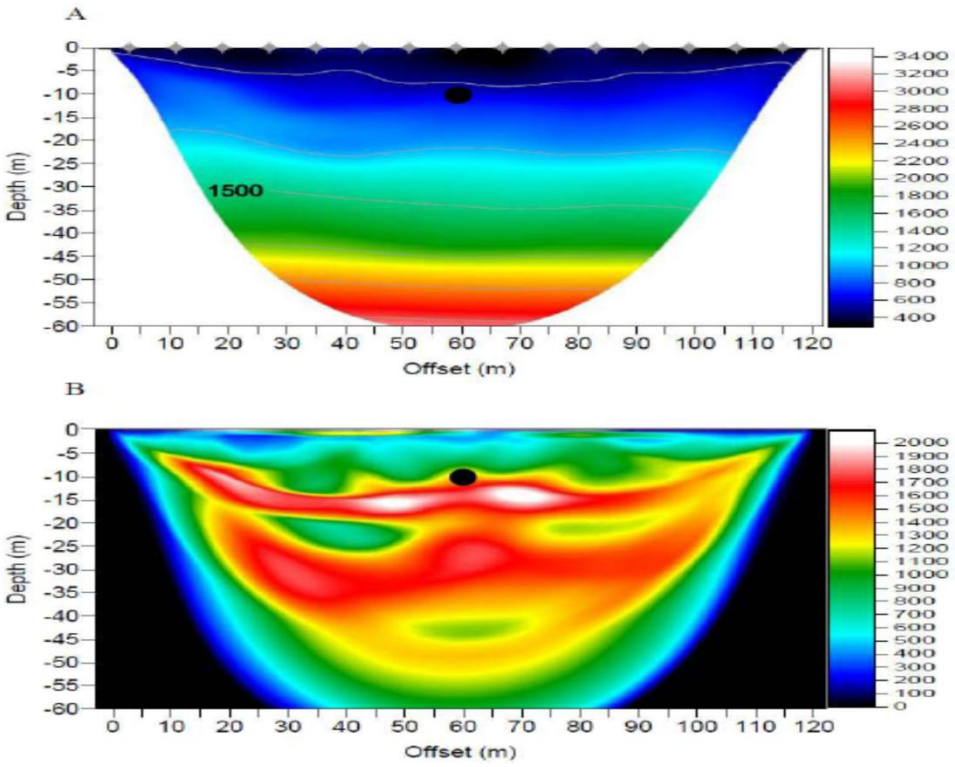

Figure 6-6 this is the tunnel 1 location, this site has an approximate tunnel depth of 10-12m and is a approximately 1m wide. Top: refraction tomography of the subsurface of depth up to 60m. Bottom: This is the ray coverage plot showing how the rays traveled through the subsurface. The inversion used a 1D gradient initial model and 20 iterations.

6.3.4 Discussion

nine different test sites were measured at Oxford, MS (see Appendix for details of each site). The tunnels that could not be detected were Tunnels 1 (as just shown) and 8 and the dam site. Although some of the remaining sites required additional processing the existence of the tunnel, or more precisely the zone of disturbed materials surrounding the tunnel, was detected. The most important finding of this investigation is that the ray coverage density maps highlighted the location of the tunnel much more effectively than the velocity tomogram itself.

Additional processing was not successful at the Tunnel 1 and the dam sites. This is likely due to the fact that the near surface conditions did not allow sufficient

refracted energy to be detected properly particularly with the contamination of high amplitude surface waves to the record.

Unfortunately, this study is not yet able to come up with definitive indications of the existence of tunnels. Even in some of the 'successes' the evidence for the tunnel, known to exist in reality, is tenuous; and complementary schemes to reduce the failure of the detection (both false positives and negatives) is necessary and will be discussed in the next chapter. The experiences gained at Oxford were then taken to Douglas, AZ to help increase the chance of finding the tunnel site there. The key factors that were changed in acquisition for the Douglas site were,

1) Using a sledge hammer as the source to limit the effect of lateral ray tracing of the seismic waves.
2) Further use a sledge hammer as the source to decrease the noise produced by the engine used to operate the hydraulics of the weight drop source.
3) Use broader band geophones with a lower frequency cutoff geophones in order to increase the sharpness of the detected refracted pulse.
4) Decrease geophone spacing to help increase lateral resolution and allow for denser ray path sampling.

These were some of the key findings in the Oxford, MS result and then more seismic data was collected at the Douglas, AZ test site

6.4 DOUGLAS, AZ

Urban barriers of fences, paved roads, ditches, and the significant barriers at the border itself over the allowed for a survey on the roadside and a survey in the ditch to be carried out.

The roadside data site was along the road parallel and adjacent to a high wire metal fence. The surface consisted of hard gravel that was difficult to properly plant geophones in. The geometry of the paved streets forced the centre of the geophone profile to be offset from the tunnel. Nearby traffic noise was a minor irritant at this site also. The roadside site was further interesting in that a number of

shallow boreholes had been emplaced by earlier researchers who had hoped to use cross well tomographic methods to image the tunnel, but to our knowledge this work has never been made publicly available.

The other location is known as the ditch site and it was carried out in a deep ditch running parallel to the road, the ditch had been recently dug to provide an additional barrier to crossing the US-Mexican border and fortunately had not yet been paved with concrete. This site too was contaminated by traffic noise on a busy parallel road immediately across the fence in Mexico, although the depth of the tunnel appeared to reduce this problem.

In the situation in Douglas, AZ we have the roadside borehole tunnel site has the refraction tomography done by SeisOpt® Pro™ software (provided by Optim Software and Data Solutions, USA), this was due to the capabilities of the program to handle borehole tomography. The refraction data along the surface seismic was done by Dr. Craig Hickey using the Rayfract™ software. The seismic was collected using both 14Hz and 40Hz geophones and both surveys used hammer seismic as the main source.

6.4.1 DITCH DATA

The seismic data that was collected in the ditch just consistent of two surveys in which the 14 Hz or the 40 Hz geophones were used. As indicated in the last section, this was just a test to see if the seismic refraction arrivals did indeed depend on the frequency of the geophone and if our results were skewed. What was found is that both geophones gave very similar results and the tomography is nearly identical. The higher frequency phones had less ground roll but the signal amplitude was comparable to the that obtained with the 14 Hz geophones. The ditch profile was a 48m seismic spread with 96 geophones spaced at a 0.5m; the tighter sampling was used to help increase resolution again as recommended on the basis of the earlier Oxford surveys.

Another difference between the Oxford and Douglas surveys is that in the former the locations of the tunnels or culverts were unambiguously known as they

could easily be seen. As the tunnel was completely buried at Douglas, and because no exact information was available on its exact location, we could not guarantee that the observing geophone profiles were centered. The advantage of this is that it was closer to a true blind survey.

Two shot gathers are shown for example in Fig. 6-7 with the source either near the end or at the this result has a mean scale applied and a slight gain attached, the desired first arriving refracted signal is good but there is substantial surface wave energy. No reflections can be seen in the data and any reflections that would come off the tunnel would be in the top 100ms.

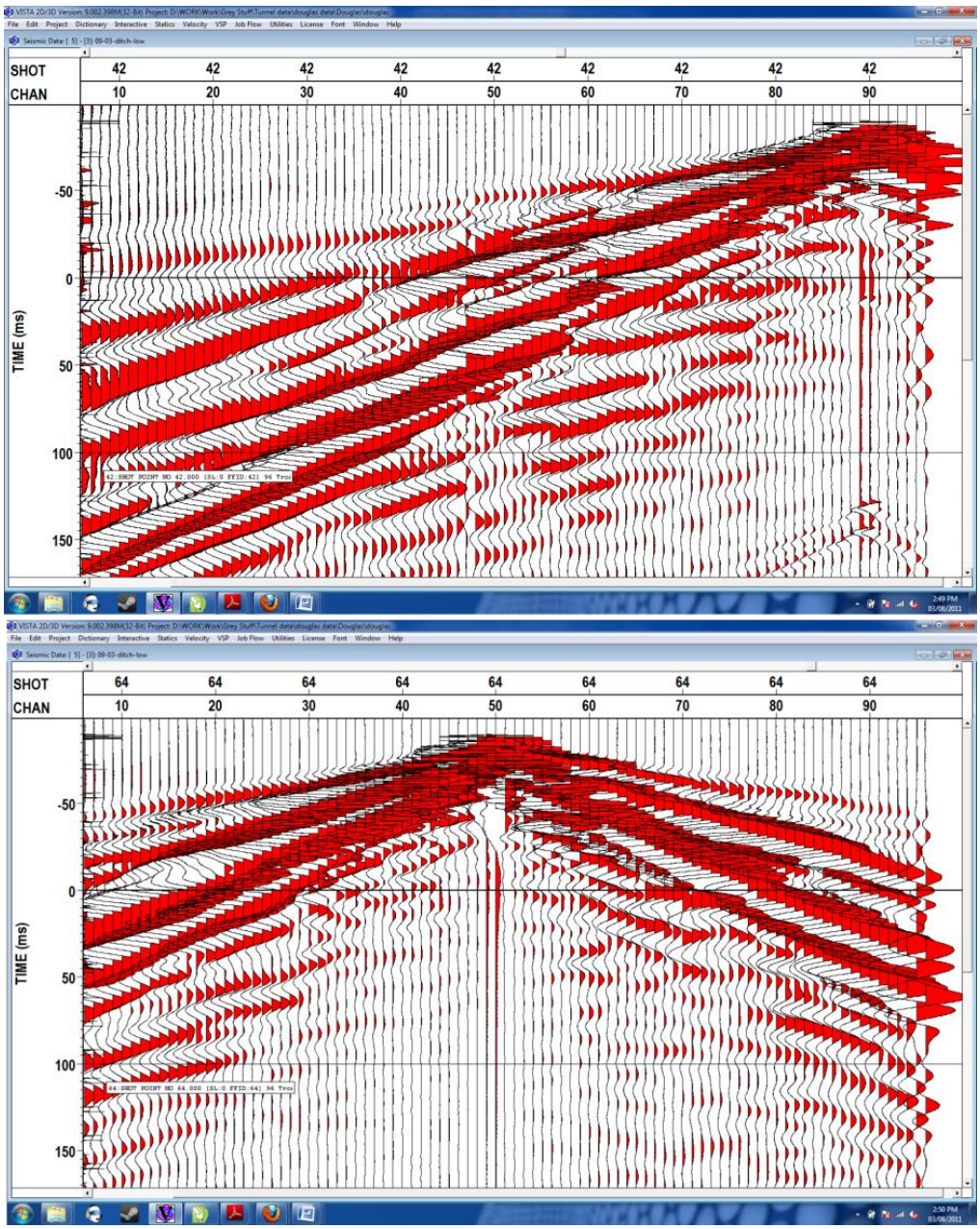

Figure 6-7 Sample shot gather for the Douglas, AZ ditch data using the 14Hz geophones. Top: this is at shot record 42 where we have the shot at the 90th channel or 3m into the spread. Bottom: This is in the middle of the spread where the shot is at channel 50, or 25m into the spread. The first arrivals can be seen clearly and only a gain and a mean scaling were applied.

The seismic data initially had the first arrivals automatically picked and then the bad ones were manually picked to the correct times. Overall, this set consisted of 97 shots with the 96 receivers that resulted in 9312 first break time picks deemed acceptable for the inversion. The starting model was the 1D gradient model and an

initial 20 iterations were done for the ditch data. The result can be seen in figure 6-8 where the velocity tomogram is displayed with two anomalies located on it. These anomalies are come from the ray coverage plot where we see a zone of low ray coverage. The approximate velocity of this tunnel site is significantly higher then what was seen in the Oxford, MS test sites, at around 1000m/s the ray coverage plot shows that most rays are traveling though around 10m down and very few rays go below this point. The two anomalies are labeled have, S1 which is around the center of the spread and S2 which is on the end of the spread. Both these anomalies were marked since the result could in fact be another tunnel.

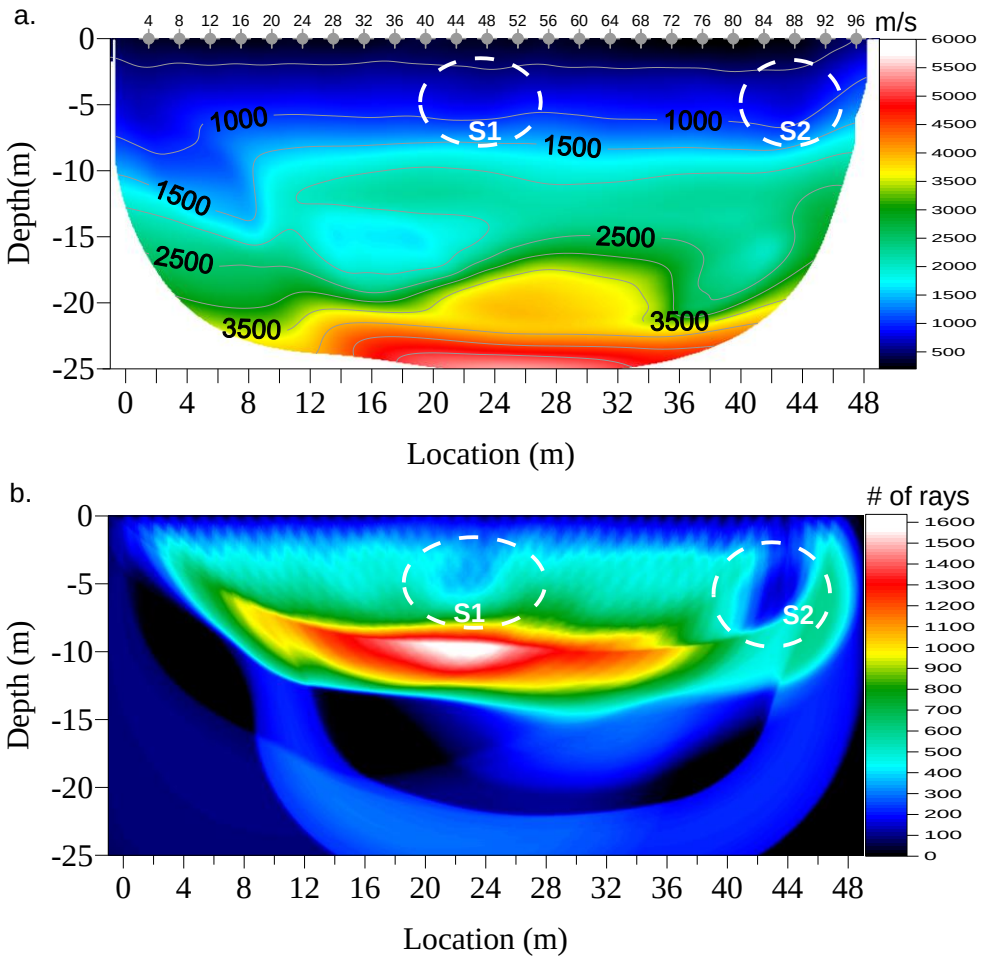

Figure 6-8 This is the refraction tomogram result for the ditch data in Douglas, AZ. Top: the velocity tomogram which is a vertical cross-section of depth vs. surface location. Bottom: This is the ray coverage plot of how the waves traveled through the subsurface. S1 is labeled as a low velocity zone and is indicative of where the tunnel is and S2 is an unknown anomaly.

The tunnel location that we were looking for would be S1 in figure 6-8 and the location of this is slightly off the center of the refraction tomogram but approximately the right depth of around 5m in the ground. The seismic data was then reprocessed using a shortened spread length that focused around S1 anomaly. This is a perception issue so we can see how the ray coverage similar to what was done for tunnel 6 in Oxford, MS. using smaller offsets. To look at this we only used stations from 12m-36m giving ample coverage to see the anomaly. With this reduced data set, at 20 iterations the anomaly is still detectable but the image continued to improve with every additional iteration, The final result at 50 iterations can be seen in figure 6-9 where we have in the top the velocity tomogram, the middle the ray coverage plot, and the bottom and threshold ray coverage plot to better delineate the paucity of ray density at the tunnel location. The tunnel anomaly can be seen 1.5m off the center of the spread, the velocity image shows a drop down at about 6m depth. The ray coverage takes a banana shape with an elongated circle in the middle. The threshold ray coverage plot is used to better delineate the tunnel for easy referencing, this is done by just setting a maximum amount of rays that can go though and once you are at the minimum threshold then that should be the region of the tunnel. The data shows the approximate location of a low velocity zone quite well which is around the tunnel location, the next site in the roadside has the tunnel quite a bit deeper and the surface conditions are substantially more problematic.

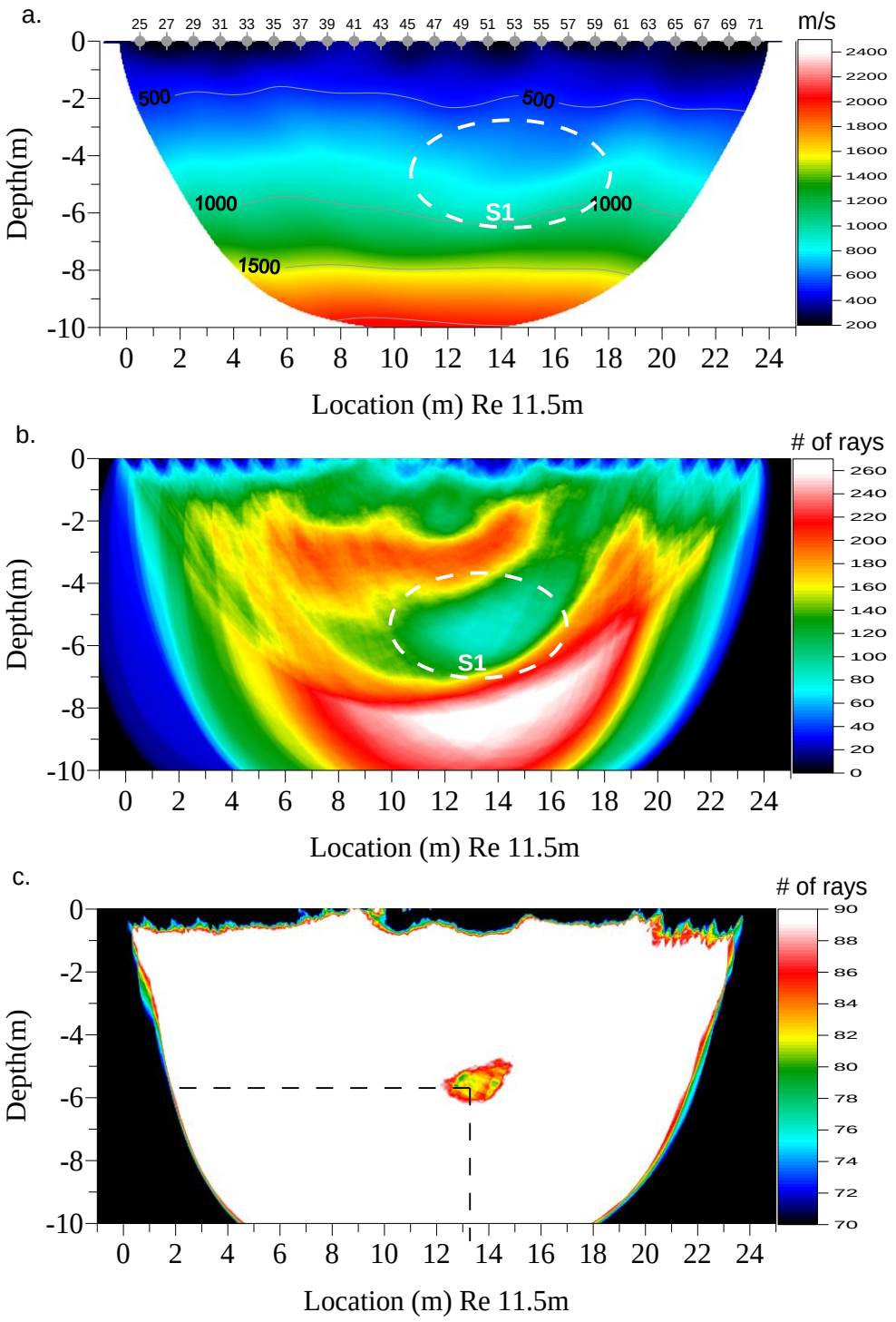

Figure 6-9 this is the refraction tomography for the Douglas, AZ ditch site with reprocessing to enhance the S1 anomaly seen in figure 6.8. Top: This is the refraction velocity tomogram showing the approximate location of the S1 anomaly and also shows the dropdown in velocity seen. Middle: this is the ray coverage plot of where the rays traveled through in the subsurface. Bottom: this is the threshold ray coverage plot showing the location of least amount of rays traveled. The hot spotting technique makes a bulls eye around the tunnel.

6.4.2 ROADSIDE SURVEY

The Roadside survey was much more difficult to implement. The near surface was more heterogeneous and there was substantially more traffic nose. In particular, the necessary first arrivals were highly attenuated at distances greater than about 40m from the shot point primarily because wind and traffic noise amplitudes were comparable to the signal. The seismic data could only be obtained 18m to the west side of the spread due to a paved concrete road.

However, a number of shallow boreholes were drilled for cross bore tomography, and during the surveys a downhole geophone package was placed in them to assist in characterizing the site. The dowhnhole tool consists of 3 geophones mounted on a weighted gimbal system that allowed one vertical and 2 horizontal components of the wavefield to be obtained. When a seismic shot was taken we get a direct 1–way travel time and thus the results give accurate velocity information. The seismic profile was 60m long with a 0.5m geophone spacing, the tunnel was located approximately 18m from the west end of the the spread. The borehole in which the geophone was emplaced was approximately 12m into the spread. Multiple shots for purposes of stacking were taken every 1m. As noted, the energy transmitted across the array was significantly attenuated due to poor coupling of the geophones to the hard ground and due to the low energy source employed. Consequently, not all of the first arrivals could be reliably time picked on the eastside of the data set.

The seismic survey carried out for the seismic refraction tomography shown in figure 6-10 used 14Hz geophones, and the seismic data was inverted commencing with a 1D gradient and 20 iterations. Refraction result shows that nearly all the rays are traveling through to 5m of depth with, regrettably, few are going any deeper. The velocity tomogram does not show the same anomaly it shows an increasing velocity with depth, this just follows what the initial model was. The few rays that go through that cause the model to not be updated and thus we won't get a good idea how the velocity changes at this test site. This reduction in depth of investigation could be a result of a zone of better cemented sands and soils as were seen in the

drainage ditch walls. With this the tunnel site most likely won't be able to be detected using seismic refraction techniques or using the first arrivals, other techniques are needed to detect the tunnel.

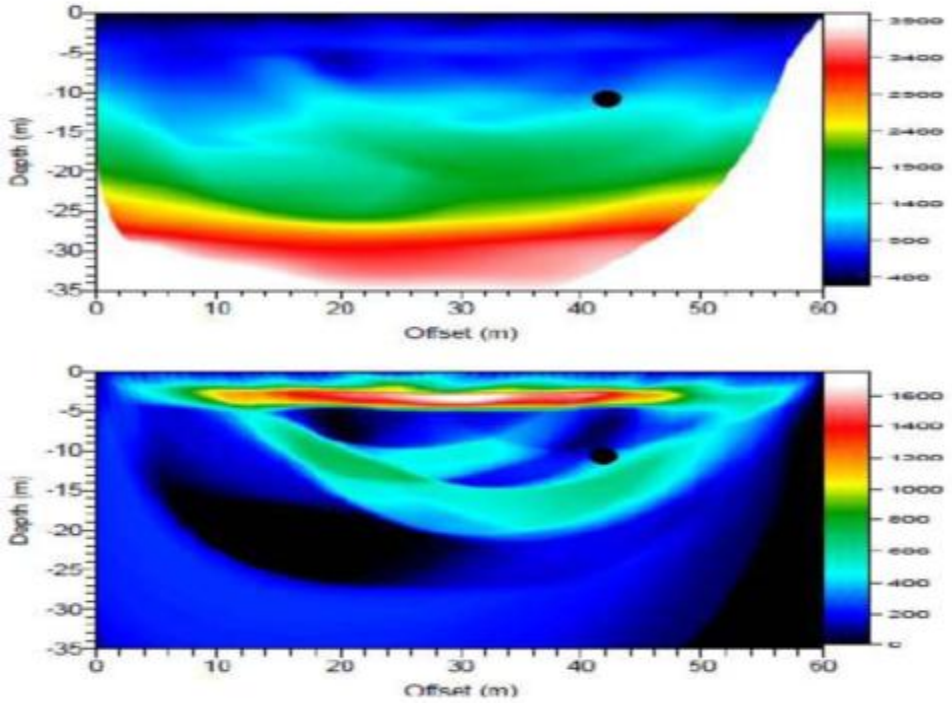

Figure 6-10 this is the roadside refraction tomography result using 20 iterations and a 1D gradient used. Top: this is the velocity image showing the location of the tunnel at around the 42m offset range and 10m depth. Bottom: the ray coverage plot for the seismic that was recorded. Most the rays are getting trapped at around 3m down, and thus the tunnel was not imaged.

The other data that was collected on this site was the borehole data, which was used a 1 station walkway seismic survey. This technique is known as vertical seismic profiling (VSP), where we have a constant receiver location and the source location changes. The goal was to see if the direct arrival of the seismic wave could detect the presence of the void and see if the wave bends around the tunnel. The little amount of data and small geometry made it possible to use SeisOpt™. We did this an initial model of constant velocity of 1000m/s and iterated the procedure until the tomography converged on a result. The inversion took around 2 days to run on 1 windows computer, which has a dual core Pentium 4, 2.0Ghz processor with 4 Gb of ram even with their being only 100 first arrivals to fit. The result can be

seen in figure 6-11 where we have the borehole and the approximate tunnel location specified. The tunnel is approximately 10m in depth and at 18m on the surface. The length of the spread is large since some far offset data was acquired for this result. The borehole shows that some of the velocities are curving around the tunnel which is actually a faster velocity. The truth here is that no rays are going underneath the tunnel expect some of the far offsets so the tunnel location is not truly seen. The results show that if another downhole tool was place in a borehole on the other side of the tunnel then there could be solid evidence e for the tunnel. Looking at the velocities though we see that there is a change from about 400m/s to 800m/s at about the 7m mark in the subsurface, this could be the velocity change that was seen in the surface seismic data. As you can see the simulated annealing approach also shows lots of holes and false artifacts in the data.

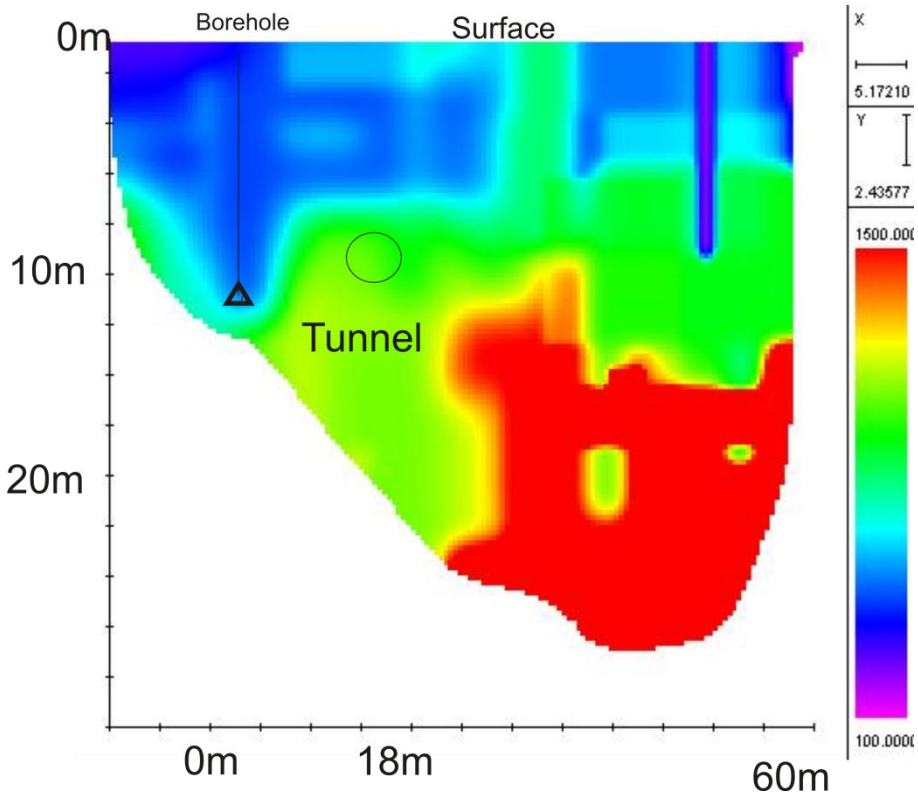

Figure 6-11 This is the borehole tomography using far offsets in the model. the tomography is zoomed in onto the length of the spread. The approximate location of the tunnel is shown and the velocity bending around the tunnel can be seen. The rays are all above the tunnel location and very little data goes below the tunnel site. Only some of the far offset data goes around the tunnel and the red velocities have no real rays going through it.

6.4.3 DISCUSSION

The results in Douglas, showed that refraction methods can be used to detect tunnels if the conditions are appropriate, but it also illustrates the limitations of the technique and the influence of noise, depth, and the actual geological velocity structure on the results. To some degree one good analogy to this comes from Sonar where it is well known that submarines can use the low velocity SOFAR subsea channel to avoid the interrogating ray paths and hence detection. Using smaller geophone spacing helped increased the resolution of the survey and increases the number of travel time picks. At least in the tests here, using different geophones proved to have little to no effect and the seismic traces gathered were quite similar. Shortening the spread helped improve identifying the tunnel due to making the window smaller but a large survey is still needed especially in cases where the actual location of the tunnel is unknown. The velocity drop down seen was still minimal but using the ray threshold coverage plot helped in zoning out possible zones of low velocity.

6.5 SUMMARY

The use of seismic refraction tomography has proved to be a useful technique in identifying subsurface voids, the methods of data analysis were dealt with were discussed in this chapter. The refraction method compared to what was seen in modeling shows that there is a reduction in velocity around the tunnel. The rays bend around the low velocity range of the tunnel and using the ray coverage plot we can use this as an indicator of a tunnel. This can be seen in seismic ray tracing and particularly evidenced by regions of low ray density coverage and, to a lesser extent, as zones of decreased velocity in the tomogram. The seismic wave does ‘see’ the tunnel as in most cases it is below the resolving limits at the wavelengths employed. The results in Oxford, MS showed that the tunnel could be detected in six out of nine sites and that in Douglas, AZ 1 out of 2 sites were detected

using surface refraction tomography. Failures are a results of differing aspects that include: 1) Ray trapping in the slow near surface materials that do not allow lower sections to be properly interrogated (e.g. Douglas Roadside), 2) Similarly, ray trapping due to velocity gradients that force most of the ray paths to go deeper than the tunnel (e.g. Oxford Tunnel 1), 3) high levels of cultural noise, and 4) tunnel is too small and deep. Additional processing for some sites was required because the anomaly was so small that additional processing was needed to further ensure that the 'detection' was really a false positive artifact. There were very few surveys that had the tunnel come out distinctly; and the reliability of the survey depended critically on the quality of the data acquired.

CHAPTER 7
7.0 JOINT INTERPRETATION AND FUTURE WORK

The previous two chapters discussed how seismic methods and electrical methods can be used to detect clandestine tunnels. The goal of this chapter at first is to show how using both electrical and seismic methods can be used to gather to help delineate artifacts, and improve detection. Then after this the future work will be discussed and how other methods could be used to help detect tunnels on the US-Mexico border. This is followed by some of the key issues associated with this study and how to resolve them such as repeatability, tunnel detection criterion for future work.

7.1 JOINT INTERPRETATION

The goal of this chapter is to illustrate how seismic and electrical methods can be used to jointly help delineate anomalies and also how they can be used more effectively. One crucial issue is that both ERT and seismic refraction tomography methods is that they detect multiple anomalies such as a highly resistive zone for ERT and or a low velocity zone for SRT but knowing which of these are actually tunnels or whether they are false positive indicators is difficult. The tunnel anomaly that is detected in a velocity tomographic image as an anomalously low velocity localized zone can be used to detect a subsurface tunnel. However in situations of poor data this can problematic as the experimental errors in the travel times could result in false anomalies in the final tomogram. In a ray density coverage plot we should see few rays in the presence of a low velocity zone, but the zone can be quite large. Further, depending on the local velocity structure, sometimes the rays are trapped by a high velocity zone, and don't go near the tunnel location. In electrical methods the subsurface void can full of air which is highly resistive anomaly or full of water, which can be a conductive anomaly.

In near surface studies the amount of near surface heterogeneity can cause the physical properties of the surface materials to change quite drastically due to

different levels of cementation and water saturation. The factors that will change the resistivity in partially saturated near surface rocks are the ionic concentration, porosity surface conduction, tortuosity and connectivity of fluid or conductive solid phases (Gueguen and Palciauskas 1994). For seismic methods the main factors that will change velocity in the subsurface are the lithology, the porosity, the fluid saturation, the pressure, and the temperature. (Yilmaz 2001). Both methods are sensitive to the porosity and fluid saturation, but in addition seismic methods are sensitive to the elastic parameters of the rock frame. The electrical methods are sensitive to the fluid motion and how the fluids move through the subsurface. Taking this into account the different methods are going to show different ways of detecting the tunnel and so should help discriminate between false and positive anomalies.

Using seismic methods and electrical methods to help delineate subsurface features have been done in the past to detect sinkholes (Dobecki and Upchurch 2006) or even cavity detection(Piro et al. 2001),(Cardarelli, Fischanger and Piro 2008). This method can be taken a bit farther and use electrical and seismic methods for joint inversion to help increase tunnel detection by (Cardarelli et al. 2010). All these studies found that using multiple geophysical methods increases the reliability of detecting subsurface voids. The electrical methods are very popular for void detection because of the contrast in resistivity's between air and near surface soils (van Schoor 2002). The situations where electrical methods won't work are when in zones of very resistive materials, this is due to not getting enough current through the rock. When in zones where the rock is very resistive it is generally indicative of stiff and fast velocity rocks which should help delineate seismic contrast with air (Cardarelli et al. 2010). The goal of using both these methods was to help make sure that the anomalies that were seen in both electrical and seismic methods were real.

To display these results the seismic and electrical results will be discussed in detail for the Douglas, AZ ditch site, and the Oxford, MS Tunnels 1 and 5. The reason the Douglas, AZ test was chosen was to compare the tunnel related anomalies that were seen in both the SRT and ERT images. The tunnel 5 site was chosen because two anomalies are seen in the dipole-dipole array and as such it is good to contrast

this result with the SRT images to see if it is actually a tunnel site. The Oxford Tunnel 1 site illustrates a case in which neither of the methods were able to find any anomaly related to the known tunnel.

The Douglas, AZ test site was already discussed in previous chapters but what we need to remember for this section is that both the electrical and seismic method was performed 3m laterally offset from each other and both had similar spread arrays. Briefly, the seismic tomography had 0.5m geophone spacing and 48m spread while the electrical method was a 50m dipole-dipole array with 1m electrode spacing seen in figure 7-1A. The electrical anomaly that was seen was inverted and two anomalies were observed E1 and E2 in Fig. 7-2C. E1 is the approximate location of the known tunnel, but anomaly E2, which is slightly shallower and 6m laterally offset, is very similar. Since the inversion creates both these anomalies so both have a legitimate chance to be the tunnel and if the location of the tunnel was unknown then the confidence of the tunnel would be low.

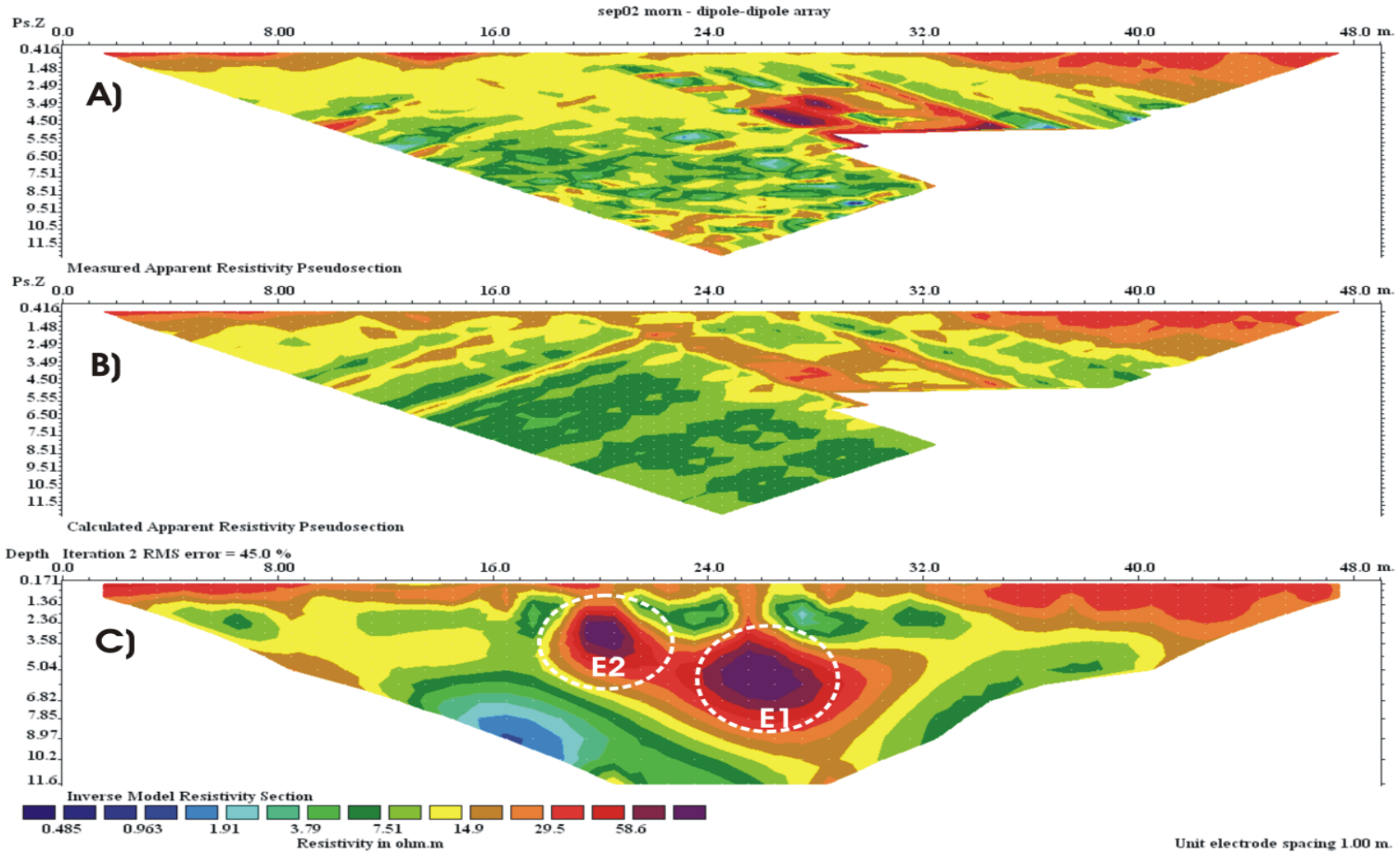

Figure 7-1 the ERT image for the dipole-dipole array in Douglas, AZ. Top: this is the measured apparent resistivity pseudosection. Middle: The calculated apparent resistivity pseudosection. Bottom: The inverse modeled resistivity section. The tunnel analogies are highlighted as E1 and E2.

The seismic profile was acquired 3m laterally offset from the ERT line. The initial SRT displayed two possible anomalies S1 and S2 in Fig. 7-2. In this case the two anomalies were both approximately 5m in depth but were laterally offset by 20m. Additional processing was carried out over the S1 anomaly but not at the S2 which was at the end of the spread. Looking at figure 7-2 we can see the velocity image with the anomalies S1 and S2, these anomalies are see a lack of ray coverage but display only a slight drop down in velocity. The ray coverage shows a small amount of rays not going through the tunnel area, the confidence in this plot is quite small if the location of the tunnel was not known.

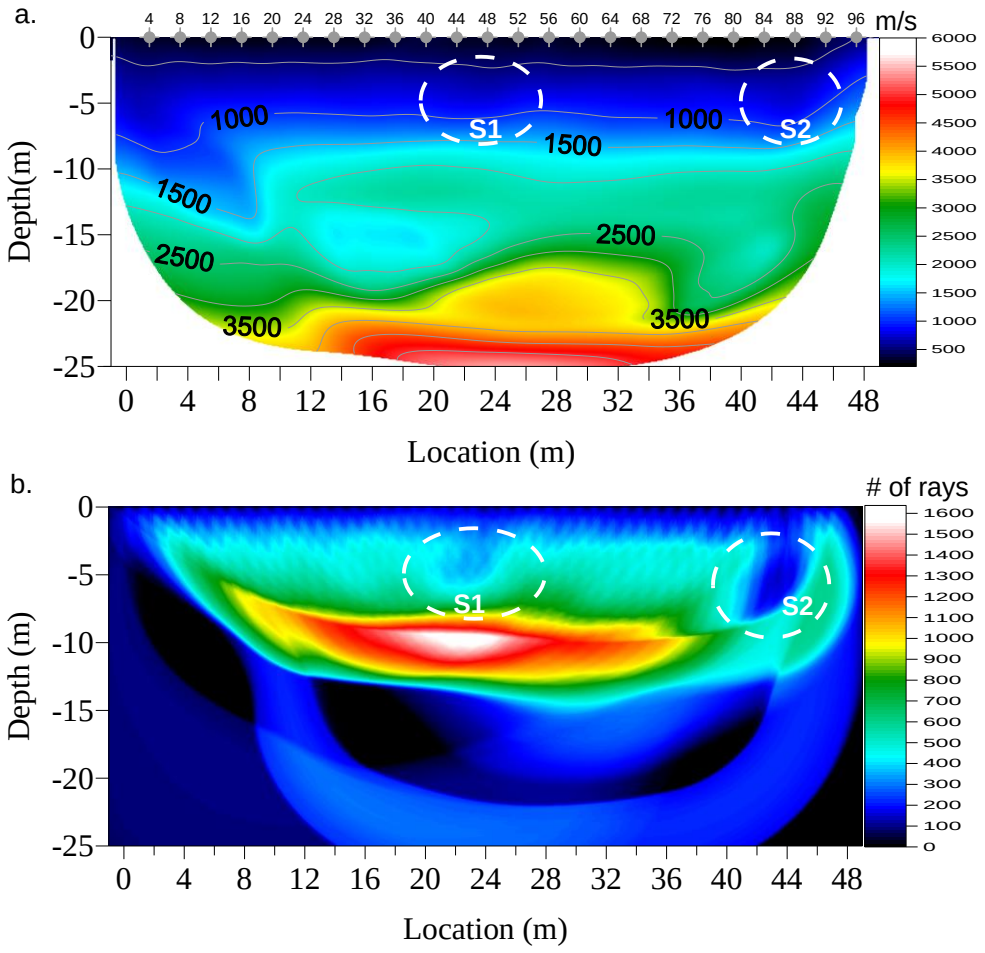

Figure 7-2 this is the refraction tomography for the ditch data in the Douglas, AZ test site. Top: This is the velocity tomogram for the surface with both S1 and S2 anomalies present. Bottom: this is the ray coverage, the two zone s of low ray coverage are the estimated tunnel anomaly sites

Looking at figure 7-1 and figure 7-2 we can see that the results show that both have a depth of investigation of approximately 12 m. The survey site shows the resistivity of surrounding rock around the tunnel ranging from 10-30 Ω.m while the seismic velocities range from 200-1000 m/s. The resistivity's are smallest nearest the surface and increase with depth which is indicative of having an increasing value of water content in the rock, around 10-15m of depth we have a velocity of around 1500-2000m/s which is indicative of fully saturated sandstones (Gueguen and Palciauskas 1994). The resistivity decreases with depth which may indicate increased fluid content in the sandstone, thus the location of the tunnel is in partially-saturated and relatively well consolidated. Promisingly, the E1 (high resistivity) and S1 (low ray density) anomalies match position well. In contrast, the E2 anomaly is resistive but there is no corresponding seismic velocity or ray coverage density in this location. The region around site S2 is fairly resistive compared to other areas but show no resistive anomaly at this location. The interpretation of the tunnel site makes sense and by using both electrical and seismic methods have helped increase the confidence in detecting this tunnel location.

Oxford Tunnel 5 was an interesting site since the culvert is only 2m deep and generally most of the other survey sites were a lot deeper. The electrical used was 3m laterally offset from seismic array, and the seismic survey was only 24m long. The apparent resistivities from the dipole-dipole array can be seen in figure 7-3 where the 1m dipole-dipole electrical array is found and the electrical survey shows 2 resistivity anomalies where the approximate location of the tunnel is in the middle of these tunnel sites. We saw that in chapter 5 that the electrical array does show the presence of the anomaly but we can see is quite large anomaly for only a 0.4x0.4m size tunnel.

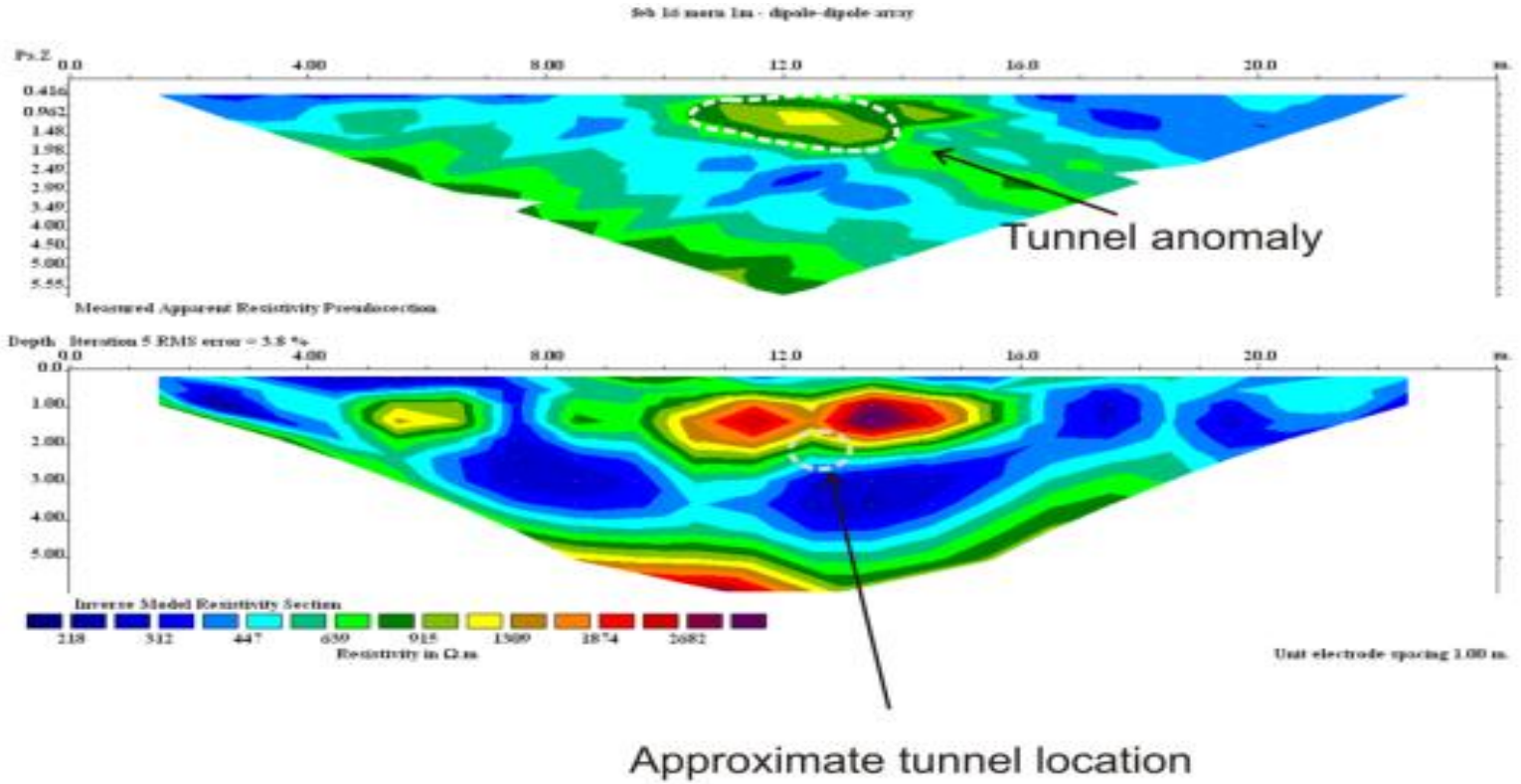

Figure 7-3 this is tunnel 5 of the Oxford, MS test site culverts; the tunnel is approximately 2-3m deep and 0.4x0.4m in dimensions. Top: The measured apparent resistivity pseudosection, there is 232 data points on a 25m dipole-dipole array with 1m electrode spacing. Bottom: this is the inverse model resistivity section of, where the approximate location of the tunnel is indicated.

Its seismic data was not discussed in Chapter 6 so a brief overview will be given for the tunnel 5 test site. The seismic data that was gathered was 28.8m long and the seismic data had 0.6m geophone spacing with shot spacing of 0.6m. The seismic refraction arrivals were collected with the sledge hammer source had good energy throughout the whole spread; the velocity tomogram and ray coverage can be seen in figure 7-4. The tunnel anomaly is indicated by the low ray coverage while there is only a slight velocity perturbation and not even at the approximate location of the tunnel.

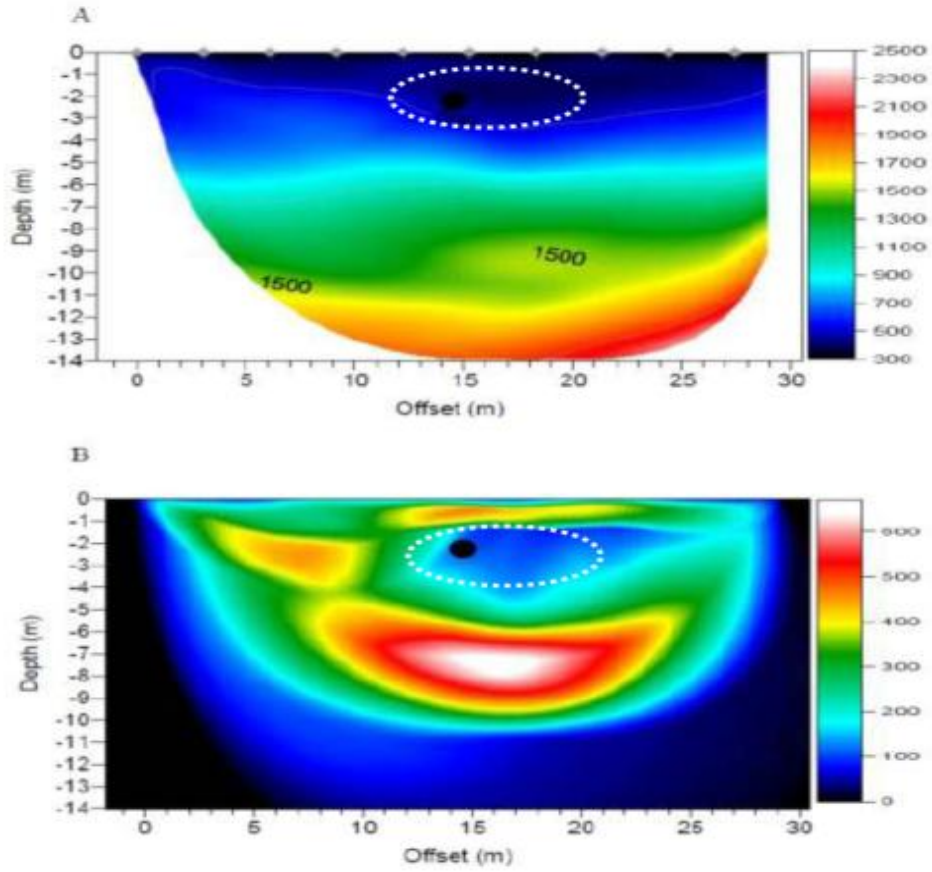

Figure 7-4 this is the refraction tomography for tunnel 5. Top: This is the velocity tomogram for the site; the tunnel is approximately 0.4x0.4m and is only 2m deep. Bottom: the ray coverage of the seismic site.

The tunnel anomaly seen in figure 7-4 shows a large zone of low ray coverage and in comparison to figure 7-3 this is near the same position as the resistive anomaly. The tunnel site in this location was only 0.4x0.4m in dimensions

and it was partially filled with debris. This might be the reason why the anomaly that is seen is so large and deals with that this whole region may be a region of quite low velocity. The reason the velocity barely changes in this region is that the velocity around the tunnel is approximately 200-500m/s which is similar to that of air and thus the velocity model won't change. The low ray coverage is just showing that most the energy is traveling along the surface and then to the competent material below the tunnel. Looking at the resistivity model we can see that the resistivity of the tunnel anomaly is quite large and the resistivity of the surrounding rock is around 200-500Ωm. This evidence shows that the anomaly can't be partially saturated with water and the zone is probably filled with loosely consolidated sands with little to no water in this region. The area is still disrupted so the tunnel site is predicted to be quite large and possibly could have been constructed or has been worked on recently. With both of this information the tunnel anomaly can be confidently be detected with a velocity, low ray coverage zone and a highly resistive region.

Tunnel 1 was the deepest tunnel site and also one of the few sites that seismic and electrical methods could not find any indication of the tunnel. The reason for this makes more sense when looking at both the electrical and seismic methods. Looking at figure 7-5 we can see the velocity tomogram for tunnel 1 site, the location has the approximate location of a zone of fairly consistent velocity and

the tunnel a location of large amount of rays traveling through it.

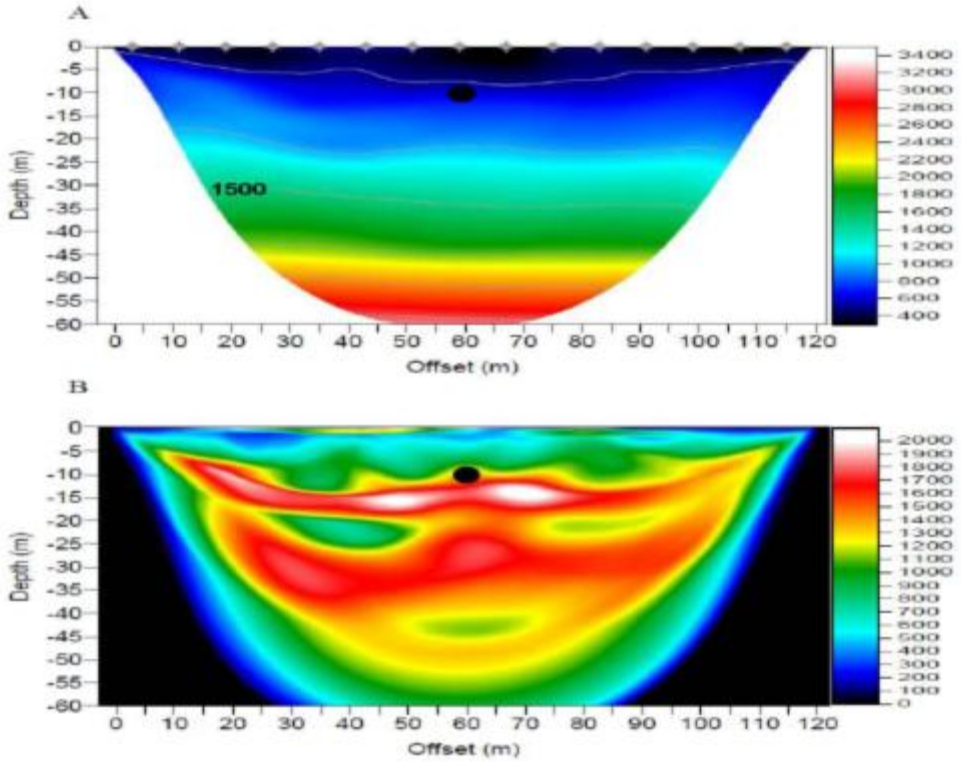

Figure 7-5 this is the refraction tomography for tunnel in Oxford, MS. Top: the velocity tomogram. Bottom: The ray tracing plot. The black dot is indicative of the approximate tunnel location.

This was one of the few sites where the Wenner array and a dipole-dipole array were both done over the seismic profile. The Electrical array was 100m similar to that of the seismic array which was 120m. The Wenner array can be seen in figure 7-6 where we see that on the left hand side of the array we have a resistive material and then on the right hand side we have a region which is less conductive. The region on eh left is fairly resistive with an approximate resistivity of about 750Ωm and the right side as an approximate rock resistivity of 200Ωm.

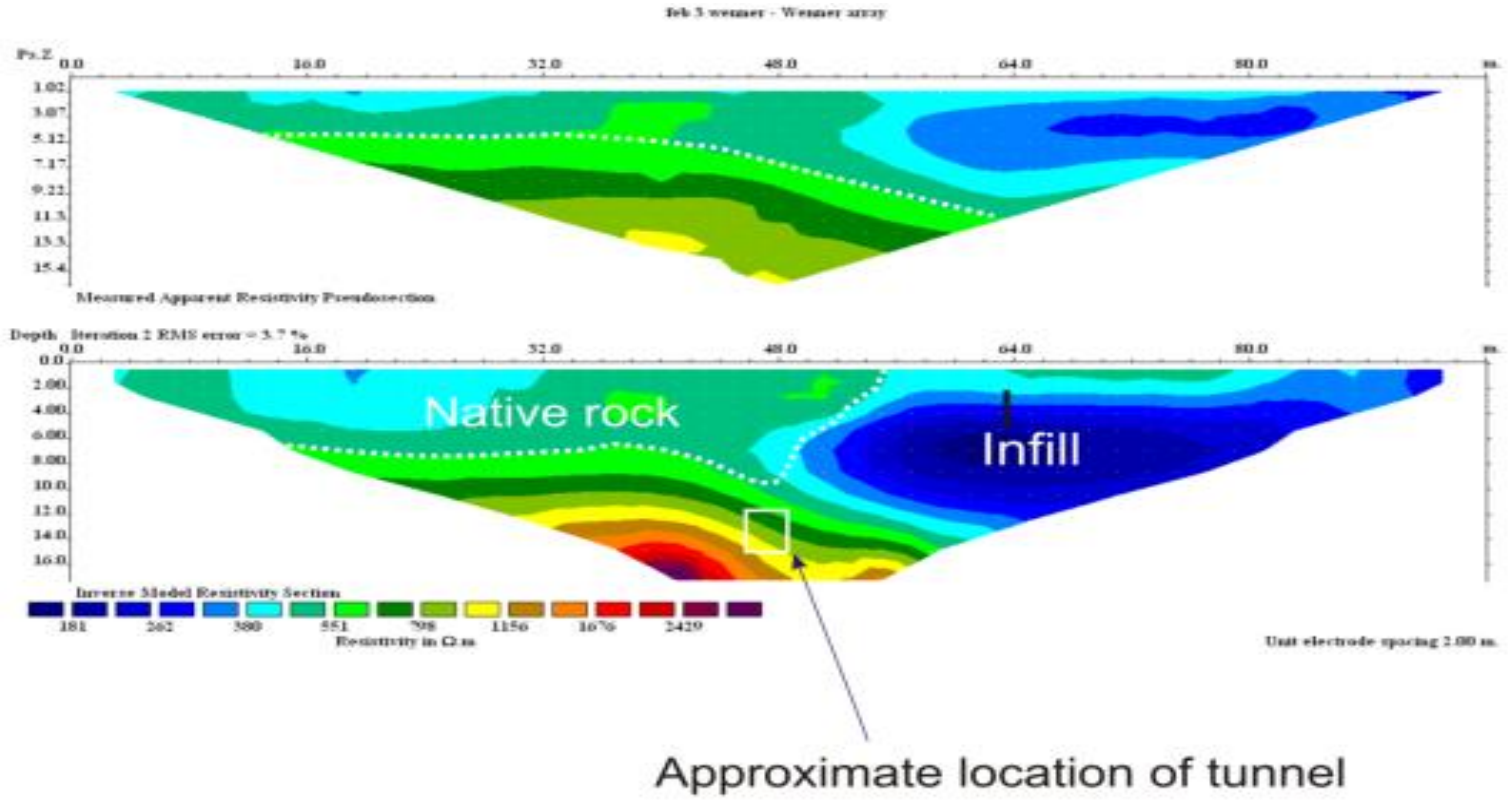

Figure 7-6 this was the first survey performed site in Oxford, MS and was also the largest. The survey has 2m electrode spacing with 100m Wenner array. Top: This is the raw collected data gathered over the first tunnel site. Bottom: This is the inverted pseudosection for true apparent resistivity

Both the SRT and ERT methods could not detect the presence of the tunnel, the tunnel was quite large but still nothing is detected. When looking at figure 7-6 two regions of the reisitivty array are indicative of two diffferent materials. When we look at figure 7-5 we can see in contrast that the seismic image is more laterally uniform with a consistent velocity.. The ray coverage plot shows that most of the rays are traveling beneath the tunnel to about 12-15m depth and then coming back to the surface. The ray coverage shows that there is a consistent amount of rays traveling at least 15m deep but some go as deep as 30m. The change of resisitivity of the differnet sides of the tunnel site can be seen in Wenner array, but the seismic tomogprahy does not take that into account. The site was believed to have had some repairs done to it after the insertion of the tunnel, but the material that filled must have been the same material prior to constuction. The interesting thing is that the construction appears to have happened all the way from the tunnel to point past the seismic line. The seimic refraction methods sees very little evidence for this and thus other seismic methods or electriical methods would be critcal . Other tehcniques that don't use the first arrival energy or tehcniques that use surface waves might be more benfiical to help detect some of these tunnel sites.

What was shown is that using seismic refraction and electrical methods can help delineate some artifacts that are seen in the data. Using multiple geophysical techniques can also help increase the likelyhood that your anomly is true or also can be used to help understand why the method did not work. All the tunnel sites had both the electrical and seismic tomography methods looked at side by side to see if the tunnel was truly detected and also to see if any intricacies could be used to help improve the interpretation.

7.2 Future Work

The goal of this thesis was to test the ability of seismic refraction and electrical resistivity tomography to find subsurface tunnels. While using refraction methods other seismic methods were entertained and tried to see if we could detect the presence of the tunnel. Other seismic methods were tested but could be taken further to try and get a better idea if other seismic methods would work better.

The first was to use reflection profiling to detect the tunnel. To do this a conventional processing scheme was used but the noise removal of the data could not remove the actual reflection of the data. This was tried and the technique did not see any reflection energy so the method could not be used. What was seen in the modeling chapter was that the tunnel should be able to diffract the energy and act as a scattering point for and treated as a reflection on the surface. Numerous studies have found that you can use reflection profiling to detect abandoned mines (Yancey et al. 2007, Curro, Cooper and Ballard 1981) or delineated karst cavities. More advanced processing techniques in which the reflection profile is migrated to collapse diffractions have shown some promise in detecting voids. (Grandjean and Leparoux 2004). The main problem with using the reflection method to detect tunnels is that the tunnels are small relative to the wavelengths of the seismic energy such that they cannot really be properly imaged. Another series problem is that any reflections coming from the tunnel are usually swamped by the much stronger direct refractions and surface waves that will arrive at the same time.

An alternative approach may be to attempt to image the diffracted seismic energy scattered by the tunnel. The full elastic wave modeling of Chapter 4 showed two strong diffractions: a P-wave diffraction and a P-SV diffraction. These diffractions occur because the large variation in the impedance between the tunnel and the surrounding earth materials causes it, by Huygens's principle, to act as a new point source. This incoming wave could possibly diffract and create both a shear and a compressional component (Meier and Lee 2009). Knowing this studies have used the diffracted wave to help delineate a void (Keydar et al. 2010), or to gather the velocity and depth of a diffraction (Xia et al. 2007). Referring back to the models of figure 4-7 we can see that the P-SV wave diffraction later than the surface wave and the first refracted arrival, hence in principle it should not be as easily masked as the pure P-wave diffraction To help enhance the diffraction methods of using radon transforms are used to separate the surface and primary wave energy and also the diffraction (Bansal and Imhof 2005). Once the diffraction is enhanced then the detection can either image using the migration techniques to collapse the diffraction to a point (Keydar et al. 2010) along a seismic profile.

The methods of (Xia et al. 2007) were tested as a possible method and found that from the P-SV diffraction seen in the synthetic data (e.g. Fig. 4-7) the depth of the tunnel and seismic velocity around it could be determined. When used in real data where the velocity of the diffractor was given for a range of possible diffraction imaging showed it could not be imaged. This was done by Xia himself and the results proved to be inconclusive for the tunnel 1 data set. This data set was used since it was the deepest and the diffraction had a better chance of not being overwhelmed by the primary and surface waves. The reasoning is that the surface waves are still so strong that even with processing they mask the diffraction energy and cannot image the tunnel. Unfortunately, the use of diffraction techniques did not appear to delineate Tunnel 1.

Up to now we have completed ignored the seismic surface waves assuming they are no more than noise relative to either the refractions or reflections. However, the surface wave as a source has been used for some time in near surface studies (Park et al. 1999) and even applied for cavity detection (Karray and Lefebvre 2009, Xu and Butt 2006, Gelis et al. 2005). Surface waves differ significantly from body waves in that the former are usually highly dispersive, that is the phase velocities that make up the surface wave packet are dependent on frequency. As such, this dispersion can be studied to better understand the velocity structure of the subsurface. The method requires the spectral transformation of the surface wave and you then look at the frequency vs. velocity component of the Rayleigh. The Rayleigh wave velocity is dispersive and so when put into the spectrum the velocities of the Rayleigh can be picked and inverted for to give a S-wave tomography (Xia et al. 1999). The frequency that is required is usually from 4.5-20Hz since that is the dominant frequencies of ground roll. The reason surface wave techniques are so useful is that since there is a shear component in the presence of air, the velocity goes to 0 and thus the tunnel can significantly influence the surface wave. The problem is that in near surface studies is its can be difficult to distinguish a tunnel site from other heterogeneities. The advantage of the method, however, is that since the surface wave amplitudes are usually the strongest it allows for detection of concrete covered cavities or in noisy urban environments (Karray and Lefebvre 2009). This method was not used for are tunnel sites since the frequency of the geophones was quite high for the Oxford, MS test sites at 40Hz, and in the sites

that there was 14Hz, the surface wave energy could not have each mode picked very well. The acquisition for a survey using surface wave studies is different but should be investigated to see if doing with conjunction with traditional P-wave tomography acquisition.

Using the different wave components of the seismogram can help us image the subsurface but each method has its own limitations and benefits. To truly image the near surface the entire waveform needs to be taken into account and in particular issues such as dispersion and attenuation considered. Methods such as full waveform inversion (FWI) can be used to image the subsurface (Lee et al. 2010, Brossier 2011). The method tries to image the subsurface by modeling the entire wave field spectrum and iterates until the original seismic gather is similar to that of the synthetic gather. However, at the present time such a method is both highly labour intensive and computationally expensive. The technique also requires very high quality data and this data must be carefully processed to minimize difference in the character between source point to source point. The full frequency spectrum is needed to image the waves so broadband data is required. This method is technically not used for any near surface modeling yet to our knowledge but despite the handicaps this technique has some potential and should be attempted in the future.

Due to the large amount of surface heterogeneity that was discussed in the near surface, issues associated with trying to resolve a subsurface void are quite difficult. There are two major considerations that were ignored for most of the report and need to be looked at greater detail in the future before larger studies could be pursued. The first is repeatability the ability to have different groups of contractors able to detect the same void using the same technique. The second major pitfall is a criterion of what makes the anomaly a tunnel for regions where the tunnel is not known. The test for repeatability should be easy enough to approach with trying to run a similar survey over a given tunnel site without giving any prior information to the groups of people. Since the anomalies are also quite small a time lapse approach to make sure local changes of weather and season don't affect the result should also be done. Especially with changing water table levels,, which could drastically change the interpretation of the tunnel anomaly. I think the harder issue is to classify what a tunnel anomaly is in a global sense to try and make a tunnel

detection criteria book for everyone to use. I think to do this multiple geophysical techniques would need to be used and do a similar study as (Cardarelli et al. 2010) where the use of joint inversion. To do this study site doing correlations between multiple different methods would need to be done to look at the relative anomaly for multiple different sites.

7.3 SUMMARY

The use of both seismic and electrical methods can help improve the interpretation of tunnel sites by eliminating possible false artifacts. The joint interpretation was found useful to both detect the actual location of the tunnel, to confirm the presence of a tunnel, and to help describe why the method did not work. The next section was to describe the future work to be done on the tunnel detection field and some notes about what was seen when trying to use other seismic techniques. The details about using seismic diffraction techniques showed that they can detect tunnels but in the situation we were in with loose gravel and sand the surface wave energy was to great and masked the diffractor energy. The next method that discussed was surface wave techniques such as MASW that were not sued due to the low frequency nature that was needed. The final area that was talked about was using the full waveform to image the subsurface using techniques such as full waveform inversion but the code is not readily available.

CHAPTER 8
8.0 CONCLUSION

Along the US-Mexico border the control of illegal immigration and transportation of goods is of utmost importance. The use of clandestine tunnels that travel through the border makes it nearly impossible to enforce control at the borders. The use of non-invasive detection techniques for the detection of these tunnels is critical when other methods such as intelligence don't work. The work presented here was to use seismic refraction and electrical resistivity tomography to detect the subsurface tunnels. The project was split into two different test areas. The first was Oxford, MS where surveys were tested over an area of where culverts were used as surrogate tunnels. The culverts were of various shapes, compositions and depths; this site was used as a test area before a real clandestine tunnel was surveyed. The next test area was Douglas, AZ, this is a tunnel along the US-Mexico border that was found in 1990 and is used as a test site for the DHS and CBP. The goal was to see the feasibility of using seismic and electrical methods for the detection of clandestine voids. The contrast in physical properties of a tunnel and the surrounding rock should be able to imaged and used for the detection of clandestine tunnels

The use of seismic and electrical methods were done along the surrogate and real tunnel sites for the detection using the equipment from both the University of Alberta, and the National Center of Physical Acoustics. The research involved the acquisition, processing and interpretation of the seismic and electrical data. The use of different acquisition parameters and survey arrays were used to help optimize what technique is best for the detection of seismic tunnels. Background information about tunnel detection was described and how other geophysical techniques have been used to detect tunnels.

Before any data was collected synthetic data was used to help simulate what would be seen in the test sites. To simulate how the electrical data would be affected for the detection of a tunnel a sample resistivity spread for both a Wenner and a dipole-dipole array were done. The initial model that was used was just a

homogeneous layer with an air filled void in the middle of the model. The test showed that the casing around a model had little to no affect on the inversion of the data. The inversion of a test array showed that using a dipole-dipole array could detect a high resistivity anomaly around the location of the tunnel. The use of a Wenner array showed little evidence for detecting the tunnel. Similar to the electrical data synthetic seismograms for individual shots were used to help simulate how the seismic wavefield is affected by a tunnel. The shot gathers showed little evidence for changes in the direct and refracted wave, unless a significantly large tunnel was used. The seismogram shows that there is both P and P-SV diffracted waves were diffracted back to the surface from the tunnel. The synthetic data that was collected showed that using a dipole-dipole array could be used for the detection of the tunnel. The synthetic seismograms data showed that only a large tunnel could be detected with direct and refracted waves.

The acquisition of the data at the Oxford, MS was used as test data before the acquisition at Douglas, AZ. The Oxford, MS test site was an abandoned railway track that is now used as a walking path, along the path culverts are placed with various depths. The culverts that were placed in the railway had different compositions ranging from metal pipes, concrete, to sandstones blocks. The depths of the culverts also change ranging from anywhere from 1.5-10m deep. The size of the array that was used depended on the perceived depth of the tunnel. The deeper the tunnel the larger the spread length, for both electrical and seismic surveys. There were 9 tunnel sites in total that had both electrical and seismic data recorded. The seismic data and electrical data were processed after the acquisition back at the University of Alberta, and at the NCPA. Taking the information gathered from Oxford, MS; data was then collected along the US-Mexico border at the Douglas, AZ test site. The Douglas, AZ test site was a real clandestine tunnel that was discovered in 1990. The test site is along the border and two survey locations were done using both seismic and electrical data. The tunnel is a concrete lined which varies from 5-10m in depth depending on the location of the spread. The seismic data had both a surface array along with a downhole geophone placed in one of the boreholes. The electrical data had both Wenner and dipole-dipole arrays surveyed. The data was post processed and interpreted later back at the office.

The electrical data that was collected was processed and using a technique known as electrical resistivity tomography (ERT). The ERT method takes the measured apparent resistivity taken at the site and is inverted to produce an image of the true reisistivities as a 2D image. The ERT method was expected to detect the air-filled void since the contrast between surface rocks and air is quite large. The ERT pseudosection should display the tunnel anomaly as a highly resistive zone. What was seen was that there could be resistive or conductive anomalies present at the approximate locations of a tunnel. In Oxford, MS there were 8 tunnel sites that were surveyed and out of all these sites only 4 detected a presence of a tunnel anomaly. Some sites showed an area of conductive anomalies which was interpreted as zones where water could flow easier due to the presence of the tunnel. The water could flow inside or just outside the tunnel to cause a pathway for the ions to move to create the anomaly. This was different then what was expected in modeling since the motion of ions was not taken into account. The main source of error and why most tunnel sites could not be detected was attributed to the contact of the electrodes causing the current to stay near the surface. The Douglas, AZ test site found that 1 out of 2 test areas detected the presence of a tunnel where only the dipole-dipole array detected it. The anomaly was a highly resistive but the inversion showed two possible locations around the approximate location of the tunnel. The site that could not detect had a metal fence causing it to not be able to inject enough current and was just imaging the fence. Overall the electrical method proved to be to detect subsurface voids, but the interpretation depends on knowing information about the subsurface.

The seismic data was processed and imaged using a technique known as refraction tomography. The refraction method tries to image the near surface using the direct and refracted waves. The velocities of the tunnel are that of air and the surrounding rock should be a higher velocity creating a strong contrast. The seismic data has its first arrivals picked and then inverted using ray tracing to give a velocity tomogram and a ray coverage plot. The velocities should show a drop down in velocities around the tunnel and the ray coverage should show a zone of little rays traveling through it. In the Oxford, MS site there were 9 tunnel sites that were imaged and 6 out of 9 tunnels showed the presence of a tunnel anomaly. Similar to

what was seen in the modeling the velocity tomogram showed very little evidence of the tunnel and at best showed a small velocity drop down. The ray coverage proved to be the best method to detect the tunnels which characterized the tunnel as a low ray coverage zone. The Douglas, AZ test site had both refraction tomography done with both surface data and downhole using a geophone in a borehole. The refraction method found the tunnel location at the same spot as the dipole-dipole array showing the drop down in velocity and low ray coverage around the approximate location of the tunnel. The borehole showed a bending around the tunnel seen in the velocity tomogram in the site which the electrical and seismic methods could not detect the tunnel. The seismic data could not detect the tunnel along a site with large surface heterogeneity. The use of other seismic techniques could not be used to image the tunnel due to the strong heterogeneity in the near surface and the large amount of surface wave noise, both reflection and diffraction methods could not work.

Both electrical and seismic methods found that the electrical and seismic methods could detect the presence of a tunnel. The anomaly that was seen in both methods was not distinct and the use of both electrical and seismic methods is thought to be critical for the interpretation of a tunnel site. In the situation where the tunnel location is not known the use of multiple geophysical techniques could be crucial to eliminate false tunnels sites. The In conclusion, using high resolution seismic and electrical methods can help detect the location of a clandestine tunnel in an urban environment.

REFERENCES

ANON. 1981. PROCEEDINGS OF THE SECOND TECHNICAL SYMPOSIUM ON TUNNEL DETECTION. GOLDEN, COLORADO.

---. 1988. PROCEEDINGS OF THE THIRD TECHNICAL SYMPOSIUM ON TUNNEL DETECTION. GOLDEN, COLORADO.

BAKER, G. S. 2002. NEAR-SURFACE SEISMIC REFRACTION TOMOGRAPHY TUTORIAL.

BANSAL, R. & M. G. IMHOF (2005) DIFFRACTION ENHANCEMENT IN PRESTACK SEISMIC DATA. *GEOPHYSICS,* 70, V73-V79.

BELFER, I., I. BRUNER, S. KEYDAR, A. KRAVTSOV & E. LANDA (1998) DETECTION OF SHALLOW OBJECTS USING REFRACTED AND DIFFRACTED SEISMIC WAVES. *JOURNAL OF APPLIED GEOPHYSICS,* 38, 155-168.

BENSON, A. K. (1995) APPLICATIONS OF GROUND-PENETRATING RADAR IN ASSESSING SOME GEOLOGICAL HAZARDS - EXAMPLES OF GROUNDWATER CONTAMINATION, FAULTS, CAVITIES. *JOURNAL OF APPLIED GEOPHYSICS,* 33, 177-193.

BISHOP, I., P. STYLES, S. J. EMSLEY & N. S. FERGUSON. 1997. THE DETECTION OF CAVITIES USING THE MICROGRAVITY TECHNIQUE: CASE HISTORIES FROM MINING AND KARSTIC ENVIRONMENTS. IN *MODERN GEOPHYSICS IN ENGINEERING GEOLOGY,* EDS. D. M. MCCANN, M. EDDLESTON, P. J. FENNING & G. M. REEVES, 153-166. BATH: GEOLOGICAL SOC PUBLISHING HOUSE.

BOHLEN, T. (2002) PARALLEL 3-D VISCOELASTIC FINITE DIFFERENCE SEISMIC MODELLING. *COMPUTERS & GEOSCIENCES,* 28, 887-899.

BROSSIER, R. B. R. (2011) TWO-DIMENSIONAL FREQUENCY-DOMAIN VISCO-ELASTIC FULL WAVEFORM INVERSION: PARALLEL ALGORITHMS, OPTIMIZATION AND PERFORMANCE. *COMPUTERS & GEOSCIENCES,* 37, 444-455.

BUTLER, D. K. (1984) MICROGRAVIMETRIC AND GRAVITY GRADIENT TECHNIQUES FOR DETECTION OF SUBSURFACE CAVITIES. *GEOPHYSICS,* 49, 1084-1096.

CARDARELLI, E., M. CERCATO, A. CERRETO & G. DI FILIPPO (2010) ELECTRICAL RESISTIVITY AND SEISMIC REFRACTION TOMOGRAPHY TO DETECT BURIED CAVITIES. *GEOPHYSICAL PROSPECTING,* 58, 685-695.

CARDARELLI, E., E. FISCHANGER & S. PIRO (2008) INTEGRATED GEOPHYSICAL SURVEY TO DETECT BURIED STRUCTURES FOR ARCHAEOLOGICAL PROSPECTING. A CASE-HISTORY AT SABINE NECROPOLIS (ROME, ITALY). *NEAR SURFACE GEOPHYSICS,* 6, 15-20.

CERJAN, C., D. KOSLOFF, R. KOSLOFF & M. RESHEF (1985) A NONREFLECTING BOUNDARY-CONDITION FOR DISCRETE ACOUSTIC AND ELASTIC WAVE-EQUATIONS. *GEOPHYSICS,* 50, 705-708.

CHAMBERLAIN, A. T., W. SELLERS, C. PROCTOR & R. COARD (2000) CAVE DETECTION IN LIMESTONE USING GROUND PENETRATING RADAR. *JOURNAL OF ARCHAEOLOGICAL SCIENCE,* 27, 957-964.

CURRO, J. R., S. S. COOPER & R. F. BALLARD (1981) CAVITY DETECTION-DELINEATION IN KARST AREAS - AN INVESTIGATION USING SEISMIC AND ACOUSTIC METHODOLOGY. *GEOPHYSICS,* 46, 452-452.

DAILY, W., W. LIN & T. BUSCHECK (1987) HYDROLOGICAL PROPERTIES OF TOPOPAH SPRING TUFF - LABORATORY MEASUREMENTS. *JOURNAL OF GEOPHYSICAL RESEARCH-SOLID EARTH AND PLANETS,* 92, 7854-7864.

DAILY, W., A. RAMIREZ, A. BINLEY & B. LABRECQUE. 2005. *ELECTRICAL REISISTANCE TOMOGRAPHY-THEORY AND PRACTICE*.

DEBEGLIA, N. & F. DUPONT (2002) SOME CRITICAL FACTORS FOR ENGINEERING AND ENVIRONMENTAL MICROGRAVITY INVESTIGATIONS. *JOURNAL OF APPLIED GEOPHYSICS,* 50, 435-454.

DEY, A. & H. F. MORRISON (1979) RESISTIVITY MODELING FOR ARBITRARILY SHAPED TWO-DIMENSIONAL STRUCTURES. *GEOPHYSICAL PROSPECTING,* 27, 1020-1036.

DOBECKI, T. L. & S. B. UPCHURCH (2006) GEOPHYSICAL APPLICATIONS TO DETECT SINKHOLES AND GROUND SUBSIDENCE. *THE LEADING EDGE,* 25, 336-341.

DOLL, W. E., J. R. SHEEHAN, W. A. MANDELL & D. B. WATSON. 2006. *SEISMIC REFRACTION TOMOGRAPHY FOR KARST IMAGING*. MONMOUTH JUNCTION: SCIENCE PRESS USA INC.

EDGE, A. B. & T. H. LABY. 1931. THE PRINCIPLES AND PRACTICE OF GEOPHYSICAL PROSPECTING. 339-341. CAMBRIDGE UNIVERSITY PRESS.

EDWARDS, L. S. (1977) MODIFIED PSEUDO-SECTION FOR RESISTIVITY AND IP. *GEOPHYSICS,* 42, 1020-1036.

EL KHAMMARI, K., A. NAJINE, M. JAFFAL, T. AIFA, M. HIMI, D. VASQUEZ, A. CASAS & P. ANDRIEUX (2007) COMBINED GEOELECTRICAL-GPR MAPPING OF UNDERGROUND CAVITIES IN THE ZAOUIT ECH CHEIKH CITY (MOROCCO). *COMPTES RENDUS GEOSCIENCE,* 339, 460-467.

ENGELSFELD, T., F. SUMANOVAC & N. PAVIN (2008) INVESTIGATION OF UNDERGROUND CAVITIES IN A TWO-LAYER MODEL USING THE REFRACTION SEISMIC METHOD. *NEAR SURFACE GEOPHYSICS,* 6, 221-231.

FURMAN, A., T. P. A. FERRE & A. W. WARRICK (2003) A SENSITIVITY ANALYSIS OF ELECTRICAL RESISTIVITY TOMOGRAPHY ARRAY TYPES USING ANALYTICAL ELEMENT MODELING. *VADOSE ZONE JOURNAL,* 2, 416-423.

GARDNER, L. W. 1939. AN AEREAL PLAN OF MAPPING A SUBSURFACE BY REFRACTION SHOOTING. GEOPHYSICS.

GELIS, C., D. LEPAROUX, J. VIRIEUX, A. BITRI, S. OPERTO & G. GRANDJEAN (2005) NUMERICAL MODELING OF SURFACE WAVES OVER SHALLOW CAVITIES. *JOURNAL OF ENVIRONMENTAL AND ENGINEERING GEOPHYSICS,* 10, 111-121.

GRANDJEAN, G. & D. LEPAROUX (2004) THE POTENTIAL OF SEISMIC METHODS FOR DETECTING CAVITIES AND BURIED OBJECTS: EXPERIMENTATION AT A TEST SITE. *JOURNAL OF APPLIED GEOPHYSICS,* 56, 93-106.

GRIFFITHS, D. H. & R. D. BARKER (1993) 2-DIMENSIONAL RESISTIVITY IMAGING AND MODELING IN AREAS OF COMPLEX GEOLOGY. *JOURNAL OF APPLIED GEOPHYSICS,* 29, 211-226.

GUEGUEN, Y. & V. PALCIAUSKAS. 1994. *INTRODUCTION TO THE PHYSICS OF ROCKS*.

HAGEDOORN, J. G. 1959. THE PLUS-MINUS METHOD OF0 INTERPRETING SEISMIC REFRACTION SECTIONS. 158-182. GEOPHYSICAL PROSPECTING.

HALIHAN, T. & J. E. NYQUIST. 2006. DETECTION OF VOIDS, TUNNELS AND COLLAPSE FEATURES. IN *PHILADELPHIA ANNUAL MEETING OF THE GEOLOGICAL SOCIETY OF AMERICA*. PHILADELPHIA, PA.

HAMPSON, D. & B. RUSSELL. 1984. FIRST-BREAK INTERPRETATION USING GENERALIZED LINEAR INVERSION. 40-50. CANADIAN JOURNAL OF EXPLORATION GEOPHYSICS.

HICKEY, C. J. & W. B. HOWARD. 2006. REFRACTION TOMOGRAPHY FOR TUNNEL DETECTION. IN *US ARMY WORKSHOP ON THE REAL-TIME DETECTION OF CLANDESTINE SHALLOW TUNNELS*. OXFORD, MS.

JETSCHNY, S., T. BOHLEN & D. DE NIL (2010) ON THE PROPAGATION CHARACTERISTICS OF TUNNEL SURFACE-WAVES FOR SEISMIC PREDICTION. *GEOPHYSICAL PROSPECTING,* 58, 245-256.

KARAMAN, A. & T. KARADAYILAR (2004) IDENTIFICATION OF KARST FEATURES USING SEISMIC P-WAVE TOMOGRAPHY AND RESISTIVITY ANISOTROPY MEASUREMENTS. *ENVIRONMENTAL GEOLOGY,* 45, 957-962.

KARRAY, M. & G. LEFEBVRE (2009) DETECTION OF CAVITIES UNDER PAVEMENTS BY MODAL ANALYSIS OF RAYLEIGH WAVES (MASW). *CANADIAN GEOTECHNICAL JOURNAL,* 46, 424-437.

KELLER, G. V. & F. C. FRISCHKNECHT. 1966. *ELECTICAL METHODS IN GEOPHYSICAL PROSPECTING*. PERGAMON PRESS.

KETCHAM, S. A., J. R. MCKENNA, R. J. GREENFIELD & T. S. ANDERSON. 2006. SEISMIC PROPAGATION FROM ACTIVITY IN TUNNELS. IN *HPCMP USERS GROUP CONFERENCE (HPCMP-UGC'06)*. DENVER, CO.

KEYDAR, S., D. PELMAN & M. EZERSKY (2010) APPLICATION OF SEISMIC DIFFRACTION IMAGING FOR DETECTING NEAR-SURFACE INHOMOGENEITIES IN THE DEAD SEA AREA. *JOURNAL OF APPLIED GEOPHYSICS,* 71, 47-52.

KHAIDUKOV, V., E. LANDA & T. J. MOSER (2004) DIFFRACTION IMAGING BY FOCUSING-DEFOCUSING: AN OUTLOOK ON SEISMIC SUPERRESOLUTION. *GEOPHYSICS,* 69, 1478-1490.

KISSLING, E., W. L. ELLSWORTH, D. EBERHARTPHILLIPS & U. KRADOLFER (1994) INITIAL REFERENCE MODELS IN LOCAL EARTHQUAKE TOMOGRAPHY. *JOURNAL OF GEOPHYSICAL RESEARCH-SOLID EARTH,* 99, 19635-19646.

KNAPP, R. W. & D. W. STEEPLES (1986) HIGH-RESOLUTION COMMON-DEPTH-POINT REFLECTION PROFILING - FIELD ACQUISITION PARAMETER DESIGN. *GEOPHYSICS,* 51, 283-294.

KNEIB, G. & A. LEYKAM (2004) FINITE-DIFFERENCE MODELLING FOR TUNNEL SEISMOLOGY. *NEAR SURFACE GEOPHYSICS,* 2, 71-93.

KNIGHT, R. L. & A. L. ENDRES. 2005. *AN INTRODUCTION TO ROCK PHYSICS PRINCIPLES FOR NEAR-SURFACE GEOPHYSICS*.

KOEFOED, O. 1979. *GEOSOUNDING PRINCIPLES 1 : RESISTIVITY SOUNDING MEASUREMENTS*. ELSEVIER SCIENCE PUBLISHINGCCOMPANY.

KORN, M. (1987) COMPUTATION OF WAVE-FIELDS IN VERTICALLY INHOMOGENEOUS-MEDIA BY A FREQUENCY-DOMAIN FINITE-DIFFERENCE METHOD AND APPLICATION TO WAVE-PROPAGATION IN EARTH MODELS WITH RANDOM VELOCITY AND DENSITY PERTURBATIONS. *GEOPHYSICAL JOURNAL OF THE ROYAL ASTRONOMICAL SOCIETY,* 88, 345-377.

KRUSE, S., M. GRASMUECK, M. WEISS & D. VIGGIANO (2006) SINKHOLE STRUCTURE IMAGING IN COVERED KARST TERRAIN. *GEOPHYSICAL RESEARCH LETTERS,* 33, 6.

LANZ, E., H. MAURER & A. G. GREEN (1998) REFRACTION TOMOGRAPHY OVER A BURIED WASTE DISPOSAL SITE. *GEOPHYSICS,* 63, 1414-1433.

LEE, H. Y., J. M. KOO, D. J. MIN, B. D. KWON & H. S. YOO (2010) FREQUENCY-DOMAIN ELASTIC FULL WAVEFORM INVERSION FOR VTI MEDIA. *GEOPHYSICAL JOURNAL INTERNATIONAL,* 183, 884-904.

LEE, T. K., S. O. PARK, J. W. RA & S. Y. KIM (1989) NEAR-FIELD DIFFRACTION PATTERN BY AN UNDERGROUND VOID OF CIRCULAR-CYLINDER. *MICROWAVE AND OPTICAL TECHNOLOGY LETTERS,* 2, 179-183.

LEGCHENKO, A., M. EZERSKY, C. CAMERLYNCK, A. AL-ZOUBI & K. CHALIKAKIS (2009) JOINT USE OF TEM AND MRS METHODS IN A COMPLEX GEOLOGICAL SETTING. *COMPTES RENDUS GEOSCIENCE,* 341, 908-917.

LEUCCI, G. & L. DE GIORGI (2010) MICROGRAVIMETRIC AND GROUND PENETRATING RADAR GEOPHYSICAL METHODS TO MAP THE SHALLOW KARSTIC CAVITIES NETWORK IN A COASTAL AREA (MARINA DI CAPILUNGO, LECCE, ITALY). *EXPLORATION GEOPHYSICS,* 41, 178-188.

LEUCCI, G., S. MARGIOTTA & S. NEGRI (2004) GEOPHYSICAL AND GEOLOGICAL INVESTIGATIONS IN A KARSTIC ENVIRONMENT (SALICE SALENTINO, LECCE, ITALY). *JOURNAL OF ENVIRONMENTAL AND ENGINEERING GEOPHYSICS,* 9, 25-34.

LEVANDER, A. R. (1988) 4TH-ORDER FINITE-DIFFERENCE P-SV SEISMOGRAMS. *GEOPHYSICS,* 53, 1425-1436.

LINES, L. R. & S. TREITEL (1984) TUTORIAL - A REVIEW OF LEAST-SQUARES INVERSION AND ITS APPLICATION TO GEOPHYSICAL PROBLEMS. *GEOPHYSICAL PROSPECTING,* 32, 159-186.

LO MONTE, L., D. ERRICOLO, F. SOLDOVIERI & M. C. WICKS (2010) RADIO FREQUENCY TOMOGRAPHY FOR TUNNEL DETECTION. *IEEE TRANSACTIONS ON GEOSCIENCE AND REMOTE SENSING,* 48, 1128-1137.

LOKE, M. H. 2002. *TUTORIAL: 2-D AND 3-D ELECTRICAL IMAGING SURVEY*.

LOKE, M. H. & R. D. BARKER (1996) RAPID LEAST-SQUARES INVERSION OF APPARENT RESISTIVITY PSEUDOSECTIONS BY A QUASI-NEWTON METHOD. *GEOPHYSICAL PROSPECTING,* 44, 131-152.

MARION, D., A. NUR, H. YIN & D. HAN (1992) COMPRESSIONAL VELOCITY AND POROSITY IN SAND-CLAY MIXTURES. *GEOPHYSICS,* 57, 554-563.

MARKIEWICZ, R. D. & B. D. RODRIGUEZ (1986) DETECTION OF VOIDS BENEATH AN INTERSTATE HIGHWAY USING A REFRACTION SEISMOGRAPH. *GEOPHYSICS,* 51, 445-445.

MCKENNA, J. R. & S. A. KETCHUM. 2006. TUNNNEL DETECTION, MONITORING, AND MODELING. IN *NS21A, 2006 AGU, GSS, MAS, MSA, SEG, UGM JOINT ASSEMBLY*. BALTIMORE, MD.

MEIER, M. A. & P. J. LEE (2009) CONVERTED-WAVE RESOLUTION. *GEOPHYSICS,* 74, Q1-Q16.

MILLER, R., C. B. PARK, J. XIA, J. IVANOV, D. W. STEEPLES, N. RYDEN, R. F. BALLARD, J. L. LLOPIS, T. S. ANDERSON, M. L. MORAN & S. A. KETCHAM. 2006. TUNNEL DETECTION USING SEISMIC METHODS. IN *AGU FALL MEETING*. SAN FRANCISCO, CA.

MOURATIDIS, A., S. LAMBROPOULOS & E. SAKOUMPENTA. 2005. THE "COVER AND CUT" METHOD IN TUNNEL AND ROADWAY CONSTRUCTION. IN *PROC. 1ST CONFERENCE EARTHWORKS IN EUROPE*. PARIS.

NABIGHIAN, M. & J. MACNAE. 1991. *TIME DOMAIN ELECTROMAGNETIC PROSPECTING METHODS*. SOCIETY OF EXPLORATIONAL GEOPHYSCIS.

NASSERI-MOGHADDAM, A., G. CASCANTE, C. PHILLIPS & D. J. HUTCHINSON (2007) EFFECTS OF UNDERGROUND CAVITIES ON RAYLEIGH WAVES - FIELD AND NUMERICAL EXPERIMENTS. *SOIL DYNAMICS AND EARTHQUAKE ENGINEERING,* 27, 300-313.

NEGRI, S., G. LEUCCI & F. MAZZONE (2008) HIGH RESOLUTION 3D ERT TO HELP GPR DATA INTERPRETATION FOR RESEARCHING ARCHAEOLOGICAL ITEMS IN A GEOLOGICALLY COMPLEX SUBSURFACE. *JOURNAL OF APPLIED GEOPHYSICS,* 65, 111-120.

OCONNELL, R. J. & B. BUDIANSKY (1978) MEASURES OF DISSIPATION IN VISCOELASTIC MEDIA. *GEOPHYSICAL RESEARCH LETTERS,* 5, 5-8.

PALACKY, G. J. 1987. *RESISTIVY CHARACTERISTICS OF GEOLOGICAL TARGETS*.

PALMER, D. (1981) AN INTRODUCTION TO THE GENERALIZED RECIPROCAL METHOD OF SEISMIC REFRACTION INTERPRETATION. *GEOPHYSICS,* 46, 1508-1518.

PAPADOPOULOS, N. G., M. J. YI, J. H. KIM, P. TSOURLOS & G. N. TSOKAS (2010) GEOPHYSICAL INVESTIGATION OF TUMULI BY MEANS OF SURFACE 3D ELECTRICAL RESISTIVITY TOMOGRAPHY. *JOURNAL OF APPLIED GEOPHYSICS,* 70, 192-205.

PARK, C. B., R. D. MILLER & J. H. XIA (1999) MULTIMODAL ANALYSIS OF HIGH FREQUENCY SURFACE WAVES. *PROCEEDINGS OF THE SYMPOSIUM ON THE APPLICATION OF GEOPHYSICS TO ENGINEERING AND ENVIRONMENTAL PROBLEMS*, 115-121.

PIRO, S., P. I. TSOURLOS & G. N. TSOKAS (2001) CAVITY DETECTION EMPLOYING ADVANCED GEOPHYSICAL TECHNIQUES: A CASE STUDY. *EUROPEAN JOURNAL OF ENVIROMENTAL AND ENGINEERING GEOPHYSICS,* 6, 3-31.

PULLAMMANAPPALLIL, S. K. & J. N. LOUIE (1993) INVERSION OF SEISMIC-REFLECTION TRAVEL-TIMES USING A NONLINEAR OPTIMIZATION SCHEME. *GEOPHYSICS,* 58, 1607-1620.

QIN, F. H., Y. LUO, K. B. OLSEN, W. Y. CAI & G. T. SCHUSTER (1992) FINITE-DIFFERENCE SOLUTION OF THE EIKONAL EQUATION ALONG EXPANDING WAVE-FRONTS. *GEOPHYSICS,* 57, 478-487.

RAMIREZ, A., W. DAILY, D. LABRECQUE, E. OWEN & D. CHESNUT (1993) MONITORING AN UNDERGROUND STEAM INJECTION PROCESS USING ELECTRICAL-RESISTANCE TOMOGRAPHY. *WATER RESOURCES RESEARCH,* 29, 73-87.

RECHTIEN, R. D., R. J. GREENFIELD & R. F. BALLARD (1995) TUNNEL SIGNATURE PREDICTION FOR A CROSS-BOREHOLE SEISMIC SURVEY. *GEOPHYSICS,* 60, 76-86.

RIDDLE, G. I., C. J. HICKEY & D. SCHMITT, R. 2010. SUBSURFACE TUNNEL DETECTION USING ELECTRICAL RESISTIVITY TOMOGRAPHY AND SEISMIC REFRACTION TOMOGRAPHY: A CASE STUDY. IN *SAGEEP*, 11. KEYSTONE, CO.

ROBERTSSON, J. O. A. (1996) A NUMERICAL FREE-SURFACE CONDITION FOR ELASTIC/VISCOELASTIC FINITE-DIFFERENCE MODELING IN THE PRESENCE OF TOPOGRAPHY. *GEOPHYSICS,* 61, 1921-1934.

ROBERTSSON, J. O. A., J. O. BLANCH & W. W. SYMES (1994) VISCOELASTIC FINITE-DIFFERENCE MODELING. *GEOPHYSICS,* 59, 1444-1456.

SABATIER, J. M., G. M. MATALKAH & IEEE. 2008. *A STUDY ON THE PASSIVE DETECTION OF CLANDESTINE TUNNELS*. NEW YORK: IEEE.

SABATIER, J. M. & T. G. MUIR. 2006. WORKSHOP ON REAL-TIME DETECTION OF CLANDESTINE SHALLOW TUNNELS. NATIONAL CENTER FOR PHYSICAL ACOUSTICS, UNIVERSITY OF MISSISSIPPI.

SASAKI, Y. (1992) RESOLUTION OF RESISTIVITY TOMOGRAPHY INFERRED FROM NUMERICAL-SIMULATION. *GEOPHYSICAL PROSPECTING,* 40, 453-463.

SCHUSTER, G. T. & A. QUINTUSBOSZ (1993) WAVEPATH EIKONAL TRAVEL-TIME INVERSION - THEORY. *GEOPHYSICS,* 58, 1314-1323.

SENGLAUB, M., M. YEE, G. ELBRING, R. ABBOTT & B. N. 2010. SENSOR INTEGRATION STUDY FOR A SHALLOW TUNNEL DETECTION SYSTEM. SANDIA NATIONAL LABORATORIES.

SHEEHAN, J. R., W. E. DOLL & W. A. MANDEL. 2006A. VOID DETECTION USING SEISMIC REFRACTION TOMOGRAPHY. IN *PHILADELPHIA ANNUAL MEETING*, 526. PENNSYLVANIA.

SHEEHAN, J. R., W. E. DOLL & W. A. MANDELL (2006B) AN EVALUATION OF METHODS AND AVAIABLE SOFTWARE FOR SEISMIC REFRACTION TOMOGRAPHY ANALYSIS. *ENVIROMENTAL AND ENGINEERING GEOPHYSICS,* 10, 21-34.

SHERIFF, R. E. & L. P. GELDART. 1985. EXPLORATION SEISMOLOGY I: HISTORY THEORY AND DATA ACQUISTION. CAMBRODGE UNIV. PRESS.

SILVESTER, P. P. & R. L. FERRARI. 1990. *FINITE ELEMENTS FOR ELECTRICAL ENGINEERS (2ND. ED.).* CAMBRIDGE UNIVERSITY PRESS.

SOGADE, J., Y. VICHABIAN, A. VANDIVER, P. M. REPPERT, D. COLES & F. D. MORGAN (2004) ELECTROMAGNETIC CAVE-TO-SURFACE MAPPING SYSTEM. *IEEE TRANSACTIONS ON GEOSCIENCE AND REMOTE SENSING,* 42, 754-763.

SONG, J. L. & U. TEN BRINK. 2004. RAYGUI 2.0 - A GRAPHICAL USER INTERFACE FOR INTERACTIVE FORWARD AND INVERSION RAY-TRACING. IN *U.S. GEOLOGICAL SURVEY OPEN-FILE REPORT*.

TELFORD, W. M., L. P. GELDART & R. E. SHERIFF. 1990. *APPLIED GEOPHYSICS SECOND EDITION*.

VAN SCHOOR, M. (2002) DETECTION OF SINKHOLES USING 2D ELECTRICAL RESISTIVITY IMAGING. *JOURNAL OF APPLIED GEOPHYSICS,* 50, 393-399.

VESECKY, I. F., W. A. NIERENBERG & A. M. DESPAIN. 1980. TUNNEL DETECTION. SRI INTERNATIONAL.

VIDALE, J. (1988) FINITE-DIFFERENCE CALCULATION OF TRAVEL-TIMES. *BULLETIN OF THE SEISMOLOGICAL SOCIETY OF AMERICA,* 78, 2062-2076.

VIRIEUX, J. (1986) P-SV-WAVE PROPAGATION IN HETEROGENEOUS MEDIA - VELOCITY-STRESS FINITE-DIFFERENCE METHOD. *GEOPHYSICS,* 51, 889-901.

WIDESS, M. B. (1973) HOW THIN IS A THIN BED. *GEOPHYSICS,* 38, 1176-1180.

WILLIAMSON, P. R. (1991) A GUIDE TO THE LIMITS OF RESOLUTION IMPOSED BY SCATTERING IN RAY TOMOGRAPHY. *GEOPHYSICS,* 56, 202-207.

XIA, J. H., R. D. MILLER & C. B. PARK (1999) ESTIMATION OF NEAR-SURFACE SHEAR-WAVE VELOCITY BY INVERSION OF RAYLEIGH WAVES. *GEOPHYSICS,* 64, 691-700.

XIA, J. H., J. E. NYQUIST, Y. X. XU, M. J. S. ROTH & R. D. MILLER (2007) FEASIBILITY OF DETECTING NEAR-SURFACE FEATURE WITH RAYLEIGH-WAVE DIFFRACTION. *JOURNAL OF APPLIED GEOPHYSICS,* 62, 244-253.

XU, C. Q. & S. D. BUTT (2006) EVALUATION OF MASW TECHNIQUES TO IMAGE STEEPLY DIPPING CAVITIES IN LATERALLY INHOMOGENEOUS TERRAIN. *JOURNAL OF APPLIED GEOPHYSICS,* 59, 106-116.

YANCEY, D. J., M. G. IRNHOF, J. E. FEDDOCK & T. GRESHAM (2007) ANALYSIS AND APPLICATION OF COAL-SEAM SEISMIC WAVES FOR DETECTING ABANDONED MINES. *GEOPHYSICS,* 72, M7-M15.

YILMAZ, O. 2001. SEISMIC DATA ANALYSIS: PROCESSING, INVERSION, AND INTERPRETATION OF SEISMIC DATA (INVESTIGATIONS IN GEOPHYSICS, NO 10). SOCIETY OF EXPLORATION GEOPHYSICISTS.

ZHANG, S. X., L. S. CHAN & J. H. XIA (2004) THE SELECTION OF FIELD ACQUISITION PARAMETERS FOR DISPERSION IMAGES FROM MULTICHANNEL SURFACE WAVE DATA. *PURE AND APPLIED GEOPHYSICS,* 161, 185-201.

ZHOU, W., B. F. BECK & J. B. STEPHENSON (2000) RELIABILITY OF DIPOLE-DIPOLE ELECTRICAL RESISTIVITY TOMOGRAPHY FOR DEFINING DEPTH TO BEDROCK IN COVERED KARST TERRANES. *ENVIRONMENTAL GEOLOGY,* 39, 760-766.

APPENDIX A
DESCRIPTION OF TUNNEL SITES

In this appendix the details of each tunnel site are presented, this includes photographs of the tunnels sites at each location. The information presented will be the field notes and description that were taken at each site location. The information about the target areas and motivation can be seen in Chapter. This appendix will be split into two parts; the first is the Oxford, MS test sites and then the Douglas, AZ test sites.

OXFORD, MS

The Oxford, MS test site is an old rail track that was constructed in 150- 160 years ago, the site has since then had its track removed and now is used as a walk path. The site is located 1 mile from the major highway and runs away from the highway so the only major sources of noise are pedestrians walking and, in the dam site, some possible 60Hz interference. The railway has multiple culverts that are used to keep from water building up along the embankment, the culverts were constructed in multiple phases since the construction of the railway. It is not known when these different tunnels/culverts were constructed but some are believed to be much older than others. These culverts, which act as surrogate tunnels for this study, provide a variety of sizes, shapes, and depths. The material above the walkway changes from site to site, but all have crushed gravel as the surface. The surveys were collected from February 5-20 , 2009 and the coordinates can be seen in table 1.

In general we approached each site with the same idea to try and find the subsurface culvert. By estimating the depth of the tunnel we then laid the spread length to at least 5 times the depth of the tunnel. The longer the spread the higher the depth penetration for refraction tomography, but at the cost of lost lateral resolution. Once this determined, we centered the seismic section along the surface of the old railway. We also have a 1.5m lateral offset perpendicular from the

receiver array for shot points in order to avoid damaging the geophone receivers by driving over them with the truck that carried the weight drop. In contrast, The hammer seismic surveys did not need to be offset.

Table A-1 lists the different sites.

Tunnel:	**Tunnel Material:**	**Date Survey Performed**	**Latitude (N)**	**Longitude (W)**
Tunnel 1	Sandstone Block	February 5, 2009	34°20'11.04" N	89°33'34.14" W
Tunnel 2	Metal Pipe	February 6, 2009	34°20'42.06" N	89°32'58.80" W
Dam	Earthen Dam	February 7, 2009	34°21'5.45"N	89°33'21.96" W
Tunnel 3	Small Metal Pipe	February 13, 2009	34°20'45.54" N	89°32'56.52" W
Tunnel 4	Small Sandstone Pipe	February 13, 2009	34°19'47.52" N	89°33'58.32" W
Tunnel 5	Concrete Pipe	February 16, 2009	34°20'3.00"N	89°33'48.12" W
Tunnel 6	Concrete Blocks	February 16, 2009	34°19'30.54" N	89°34'12.48" W
Tunnel 7	Concrete pipe	February 18, 2009	34°20'18.96" N	89°33'19.68" W
Tunnel 8	Concrete Blocks	February 19, 2009	34°19'29.19" N	89°34'14.64" W

Table A-1 This is the coordinates and location of each tunnel site in Oxford, Ms

TUNNEL 1

This was the first tunnel site that had data collected on it. The site had both electrical and seismic methods gathered on it and the most types of surveys were used for this site. The site took 2 days to acquire al the data due to issue with equipment but the data set that is used for tomography only took approximately 4 hours to gather.

The seismic survey was 120m long with the 40Hz geophones every 1m. To gather this data set we use a shot spacing of 1 m, starting 0.5m from the edge of the spread with a 1m shot spacing through the line. . The data was sampled at 0.125ms and was measured for 0.5s. The source used for this survey was an accelerated weight drop that was 1.5m laterally offset from the geophone array. At least 3 shots were taken at each shot point for stacking purposes but the data was acquired pre-stack and stacked later in house for amplitude studies. In addition to the seismic profile along the surface of the railway, a second line of 24 3-C geophones was laid inside the tunnel. This was a test to see the results but due to the tough ground the amplitudes of this data was poor. The data energy in field showed there was a difference in seismic energy transfer from the beginning to the other end of the spread. The seismic signal was drastically getting attenuated on the south end of the spread.

Along with the seismic surveys there was also 2 electrical surveys collected at this site using a ERT Scintrex box. The data set up includes 50 electrodes collected to a smart cable with 2m electrode spacing. The total length of the spread was 100m centered over the spread, the survey was set up first and was running first then the seismic survey was set up and ran. There was a dipole-dipole array that was calculated and a Wenner array. The Dipole-Dipole array was cut short due to light and power issues.

The tunnel itself can be seen in the pictures below but it consisted of blocks of stone that were fitted together and plastered into place. This tunnel was quite large being about a 1m high and about 0.75m wide, the tunnel was big enough to crawl through conformably. The base of the tunnel was made of sandstone blocks fitted together, this can be seen in figures A-1 and A-2.

PICTURES

Figure A-1 This is the a picture of inside f tunnel 1. On the ground is a measuring tape used to put the 3-C geophones inside the tunnel during acquisition

Figure A-2 Picture of the south side of the tunnel entrance. Te yellow box is the geode and orange reel is the trigger line for the accelerated weight drop

TUNNEL 2

NOTES

This was the second survey collected in Oxford MS. This is a 1m diameter corrugated metal pipe that is approximately 6m deep. The looks of this tunnel was that this was inserted after that of the railway and was used to limit wash out of the walk path. This site had both electrical and seismic surveys on it but not to the extent of tunnel 1. The site had steep slopes and had a bit rougher gravel. This survey was carried out on a Friday afternoon and had a large amount of pedestrian traffic, the survey was stopped when people were walking by but some random noise was seen. The ground here was also exposed to the sunlight and was quite a bit drier than other surveys.

The seismic survey was 120m long with 40Hz geophone spacing of 1m. To gather this data set we use a shot spacing of 1 m, starting 0.5m from the edge of the spread with a 1m shot spacing through the line. The source used for this survey was an accelerated weight drop that was 1.5m laterally offset from the geophone array. Each shot location at least 3 shots were done for stacking purposes but the data was acquired pre-stack and stacked in house for amplitude studies. The acquisition was sampled at 0.125ms and was measured for 0.5s.

The electrical survey that was done on this site was the dipole-dipole array. The first survey that was performed had a 2m electrode spacing with 50 electrodes having 100m spread. The tunnel was centered around the center of the spread and was activated during the construction of the survey. During one of the QC checks during the survey a loop error was encountered and caused the survey to stop. skipping the data made the survey continue until that electrode was found again and a open error was encountered. This was repeated until another electrode stopped working and thus caused a large amount of data not to be collected. The reason for this was a faulty smart cable and was not used for any other surveys. On Sunday February 8, 2009 the survey was performed using a 4m electrode spacing and a 100m electrode spread. The data was collected but a lot less due to only having 25 electrodes.

PICTURES

Figure A-3 This is the south entrance of the tunnel

Figure A- this is the north hand entrance

DAM

NOTES

The dam site is technically not a dam but that is how we informally referred to it, , technically this was an earthen embankment that contained some of the runoff from the power plant. The surrogate dam/tunnel is a metal pipe that is used in times of high water level, when we performed this survey there was some water that was coming out the other side in small quantities. This site is technically not part of the railway track and is in a similar region away form the highway and only source of noise is the high voltage power lines. The tunnel is approximately 5m deep and the tunnel is only about 0.5m in diameter. Compared to the other surveys the surface was a reddish clay material that was still quite moist. The seismic source had good contact but there were numerous equipment failures. There were both seismic and electrical studies performed at this site.

The seismic survey was 42m long with 40Hz geophone spacing of 0.6m. To gather this data set we use a shot spacing of 0.6m, starting 0.6m (2 ft) from the edge of the spread with a 0.6m shot spacing through the line. The source used for this survey was an accelerated weight drop that was 1.5m laterally offset from the geophone array. At each shot location at least 3 shots were done for stacking purposes but the data was acquired pre-stack and stacked in house for amplitude studies. The acquisition was sampled at 0.125ms and was measured for 0.5s. The seismic data was collected with a large number of bad geophones. At the start of the survey there were 3 bad channels and at the end there were over 10. The last line of geophones had identified loose wiring in the electrode takeout cables and was not used for the remainder of the surveys.

There were 3 dipole-dipole surveys performed over this tunnel site the reason for this is that since the last electrode takeout was removed to try and increase the data sampling we just changed the electrode spacing and kept the middle electrode the same. This was done during seismic acquisition, the ground was quite wet and the electrodes had solid contact with the ground. The surveys consisted of a 25m long 1m electrode spacing spread, a 50m long 2m electrode spacing, and a 100m long 4m electrode spacing spread survey.

PICTURES

Figure A-5 The tunnel entrance from the on the north side of the tunnel

Figure A-6 the tunnel on the south side with the towards the drainage zone.

TUNNEL 3

NOTES

This was the 4th survey or known as tunnel 3 since the dam site was not included as part of the DHS contract. This tunnel site was a small metal pipe survey that was just off from tunnel 2. This surrogate tunnel is approximately 0.4 m in diameter and is partially filled on the south hand side of the tunnel site. This tunnel site is expected to have a kink in it since the anticipated location it should come out of is different. There were both seismic and electrical surveys done at this site. The approximate tunnel depth is around 4-6m.

The seismic survey was 45m long with 40Hz geophone spacing of m. To gather this data set we use a shot spacing of 0.6m, starting 0.6m (2 ft) from the edge of the spread with a 0.6m shot spacing through the line. The source used for this survey was an accelerated weight drop 1.5m laterally offset from the geophone array. Again, at least 3 shots were done for stacking purposes at each shotpoing but the data was acquired pre-stack and stacked in house for amplitude studies. The acquisition was sampled at 0.0625ms and was measured for 0.5s. Unlike other surveys the actual location of the tunnel is not well known so the spread is centered around the approximate location of the tunnel.

The electrical survey carried out here had a 2m electrode spacing dipole-dipole spread, the survey was performed over the same region as the seismic profile. The estimated tunnel that is seen in the seismic survey sees the tunnel anomaly 10m offset from this center of spread location. The resistivity section does not detect due to not getting deep enough to detect it.

PICTURES

Figure A-7 this is the south side of tunnel 3, the small metal pipe is barley visible

Figure A-8 This is the north side of the tunnel, the location was different then expected and thus we expect a kink in the result.

TUNNEL 4

NOTES

This was the 5th survey or known as tunnel 4. This tunnel site was a made up of small concrete blocks. This surrogate tunnel is approximately 0.5m high and 0.75m wide. There were both seismic and electrical surveys done at this site. The approximate tunnel depth is around 6m. Both seismic and electrical methods should perpendicularly transect the tunnel trace at the surface. The surface was made up of crushed gravel and was quite dry.

The seismic survey was 72m long with 40Hz geophone spacing of 1m. To gather this data set we use a shot spacing of 1m, starting 0.5m from the edge of the spread with a 1m shot spacing through the line. The source used for this survey was an accelerated weight drop that was 1.5m laterally offset from the geophone array. Each shot location at least 3 shots were done for stacking purposes but the data was acquired pre-stack and stacked in house for amplitude studies. The acquisition was sampled at 0.125ms and was measured for 0.5s. There were 3 shots at each shotpoint location and vertically stacked during processing.

The electrical survey here had a 2m electrode spacing dipole-dipole spread, the survey was performed over the same region as the seismic. The dipole-dipole array has a 50m electrode spread but had an issue with electrode contact. The electrodes that were placed were easily planted and did not achieve a solid contact with the earth even when put 8" into the ground.

PICTURES

Figure A-9 This is the south side entrance into tunnel 4, this tunnel si created of concrete blocks and is approximately 0.5m.x0.75m.

Figure A-10 This is the north side entrance into tunnel 4, this tunnel is created of concrete blocks and is approximately 0.5m.x0.75m.

TUNNEL 5

NOTES

This was the second smallest tunnel that was attempted to be gathered, for this survey hammer seismic was done due to only using a 28.8m (96)ft spread. There was both seismic and electrical surveys acquired, the reason for this tunnel was because it was partially filled and quite shallow. The ground was a harder pack and both the geophones and the electrodes could get good contact. The hammer seismic is shot directly between the receivers, there is no perpendicular offset from the array since the striking plate could fit between the geophones..

The seismic survey was 28.8m long with 40Hz geophone spacing of m. To gather this data set we use a shot spacing of 0.6m, starting 0.6m (2 ft) from the edge of the spread with a 0.6m shot spacing through the line. The source used for this survey was an sledge hammer that had no lateral offset from the geophone array. Each shot location at least 3 shots were done for stacking purposes but the data was acquired pre-stack and stacked in house for amplitude studies. The acquisition was sampled at 0.0625ms and was measured for 0.5s.

The electrical surveys had a 25m dipole-dipole array done with 1m electrode spacing; the survey was set up before the seismic and ran while the seismic survey was running. The electrodes had solid contact and the ground was fairly compact and not loose gravel.

Figure A-11 this is the surface layout of tunnel 5, on the left is the ERT survey, the right is the seismic

Figure A-12, this is the north side of the tunnel 5, the culvert is partially filled

Figure A-13, this is the south side of tunnel 5. The tunnel is partially filled.

TUNNEL 6

NOTES

This was the 7th survey or known as tunnel 6. This tunnel is very similar to tunnel 4 and the acquisition was the same. The tunnel itself is slightly deeper then tunnel 4. This tunnel site was a made up of small concrete blocks. This surrogate tunnel is approximately 0.5m high and 0.75m wide. There were both seismic and electrical surveys done at this site. The approximate tunnel depth is around 6.5m. Both seismic and electrical methods should transect the tunnel on the surface perpendicular. The surface was made up of crushed gravel and was quite dry. The slopes on either side of the railway are steep with evidence of erosion. Parts of the slope had a backfill of gravel on the south side of this tunnel because of this.

The seismic survey was 72m long with 40Hz geophone spacing of 1m. To gather this data set we use a shot spacing of 1m, starting 0.5m from the edge of the spread with a 1m shot spacing through the line. The source used for this survey was an accelerated weight drop that was 1.5m laterally offset from the geophone array. Each shot location at least 3 shots were done for stacking purposes but the data was acquired pre-stack and stacked in house for amplitude studies. The acquisition was sampled at 0.125ms and was measured for 0.5s. There were 3 shots at each shotpoint location and vertically stacked during processing.

The electrical survey here had a 2m electrode spacing dipole-dipole spread done, the survey that was performed was performed over the same region as the seismic. The dipole-dipole array has a 50m electrode spread but had an issue with electrode contact. The electrodes that were placed were easily planted and did not get solid contact even when put 8” into the ground.

PICTURE

Figure A-14 The south side of tunnel 6, the tunnel was completely covered , but is not filled

Figure A-15 The north side of tunnel 6, we cannot see if this part of the tunnel is filled or not.

TUNNEL 7

NOTES

Only a seismic survey was performed at this survey due to time constraints, and because the ERT system was still running at tunnel 6 when this tunnel was being performed. The survey was the shallowest tunnel and is estimated at only 1.5m deep. The survey was 42m long (96 feet), the tunnel is partially filled with water, The ground was quite hard and good contact was achieved between with the geophones and the ground

The seismic survey was 28.8m long with 40Hz geophone spacing of m. To gather this data set we use a shot spacing of 0.6m, starting 0.6m (2 ft) from the edge of the spread with a 0.6m shot spacing through the line. The source used for this survey was a sledge hammer that had no laterally offset from the geophone array. Each shot location at least 3 shots were done for stacking purposes but the data was acquired pre-stack and stacked in house for amplitude studies. The acquisition was sampled at 0.0625ms and was measured for 0.5s.

PICTURES

Figure A-16 This is the surface layout of Tunnel 7, the geophones are on the side of the path.

Figure A-17 This is the north side of the tunnel, it is partially filled

Figure A-18 This is the south side of the tunnel, there is a mixture of water, leaves and tree branches in the tunnel.

TUNNEL 8

NOTES

This was the last survey that was surveyed in Oxford, MS. The tunnel is also the second deepest at around 8m deep. The tunnel has quite steep sides and both a Wenner and a dipole-dipole survey were done. This was one of the few days where wind noise was an issue and can be seen in the seismic data. The seismic data also had a string of low frequency phones at the end to see the difference between them. The tunnel itself is around 0.75 wide and 0.75m high, the construction is similar to 6 and 4 with suing sandstone blocks and mortar. The tunnel itself was empty and had very little debris in it

The seismic survey was 120m long with 40Hz geophone at spacing of 1m. In addition, the last 24m had 10Hz geophone attached. To gather this data set we use a shot spacing of 1 m, starting 0.5m from the edge of the spread with a 1m shot spacing through the line. There were a large number of bad shots due to wind noise. The source used for this survey was an accelerated weight drop that was 1.5m laterally offset from the geophone array. Due to the wind energy, the elastic band that was attached was tightened for more power. Each shot location at least 3 shots were done for stacking purposes but the data was acquired pre-stack and stacked in house for amplitude studies. The acquisition was sampled at 0.125ms and was measured for 0.5s

Along with the seismic surveys there were also 2 electrical surveys collected at this site using a ERT Scintrex box. The data set up includes 25 electrodes collected to a smart cable with 2m electrode spacing. The total length of the spread was 50m centered over the spread, the survey was set up first and was running first then the seismic survey was set up and ran. There was a dipole-dipole and Wenner array that were calculated.

PICTURES

Figure A-19: This is the surface layout for tunnel 8. The right has the geophones attached, the blue geophones are the 10Hz geophones, and the 10Hz geophones are red. The left hand side of the surface has the ERT survey

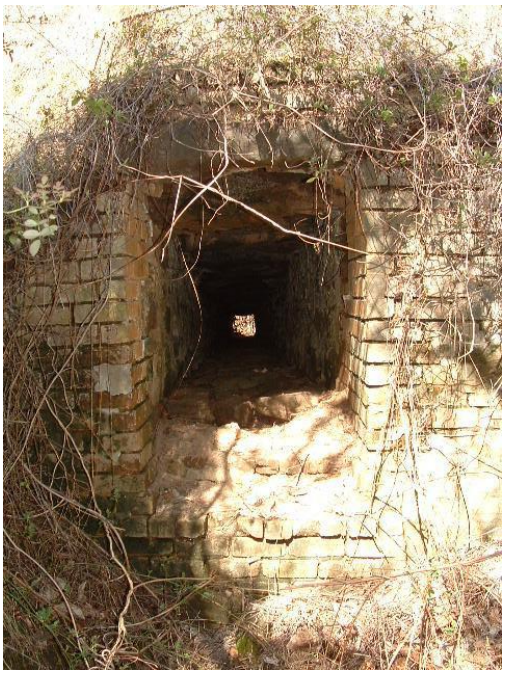

Figure A-20 The south hand side of the railway survey site for tunnel 8

DOUGLAS, AZ

The Douglas, AZ test site is a discovered clandestine tunnel that had both weapons and cocaine transferred through it. The tunnel was found in 1990 and is to date still one of the more sophisticated tunnels ever created on the US Mexico border. The tunnel was built by Corona-Verbera who was the architect for the "El Chappo" Guzman Drug Trafficking Organization. He incarcerated for 25years. The tunnel shaft was approximately 30ft deep on the Mexico side and had the use of elevator like pulley system to lower the contraband into the tunnel, the tunnel had tracks for a cart in the tunnel along with a air-conditioning and electricity for lighting. The tunnel emerged in warehouse on the US side, and there is also an underground storage area for the contraband before being brought to the surface. The tunnel is also concrete lined with a water pump and drains for when the tunnel is filled full of water.

The Douglas, AZ test site is controlled by the US customs and border patrol (CBP) and while we were there we had a representative with us and also a member of the US department of homeland security (DHS). To get permission for these tests both permission from DHS and CBP was required along with The University of Mississippi.

When we arrived at the test site there were only 2 possible areas for the seismic survey to be performed. There as a zone of gravel and sand beside the road by the warehouse, and then there was ditch beside the road and was approximately 3 m below the roadside. This had loose sands and was under construction with concrete being laid some distance away. There was also an area right beside the fence but do to safety concerns and amount of noise directly beside the fence was not done. Looking at the figures below we can see the field conditions of each seismic site.

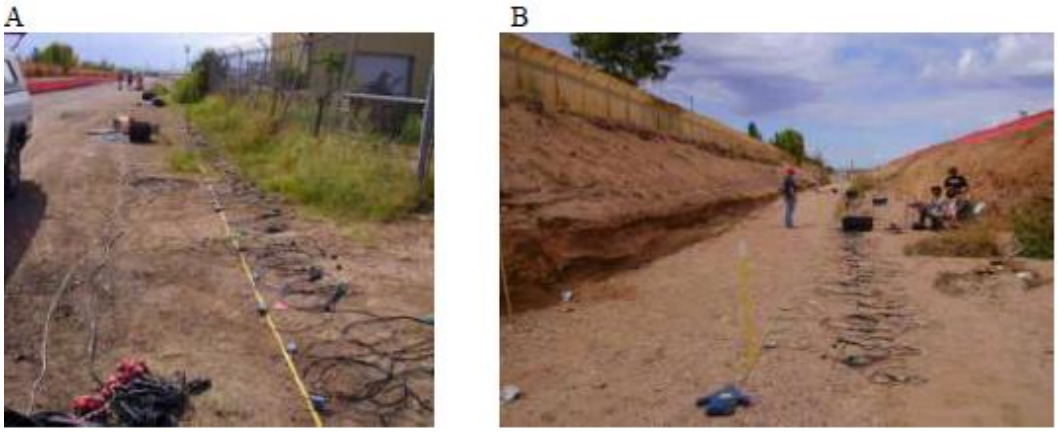

Figure A-21 Left: this is the layout for the roadside data in Douglas, AZ. This survey uses low frequency geophone. The tunnel is approximately in the middle of the warehouse running to the right. Right: This is the ditch data, the seismic was done directly in the middle and to the left hand side by the overhang the electrical survey was done. The border fence can be seen on the above the ditch on the left.

ROADSIDE

There were 4 main surveys that were acquired on the roadside data a 3-C geophone, the large hammer, small hammer and the borehole surveys. Each method was described below.

3-C survey: This was the first survey performed; it uses 24 channel 3-C geophones attached to one geode with 6 separate lines. This survey is performed by shooting 1 spread length of geophones on either side of the individual spread to increase the fold of the files. There are 6 lines, shots in-between each geophone with geophone spacing of 1m. The shot spacing for these surveys is 1m; the small hammer was used and is hit vertical into a metal plate. The geophone spacing is 1m and

Seismic 16Hz large hammer: This survey was done on Sept 2, 2009 and is the first major survey used. There were 6 separate geodes used where the first geode has the borehole component attached. On the survey file we have the first channel 1-24 as the borehole and then 25-144 as the 120 channels of the vertical component geophones. A long offset shot was taken at -30m from spread length west of the line.

This was across the road and used for the borehole data exclusively. Shot spacing is 1m and is taken inline between the geophones. The total spread length for this line is 59.5m where the tunnel is situated 18m from the west start of the line. The spread length starts from the east where 0m is the start of the line.

Seismic 16Hz small hammer: This survey was carried out just for amplitude information on the geophones which were otherwise clipped due too much energy in the close range. This data was not used for seismic refraction or reflection profiles and was gathered for amplitude studies. The shots are taken in-between the line and follow the same format as the large hammer survey.

Borehole: The data collected here is the first 1-24 channels of the large hammer survey. Channels 5-8 are the only ones active and all the rest are turned off. Channel 5 is the vertical component of the downhole tool, channel 6 is the H1 component, channel 7 is the H2 component, and channel 8 is the hydrophone. The borehole is 10.5m from the start of the line and

There were also 2 electrical surveys performed at this test site, a Wenner array and a dipole-dipole array. There was a metal fence beside the tunnel site did and also there were quite a bit of road traffic while the survey was running. The resistivity survey had a 1m electrode spacing with a 50m electrode spread. The 50 electrodes that were used worked good until the dipole-dipole survey. Similar to the Oxford, MS data set there became a bad takeout and some of the data was lost. Since there was also another road immediately to the west of the test site we could not center the tunnel in the spread.

Ditch Data

The ditch data compromised of a dug out ditch that was fortuitously under construction at the time of the surveys. The ditch would not be covered with concrete. This area had a loose sand base and was fairly flat the electrical data that was collected was over the overhang since it was moister there and the electrodes had better contact. The seismic data was collected in the middle of the ditch and was in loose sands. The ditch had a large amount of metal debris around on the surface

such as rebar, barbed wire, and other garbage. Looking at the side of the ditch we could see that there was a loosely consolidated surface by the roadside and the material got more and more competent with depth. The ditch data was under this competent layer. There were two surveys performed for this site

There were two survey performed right after another. The first used low frequency geophones, the second used higher frequency geophones which better reduce ground roll and other surface related noise, but limit the data. The goal was to compare if the frequency change in the geophones would change the result drastically. Refraction profiles were done on both to compare the difference. The second survey was identical except there was 40Hz geophones instead of the first one which had 14Hz geophones.. The seismic data had a 48m spread length with a geophone spacing of 0.5m, the data was recorded for 0.5s at a 0.0625ms sample rate. The source spacing was 0.5m and where the data started off by 0.25m.

The electrical data that was collected was a dipole-dipole array using 1m electrode spacing and with 50 electrodes. The electrodes were planted along the edge of the ditch in the shade and had water poured over them for good contact. The loose sands were causing poor contact. The

PEOPLE INVOLVED

I would like to thank the people involved for the Douglas, AZ data set for all there hard work and dedication. The people that worked on the site are

Craig Hickey	NCPA
Grey Riddle	University of Alberta
Douglas Schmitt	University of Alberta
J.D. Heffington	NCPA
Gordon Brasnett	University of Alberta
Steve Taylor	University of Alberta
Cory Schmitt	Doug Schmitt son
Lesley Blancas	DHS S&T

James Wray	CBP
Robert Shiner	CBP

PICTURES

There are no pictures of the actual tunnel. Since it is concealed and no confined space training was taken.